LARS Information Note 112174

Electrical Methods of Determining Soil Moisture Content

L. F. Silva
F. V. Schultz
J. T. Zalusky

The Laboratory for Applications of Remote Sensing

Purdue University, West LaFayette, Indiana

LARS Information Note 112174 T-1039/4

Electrical Methods of Determining Soil Moisture Content

by

L. F. Silva
F. V. Schultz
J. T. Zulusky

Laboratory for Applications
of
Remote Sensing

Purdue University
West Lafayette
Indiana

This work was supported by the National Aeronautics and Space Administration (NASA) under Grant No. NGL 15-005-112 and Contract No. NAS 914016.

TABLE OF CONTENTS

LIST OF TABLES

LIST OF FIGURES

Part Two
Figures

APPENDIX
FIGURES

LIST OF SYMBOLS

ABSTRACT

In this report electrical methods of determining soil moisture content are explored. Since the magnetic permeability and electrical conductivity of soils are known to be unreliable indicators of soil moisture content; the report focuses on the electrical permittivity of soils. The first part of the report gives an assessment of permittivity as an indicator of soil moisture content, based on experimental studies performed by the authors. The conclusion is that the electrical permittivity of soils is a useful indicator of aviilable soil moisture content.

In the second part of the report, two methods of determining the permittivity profile in soils are examined in light of the findings in Part I of this report. A method due to Becher is found to be inapplicable to this situation. A method of Slichter, however, appears to be feasible. The results of Slichter's method are extended to the proposal of an instrument design that could measure available soil moisture profile (percent available soil moisture as a function of depth) from a surface measurement to an expected resolution of 10 to 20 cm. Extension of the results to the airborne remote sensing problem is considered.

INTRODUCTION

In the field of agronomy, many scientific investigations, as well as field applications, make use of soil moisture content data. Soil moisture is also an important variable in water resources management. Unfortunately, however, soil moisture content is not easy to measure in the field. The commonly used methods (gravimetric, conductivity, neutron thermalization, gamma ray attenuation) all have important disadvantages. Thus, there is a need for a better technique which can be used in remote sensing applications to field work. The method should have better accuracy than the conductivity technique, greater speed than the gravimetric method, and better portability and safety than the radiation techniques.

Ideally, the method should permit the determination of the available (for plant growth) soil moisture profile (i.e., % available moisture as a function of depth). Electrical methods of measuring soil moisture appear to be able to satisfy these needs (32). Three properties of matter can be measured by electrical methods: magnetic permeability, conductivity, and electrical permittivity. Except under unusual circumstances, the permeability of soil is very close

to its value in free space, μ_0 (1). The conductivity of soil is not a reliable indicator of moisture content because of the large influence of ions in the soil. Measuring the conductivity of porous blocks buried in the soil overcomes this difficulty, but leads to inconvenience and inaccuracy. Only permittivity remains. It is plausible that permittivity could be a reliable indication of soil moisture, since the dielectric constant (relative permittivity) of soil is around five while water has a relative permittivity of eighty.

Furthermore, the electrical permittivity method of soil moisture measurement discussed herein has three important advantages. First, it is well suited to remote sensing, which is important from the standpoints of economy of time and financial resources required. Second, it has the capability of measuring the moisture content as a function of depth below the surface of the earth, to a depth of the order of a meter. Third, it is not affected by irregularities in the flatness of the soil, of the order of a few centimeters within a radius of a meter, or so.

It is possible, of course, to determine the amount of moisture at various depths in the soil (i.e., the moisture profile) by augering a hole and lowering some sort of probe into the soil. Another technique is to remove a core of the soil and to measure the soil moisture directly. Both of these methods are very time consuming. The proposed electrical permittivity method would not disturb the soil in any way since

the electromagnetic waves to be used (at a frequency of about 300 megahertz (MHz) or a free-space wavelength of one meter) can penetrate most soils to a depth of about a meter and also determine the available soil moisture profile with a definition in soil depth of the order of ten centimeters, or so.

Active and passive radar methods are under consideration by other organizations. These normally involve airborne instruments operating at frequencies ranging from a few gigahertz (GHz) to perhaps 25 GHz (33). In general, these methods (operating at wavelengths from about 1 to 10 centimeters) are handicapped by the existence of earth surface roughnesses of the order of a few millimeters and by the fact that, at these high frequencies, the waves penetrate the earth no more than a few centimeters, at the most, depending upon the conditions (moisture content and free ion content) of the soil. Furthermore, they give a measure of the <u>total</u> moisture content of the soil, from the surface to their deepest point of penetration. This is a serious limitation for several of the more important applications of the measurements. The use of lower frequencies (longer wavelengths) is limited by the required increase in size of the antennas to be carried by the aircraft.

The research involved in this present project naturally divided itself into two parts. The first part was concerned with determining accurate quantitative relations between soil moisture and electrical permittivity for various common soils, and the second part dealt with methods for determining the permittivity profile. The first part of this research has been

completed and the results are contained herein. The investigation of the second part seems to indicate that the most promising method for meeting the end requirements involves the development of an electrical instrument to be placed on the surface of the earth (31). The measurements made by this instrument on the soil moisture profile could then be telemetered to some central point, if desired. As mentioned previously, it is anticipated that the electrical measurements would be made at a frequency of about 300 MHz (a free-space wavelength of about one meter).

Since completing the portion of the project described in the present report, an additional report (33) has been received. It discusses many methods for measuring the permittivity of the earth, but none seems to be particularly applicable to the present need. It does contain, however, an excellent list of references on the subject.

PART I

The Relationship Between Soil Moisture and Electrical Permittivity

CHAPTER 1

STATEMENT OF THE PROBLEM

In part one of this thesis, the relationship between the electrical permittivity of soils and the moisture content of soils is explored.

Objectives of the Project

We wish to determine whether permittivity is a good indicator of soil moisture content. Certainly, moisture content influences soil permittivity. The fact that soil permittivity is a function of moisture content, however, is not sufficient to conclude that permittivity is a good indicator of soil moisture. It is necessary to explore other factors which affect soil permittivity and to assess their roles.

The objective of the study is to answer the question: Is it possible to determine soil moisture content with acceptable accuracy from knowledge of the permittivity alone?

Definitions

Since this report is an interdisciplinary investigation, it may be helpful to all to clarify some unfamiliar terminology.

Soil Moisture Content is the amount of water in the soil, generally expressed as a percentage.

1-1 $$\% \text{ Moisture Content} = \frac{\text{Mass of Water in Soil}}{\text{Mass of Dry Soil}} \times 100$$

Wilting Point Moisture is the soil moisture content at which plants undergo permanent wilting. Practically speaking, it is defined as the percentage moisture content corresponding to a soil moisture tension of 15 bars.

Field Capacity is the soil moisture content of soil which has been thoroughly wetted, but all the moisture that can drain off due to gravity has done so. This generally corresponds to a soil moisture tension of one-third bar.

Available Water is the amount of water between the wilting point and field capacity. For a given moisture content, the percentage of available moisture is (Percentage Moisture - Percentage Moisture at Wilting Point).

Soil Moisture Tension is the force per unit area which binds the water to the soil. This is measured by the "suction" (pressure difference) required to extract moisture from the soil. The usual technique for obtaining a certain moisture tension is to place a soil sample next to a porous membrane in a pressure vessel and apply air pressure to the inside of the vessel. The pressure differential removes any moisture held by the soil particles at less tension than the applied pressure.

Permittivity (ϵ) is an electrical property of materials defined by Coulomb's Law. Rationalized MKS units are used for all physical quantities.

1-2 $$F = q_1 q_2 / 4\pi \epsilon r^2$$

where F is the force between two charges,

q_1 and q_2 are the magnitudes of the two charges,

r is the distance between the two charges, and

ε is the permittivity.

ε can be expressed as $\varepsilon_o\varepsilon_r$ where ε_o is the permittivity of a vacuum in $C^2/N\text{-}m^2$. ε_r is referred to as the relative permittivity, or dielectric constant.

Dielectric Constant is defined to be the relative permittivity.

Permeability (μ) is the ratio of magnetic induction to magnetic field strength (for linear materials). In vacuum, the permeability is defined to be $4\pi \times 10^{-7}$ henry/meter. In this thesis, it is assumed that the permeability is equal to the vacuum value. This is almost exactly true, except for ferrous materials, which do not occur in the present work.

Conductivity (σ) is the ratio of volume current density to electric field strength. Conductivity can be calculated quite easily from resistance measurements.

Some Factors Which May Affect the Permittivity of Soil

Many factors influence the permittivity of soil. Some of the most important ones are introduced below.

Soil Types. Soils are composed of many different types of materials whose dielectric constants may differ considerably. Furthermore, soil and water interact. It is by no means inconceivable that different types of soil may interact differently, so that the permittivity of the mixture may differ significantly among different soils.

Soil Condition. It is possible that the physical condition

of the soil may affect its dielectric properties. Compaction is probably the most important factor. A rather highly compacted soil has less airspace than a less compacted one. This might have some fundamental effect on the permittivity of the mixture. In addition, compaction may have some other consequences. For example, suppose permittivity were proportional to the number of water molecules within a sample holder. If two samples had the same percentage moisture content, a more compacted sample would have more molecules of water and, therefore, have a higher dielectric constant.

Ion Concentration. The ion concentration in soils has a very strong effect on the electrical conductivity of soils, but it is not apparent that ion concentration will influence permittivity. If ion concentration is an important factor, this fact could have serious consequences. Ion concentration varies from place to place and time to time. Irrigation practices and fertilization alter ion concentration.

Time. A number of references have been found in the literature to the variation of measured permittivity with time. Various materials were involved, including vanadium oxide. No explanations were given except that the investigators felt that these observations were not artifacts.

Temperature. Temperature affects the permittivity of most substances. It is known that the permittivity of water decreases with increasing temperature.

Frequency. The permittivity of any material is a function of

the frequency of the electromagnetic fields used in the measurement. A material whose permittivity does not change over a certain range of frequency is said to be nondispersive in that range.

CHAPTER 2

LITERATURE REVIEW

For several decades dielectric methods of determining soil moisture content have attracted considerable attention. The first section of this chapter will review some of the papers in this area, while the second section will deal with specific aspects of soil moisture interaction.

Determination of Soil Moisture Using Dielectric Methods

The earliest article to be surveyed is "A Review of Results of Dielectric Methods for Measuring Moisture Present in Materials" by N.E. Edlefsen (2). He discussed a number of moisture meters, mainly for food products. However, he did discuss three investigations devoted to soil moisture measurement, the investigators cited being W.L. Balls (3,4), G.H. Cashen (5), and the author himself. Balls reported a linear relationship between capacitance and moisture for all moisture contents except very low ones, using buried electrodes. Cashen used a different type of condenser and obtained ir-

regularly shaped curves which were difficult to explain in terms of soil moisture. Edlefsen also found a linear relationship between capacitance and water content, although he did mention difficulties in obtaining uniform compaction. He also reported successful field tests. Edlefsen continued his research, and in 1934 reported the development of "A New Capillary Potentiometer" (6).

During the 1930's several investigators worked with dielectric properties, notably Anderson, Shaw and Muckenhirn, Aleksandrov, Bannerjee and Joshi, and Yevstigneyev. References to most of these can be found in Fletcher (7). In 1939, Fletcher published the results of his research. He built probes of plaster of Paris between metel electrodes, and his laboratory results were encouraging. Not only was he able to obtain a useful relationship between soil moisture and measured dielectric constant, but he was also able to show that between 0.1 and 20 grams of NaCl per 100 cc of water had no effect on his readings.

The next study was that of Anderson and Edlefsen (8) who worked with an apparatus similar to Fletcher's. The investigation was designed to answer three basic questions:

(1) Are the results obtained by dielectric methods reproducible?

(2) How much time must be allowed for the block to come to moisture equilibrium?

(3) What is the effect of plate separation? If electrode separation is critical, the expense of manufacturing moisture meters would be greater.

They found that the results were reproducible, the time lag was small if the probe was located near rapidly transpiring roots, and "no outstanding differences for electrode separations of 4 cm and 2 cm".

Anderson gives the equation, $C = C_0D$, which means that the capacitance of any capacitor is equal to its capacitance when filled with air multiplied by the dielectric constant of the material used to fill it. In the case of Anderson's sample holder, C_0 was no more than 0.0001 μF, the smallest value measured, and C = 0.1 μF, the largest. Then $D = C/C_0 = 1000$. Soils have a dielectric constant of around five while water has a relative permittivity of about eighty. So a simple mixing rule cannot account for this. Anderson provides a clue to the explanation when he states that changing the electrode separation by a factor of two had little effect on his readings, which suggests that most of Anderson's observations were due to something going on at the surface of the electrode.

Actually, this should not have been surprising. Anderson's collaborator, Edlefsen, reviewed an article by G.H. Cashen. The second point in Cashen's summary is:

> The results (of capacitance measurements) depend on the electrodes used. With mercury, all soils give curves of the same general type for the variation of the capacity with moisture, because the capacity effects associated with the soil-electrode interface are large compared to those due to the soil. . . The results obtained with carbon electrodes, though depending on the texture of the soil, generally confirm the. . .(results). . . with mercury electrodes.

Apparently, Edlefsen did not fully appreciate the significance of Cashen's conclusions.

Soon after Anderson's article appeared, however, E.C. Childs (9) pointed out some of these problems and stressed the effects of leaky dielectrics in capacitors. Childs assumed some reasonable values of parameters of the model and showed that Anderson's results could be explained in this way.

In 1945, E.F. Wallihan (10) of Cornell University reported on his work. He also used plaster of Paris between insulated electrodes. To begin, he noted that field tests of Fletcher's soil moisture probe were disappointing. Wallihan offered three factors which he felt were important and not given sufficient attention in earlier work:

(1) The use of medium having fixed porosity as the material between the electrodes,

(2) The relative merits of insulated and uninsulated electrodes,

(3) Choice of frequency.

Wallihan reported only preliminary results and no subsequent paper of his has been found.

In 1947, Thorne and Russell (11) published their conclusions about dielectric methods of determining soil moisture. They attempted to test Child's theory directly and found that it was confirmed, at least qualitatively. Thus the apparent capacitance is a function of sample resistance among other things. After publication of this article and subsequent mention of it in Advances in Agronomy, few articles on dielectric methods appeared in soil science journals. It is worth

noting that Thorne and Russell used electrodes which were insulated with thick pieces of glass.

Specific Aspects of Soil-Moisture Interaction

Soil Type

Many factors are involved in soil classification, but the most important is texture, which is a term referring to the size of particles. Table 1-1 gives a quantitative meaning to common textural terms.

Real soils, of course, are seldom so homogeneous as to fit into only one of these categories, but most soils are mixtures of these types. The "textural triangle" shows how combinations of soil types are named (see Figure 1-1). To determine the textural types, first project the silt content parallel to the clay side, then project the clay content parallel to the sand side. The region where the lines intersect is the texture type. For example, a soil composed of 25% clay, 35% silt, and 40% sand would be classed as a loam. The dashed lines on Figure 1-1 show how to project these various component values. The contour lines for constant silt content are parallel to the clay axis, the contour lines for constant clay content are parallel to the sand axis, and the contour lines for constant sand content are parallel to the silt axis.

How does particle size affect the permittivity of a soil-moisture mixture? Water is bound onto surfaces by adsorption,

Table 1-1. Definition of soil texture types.

U.S.D.A. System		International System	
particle size range	texture type	texture type	particle size range
2-1	very coarse sand	coarse sand	2-.2
1-.5	coarse sand		
.5-.25	medium sand		
.25-.1	fine sand	fine sand	.2-.02
.1-.05	very fine sand		
.05-.002	silt	silt	.02-.002
<.002	clay	clay	<.002
millimeters			millimeters

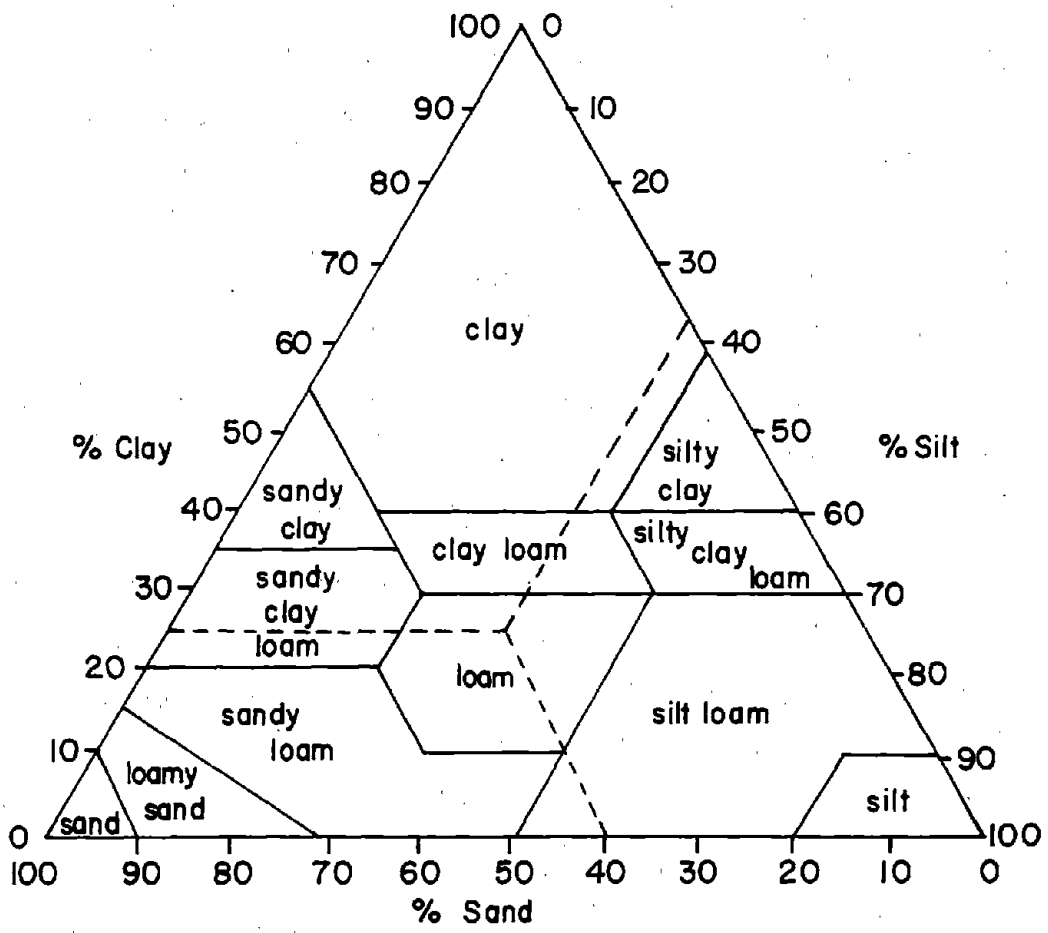

Figure 1-1. Textural Triangle.

and water that is "bound" has a lower dielectric constant than free water in the range of frequency of interest to us. An example of this is the permittivity of ice, where each molecule is bound to its neighbors. This makes it difficult for the dipolar water molecules to reorient themselves in response to an electric field. Since the permittivity of water depends largely on the motion of dipoles, the permittivity becomes very small at all frequencies except the lowest. The behavior of adsorbed water on clays is somewhat similar, according to Hoekstra (private communication). The permittivity of free water, ice, and adsorbed water on clays are illustrated in Figure 1-2.

The amount of water adsorbed depends on the available surface area. As particle size decreases, the total surface area of a given volume of soil increases dramatically. It is possible to calculate the surface area per cubic centimeter for various size particles. This shows that surface area is approximately proportional to 1/radius, with a 0.0001 cm size particle giving 31,550 cm^2 per cubic centimeter. Actually, this greatly underestimates the area available since the insides of the particles also open to admit water molecules (see Figure 1-3). So clays have far more surface area than sands and therfore adsorb much more water. Hence, a larger percentage of the water contributes very little to the dielectric constant, and one would expect clays to have a smaller dielectric constant at a given moisture content than sands or silts.

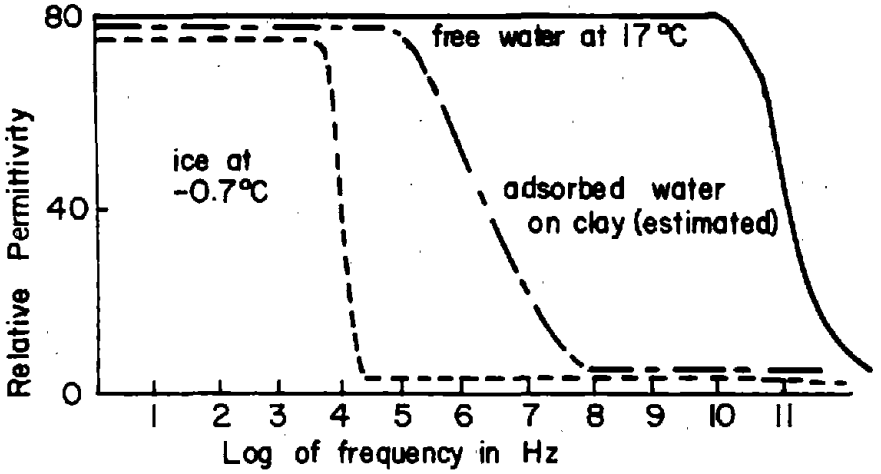

Figure 1-2. Permittivity of Water As A Function of Frequency

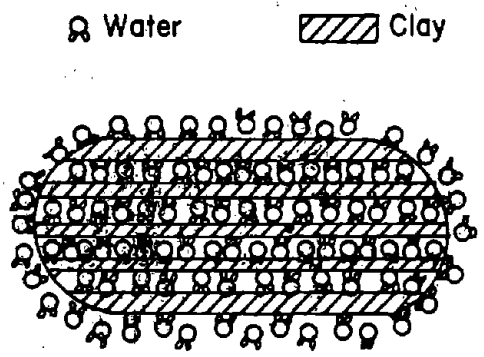

Figure 1-3. Adsorbed Water on Clay.

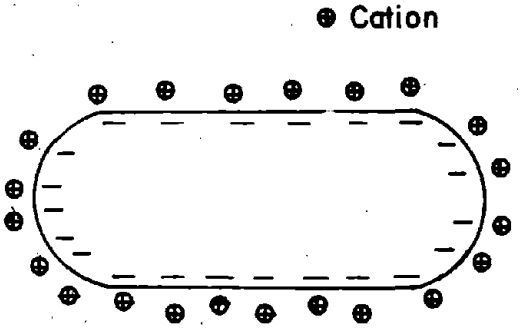

Figure 1-4. Adsorbed Cations on Clay.

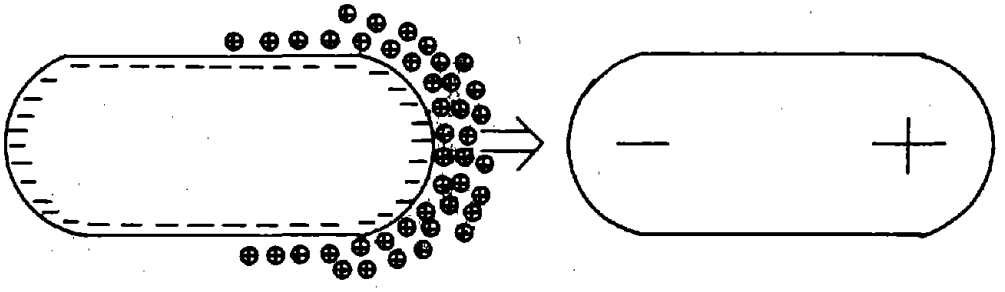

Figure 1-5. Polarization of Clay Particles.

Another problem arises from the fact that clays adsorb ions as well as water onto their surfaces (see Figure 1-4). This is because the clay particles have a structural negative charge due to substitution of lower valence ions (magnesium, etc.) for aluminum in the crystal lattice and also due to broken edges in the lattice. The cations can move freely along the surface of the clay particle in response to fields. When a field is applied, therefore, the clay particle becomes a large dipole (Figure 1-5). Hence, clays have a high dielectric constant at low frequencies (generally less than 10^4 Hz). Several investigators have formalized this intuitive explanation. O'Konski (12) introduced the notion of surface admittance to quantify the ability of ions to move in response to an applied electric field. Surface admittance is merely the ratio of the current on the surface of a clay particle to the voltage across the clay particle. Schwan (13), however, showed that this concept was not adequate to explain experimental results. Schwartz (14) extended O'Konski's concept to include complex surface admittances which imply some energy storage. This improved model is supported by Schwan's experimental results. By applying Schwartz's model to clay soils which have a lower limit (for particle size) of 0.2 micrometer, it can be shown that this phenomenon has a definite effect at frequencies below about 10^4 Hz.

Soil Condition and Time

M.L. Wiebe (15) of the Texas A & M Remote Sensing Center has recently completed a program of measurements on various soils in Texas at a frequency of 10.625 GHz. His results seem to indicate that variables such as homogeneity, compaction, and time have a significant influence on the permittivity of soils. Table 1-2 illustrates the significance of various effects. A few observations about the factors charted in the table may serve to clarify the information derived from Wiebe's graphs. Different compactions were obtained using a controlled full-compacting hammer. Curing time is the amount of time that the soil was allowed to stand in a sealed container. Only Tarrent Stoney Clay is not homogeneous, and the table shows the effect of sieving. Each entry in the table shows the relative influence of the different variables; the entries can be considered as partial derivatives evaluated at the midrange of moisture content. The table does show that these variables do have a significant influence on the permittivity.

To get a better idea of the implications of Table 1-2, consider Table 1-3. This table is designed to show the possible inaccuracies that could result from attempting to infer moisture content from the permittivity of soil. Suppose one measures the dielectric constant of soil whose moisture content, compaction, and curing time are unknown. What can be inferred about the moisture content? Table 1-3

Table 1-2. Relative Influence of Moisture, Compaction, Curing Time, and Homogeneity on Soil Permittivity.

	$\frac{\Delta\epsilon}{\Delta \text{Moisture \%}}$	$\frac{\Delta\epsilon}{\Delta \text{Compaction}}$	$\frac{\Delta\epsilon}{\Delta \text{Curing Time}}$	$\frac{\Delta\epsilon}{\Delta \text{Homogeneity}}$
Tarrent Stoney Clay	5/5	5/15	6	8
Gila Sandy Loam	10/5	2/15	1	
Hoban Sandy Loam	7/5	3/15	5	
Amarillo Fine Sandy Loam	7/5	1/15	0	
Abilene Clay Loam	10/5	2/15	3	
Houston Black Clay	6/5	3/15	4	
Miller Clay	8/5	1.5/15	3	
Lake Sand	4/5	.5/15	1	

Note that $\frac{\Delta\epsilon}{\Delta \text{ Moisture \%}}$ is defined as the ratio of the resulting change ($\Delta\epsilon$) in electrical permittivity due to a certain change (Δ Moisture %) in moisture content. Similar definitions apply to the other symbols. The difference, or change, in compaction is $20 N/cm^2 - 5 N/cm^2$ and the difference in curing time is one day. Δ Homogeneity for Tarrent Stoney Clay refers to the difference achieved by sieving the soil.

Table 1-3. The Possible Range of Moisture Content for Which ε is Constant, Provided Compaction and Curing Time Can Vary Arbitrarily.

soil type	range of moisture
Tarrent Stoney Clay	10%
Gila Sandy Loam	2%
Hoban Sandy Loam	5%
Amarillo Fine Sandy Loam	1%
Abilene Clay Loam	5%
Houston Black Clay	10%
Miller Clay	10%
Lake Sand	2%

Note that this table can be interpreted as a worst case error table. If more information were available, the error could be reduced. This additional information would involve the compaction and the curing time (at least, for laboratory samples). Presumably, field samples are thoroughly cured.

shows that the moisture content could be any number within a range of moisture contents, depending on what the compaction and curing time actually are. However, compaction and curing time are restricted to certain limits. If 20 N/cm^2 and 5 N/cm^2 represent extremes in compaction in normal soils and variations in curing time are no greater than those considered here (24 hours), it appears that these variables will cause considerable difficulty only with clay soils, as indicated by Table 1-3.

Ion Concentration

In a series of experiments, Mandel and Jenard (16) showed that salt solutions of 0.02 molarity or less differ negligibly from water in permittivity. Beyond 0.02 M, the permittivity of the solution is about (80 - 10 M), where M is the molarity of the solution (17). What is the range of molarities in soil solutions? Sea water is approximately a 0.16 M solution. Clearly, the soil solution must have a lower molarity than this in arable regions. A 0.16 M solution would have a dielectric constant only 2% less than that of distilled water. Therefore, it seems reasonable to expect that the presence of salt in soil should have little effect on the permittivity. However, one must be cautious with this kind of analysis since soil physics is very complicated and other factors may be at work. For this reason, it is important to use experimental data to

determine the role of various influences on the permittivity of soil.

Temperature

As with ion concentration, the best available experimental results deal with water, not soil and water. Dorsey (18) gives the following equation for the dependence of permittivity on the temperature of water,

$$1\text{-}3 \qquad \varepsilon = 81.47 \left[1 - 4.696 \left(\frac{T - 17}{1000} \right) + 10.2 \left(\frac{T - 17}{1000} \right)^2 \right],$$

where T is in degrees Celsius.

Frequency

The section on soil type included some information about the frequency dependence of the dielectric constant of clays. Recall that below 10^4 Hertz, the permittivity of clays can be very large due to the large surface admittance of the clay particles.

As the frequency increases above two GHz, the permittivity of water declines. According to Eisenberg (19), Figure 1-6 gives the frequency dependence of the dielectric constant of water.

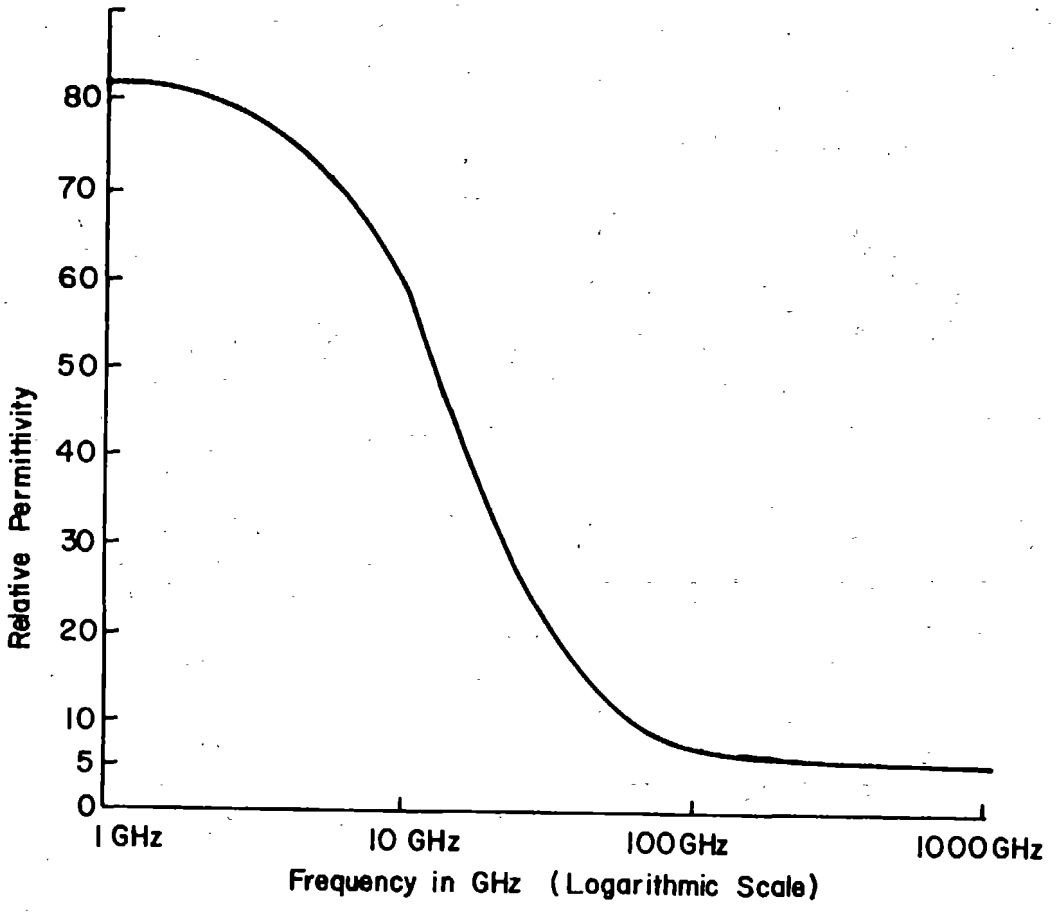

Figure 1-6. Frequency Dependence of the Permittivity of Water.

Conclusions

The conclusions from both of the previous sections are summarized below under their subheadings.

Determination of Soil Moisture Using Dielectric Methods

From the experiments of Anderson and Thorne and Russell it seems very probable that electrode polarization is responsible for many of the observed effects. This implies that resistance variations of the soil with water have a strong influence on what is actually measured. This is a serious limitation since resistance is a function of ion concentration as well as of water. The concentration of ions can vary considerably, even in one location. Fertilizer treatments, for example, can have a large effect on the measured resistance of the soil.

Fletcher claimed that salt had little effect on his results. However, Fletcher used a plaster of Paris block between the electrodes. The plaster of Paris is soluble. In fact, the block is so soluble that it dominates the situation and determines the ion concentration between the electrodes. Therefore, variations in salt content have little effect. Since it is the resistance, or something proportional to it, that Fletcher's method measures, his method does not seem to have any real advantage over resistance techniques.

In conclusion, most of the investigators cited either failed to take electrode polarization into account or to eliminate its effects.

Specific Aspects of Soil Moisture Interaction

The work of Mandel and Jenard, and others, seem to indicate that ion concentration may not be an important factor once electrode polarization is eliminated.

According to the literature, soil type should have an influence on the permittivity. For a given moisture content, clays should have a lower permittivity.

The best frequency range in which to make measurements is probably between 10^4 Hz and 10^9 Hz. Below this range clays can have a very high permittivity which is not related to their moisture content. Above this range the dielectric constant of water begins to fall off. As the permittivity of water decreases, the permittivity of the mixture is influenced more by the properties of the soil. At a few megahertz water has a dielectric constant 20 to 40 times larger than that of most soils whereas at 20 GHz the permittivity of water is only 5 to 10 times as large as that of most soils. Hence the "noise" increases considerably in this region.

CHAPTER 3
PRELIMINARY INVESTIGATION OF THE PERMITTIVITY OF SOILS

Early in the course of this project, it was decided to measure the permittivity of some soils to obtain data not available in the literature. The program of measurements explained a great deal about electrode polarization and made possible the interpretation of many of the previous investigations.

Apparatus and Measurement Procedure

A Wayne-Kerr B601 bridge together with its associated detectors and oscillators was used in this investigation. A circuit diagram is shown in Figure 1-7 and a block diagram in Figure 1-8.

The operation of the bridge was quite simple, consisting of an initial balance with the sample disconnected and a final balance with the sample in the circuit. The capacitance and resistance of the unknown (containing the soil as a dielectric) could be read directly from the balance knobs.

The soil was placed in a sample holder whose capacitance

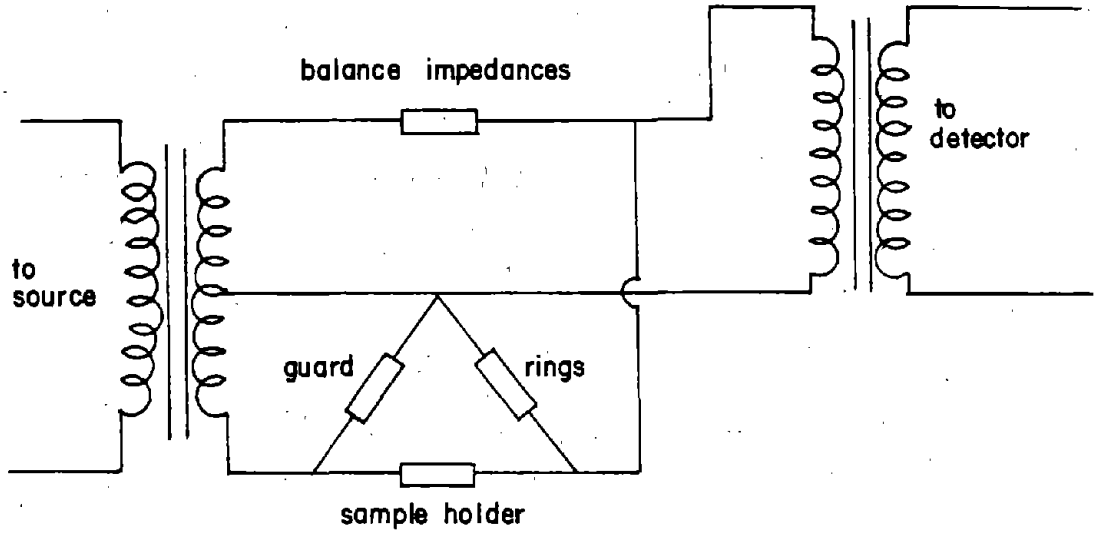

Figure 1-7. Circuit Diagram (0.02 - 2 MHz range)

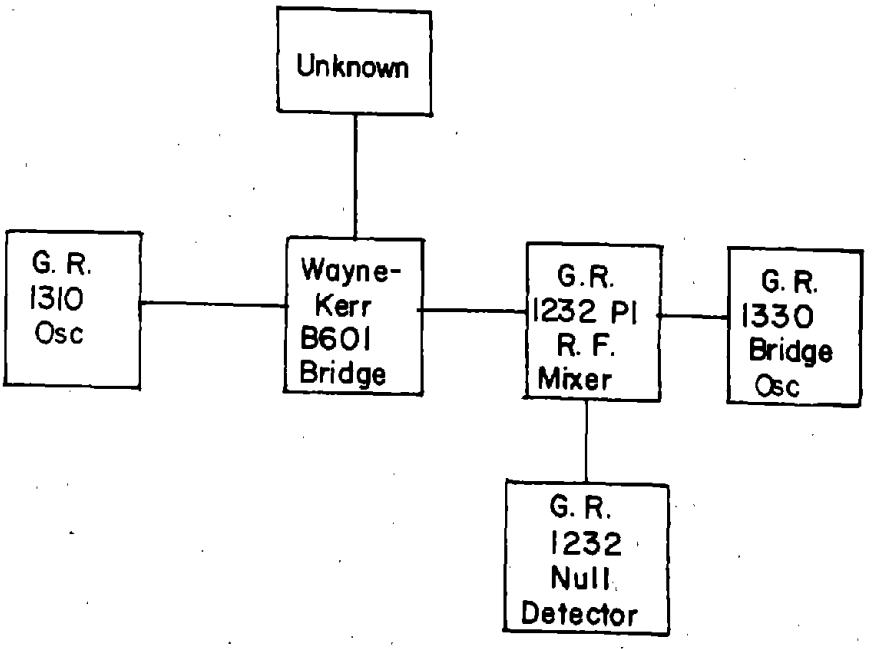

Figure 1-8. Block Diagram (0.02 - 2 MHz range)

and resistance were measured by the bridge. The sample holder underwent modification during the course of the investigation. In the beginning brass was used but it tarnished rapidly. Then a nickel-plated holder was tried which also reacted with the sample. The sample holder illustrated in Figure 1-9 was constructed of stainless steel. It seemed to resist chemical reaction and gave results which agreed with those obtained by using platinum electrodes. The sample holder is a coaxial capacitor with guard rings which serve to eliminate fringing of the electric field of the capacitor. In the absence of electrode polarization, the permittivity of the sample can be calculated by dividing the measured capacitance by the capacitance of the sample holder when the soil is removed leaving air as the dielectric.

Preparation of Samples

In the beginning, preparing soil samples presented a real problem. Samples with uniform moisture content were needed and, in addition, we wanted to be able to mix exactly the desired moisture content. Mixing water and soil directly does not give a uniform mixture. After much trial-and-error the following procedure was chosen. Soil was dried in an oven and placed in a freezer after being weighed. Percentage moisture content is defined as (weight of water)/(weight of dry soil) x 100. Using this definition, the amount of water required was calculated then increased by 5% to cover

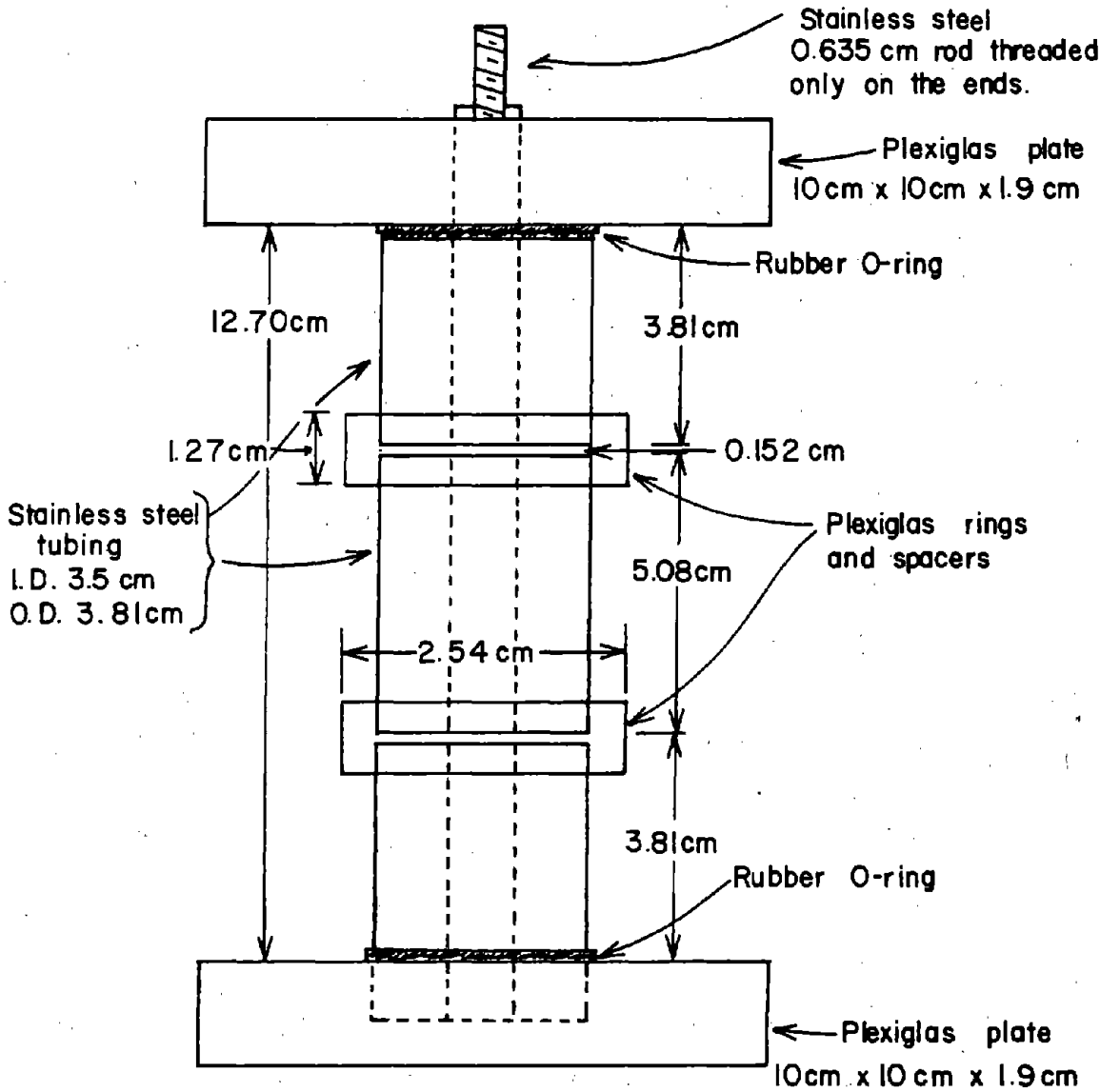

Figure 1-9. Soil Sample Holder (0.02 - 2 MHz range)
Center conductor is 19.05 cm long.

losses. This percentage was determined by experience. The water was measured with a syringe and placed in five-cc aluminum foil containers. The water was taken to the freezer and frozen. After several days, the ice was crushed and scraped into a jar where it was thoroughly mixed with the dry chilled soil. Since the freezer was maintained at -15° to -20°F, very little melting took place. The mixture was then poured into the sample holder. This was removed from the freezer and allowed to come to equilibrium for 12 to 24 hours.

Results and Discussion

The data obtained in this investigation are tabulated in Appendix I. Some representative data are shown in Figures 1-10, 1-11, and 1-12. Several points are worth noting. First, the capacitance is definitely a function of frequency. Second, the values one might infer for the permittivity of the soil-water mixture turn out to be considerably more than eighty in a number of cases. In addition, the addition of salt, even in small amounts, resulted in an increase in the capacitance of the sample. These observations led to the conclusion that electrode polarization was a significant factor in the results. This point will be covered in more detail in the next chapter.

In this series of measurements the values of capacitance occasionally varied with time. Repeated measurements on

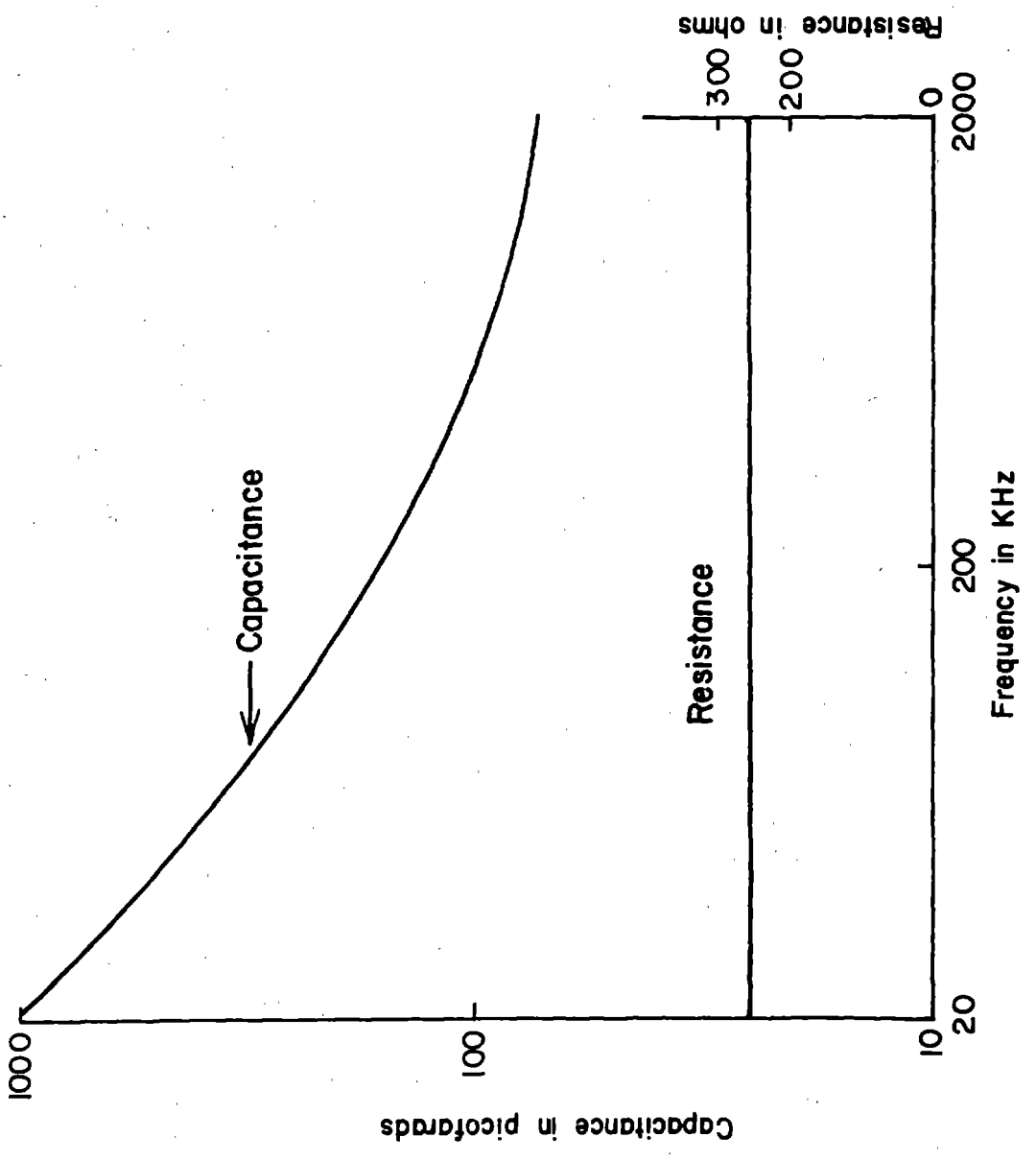

Figure 1-10. Capacitance Vs. Frequency, Crider Clay, 42.8% Moisture Content

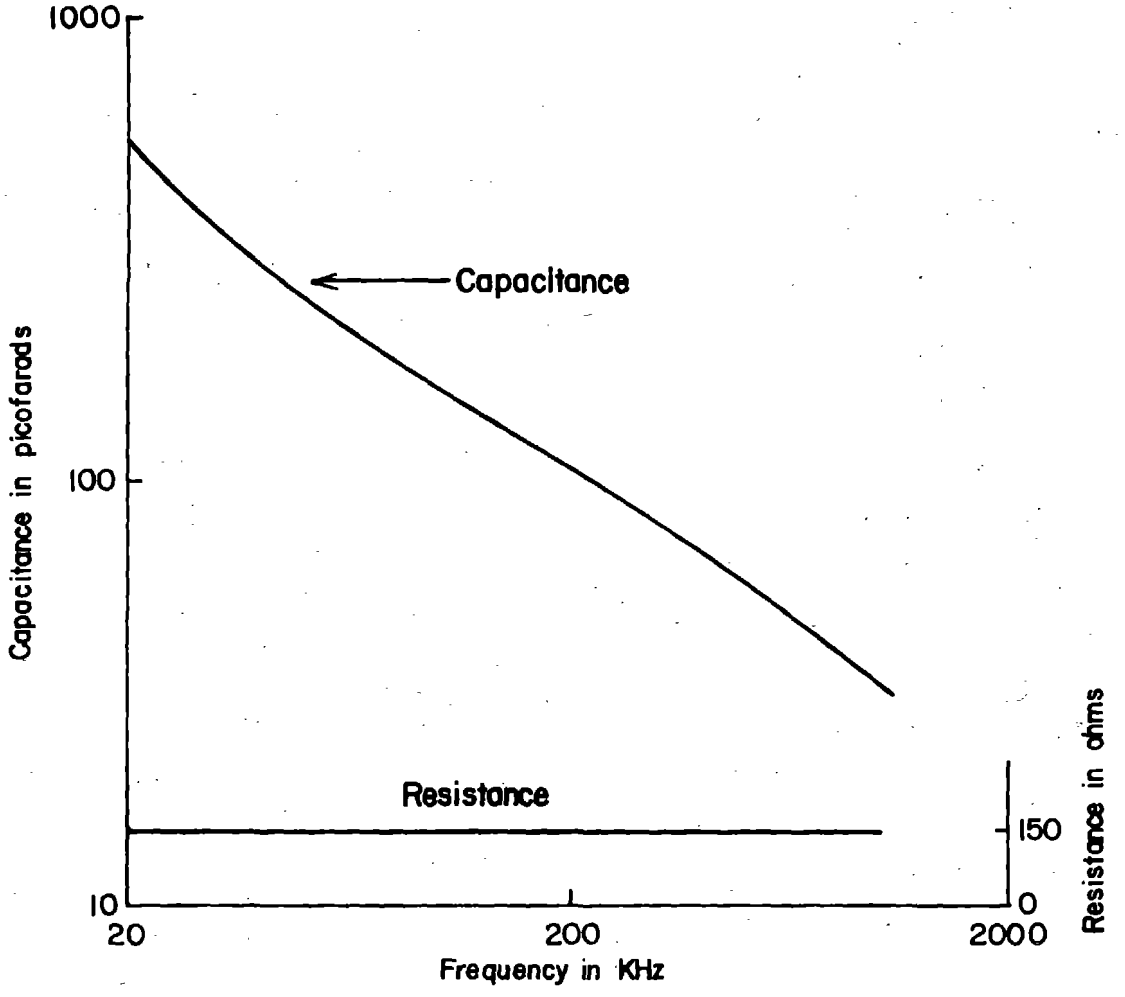

Figure 1-11. Capacitance Vs. Frequency, Muck Soil, 50% Moisture Content

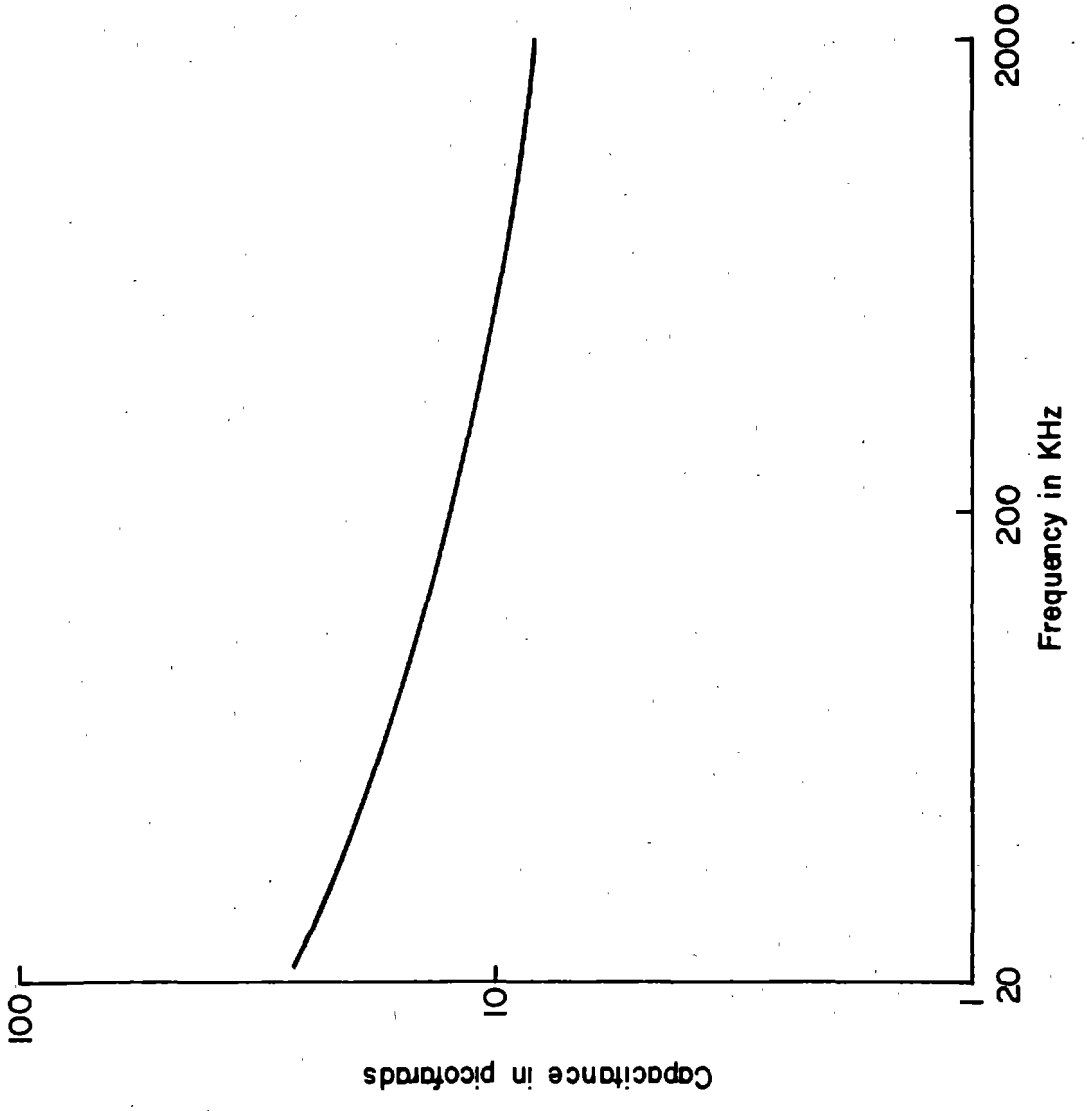

Figure 1-12. Capacitance Vs. Frequency, Sand, 5.8% Moisture Content

the empty sample holder and on commercial capacitors and resistors proved to be completely repeatable and drift free. Eventually it was concluded that the time-varying values were partly due to chemical reactions at the electrodes and partly due to something happening within the sample. The observations are summarized below.

Observations

(1) On muck soils in a brass holder the capacitance increased with time, sometimes by as much as 10% in the course of an hour. Some corrosion of the electrode was evident, but it was not possible to correlate the amount of corrosion with the time duration.

(2) A similar sample holder was nickel plated. The capacitance of Bentonite sample 5 (Bentonite is a clay mineral) decreased about 10% in one hour. A green residue was noted on the electrodes. (It may have been $Ni(OH)_2$ or some similar nickel compound. Many of them are green). In order to look into this a little more deeply, two identical samples of Bentonite wetted to the wilting point were prepared and the following experiments were performed.

Sample 1, Experiment 1

Connect the sample holder to the bridge and balance the bridge. Changing nothing else, simply rebalance the bridge every five minutes.

Sample 2, Experiment 2

Connect the sample holder to the bridge and balance

the bridge. Rebalance the bridge every five minutes but disconnect the power source from the bridge between measurements.

Sample 1, Experiment 3

Sample 1 was allowed to sit for two hours following Experiment 1. Attach it to the bridge and rebalance as often as possible.

Sample 2, Experiment 4

Attach Sample 2 to the bridge and balance the bridge. Rebalance the bridge every five minutes, disconnecting the sample from the bridge between measurements.

The data obtained from the first three experiments are shown in Figure 1-13. In Experiment 4, the capacitance varied little from measurement to measurement. A voltmeter showed a very small voltage across the terminals of the sample holder.

(3) A stainless steel sample holder was made. The capacitance of a Bentonite sample decreased 3% in an hour. No corrosion at all was observed on the electrodes.

(4) The capacitance of silts and sands without much organic matter did not vary with time.

(5) The capacitance of Bentonite samples measured using platinum electrodes decreased about 3% in an hour.

Recall that in each case where the sample holder had an electrical discharge path (through the bridge), the capacitance values changed with the passage of time. This fact, together

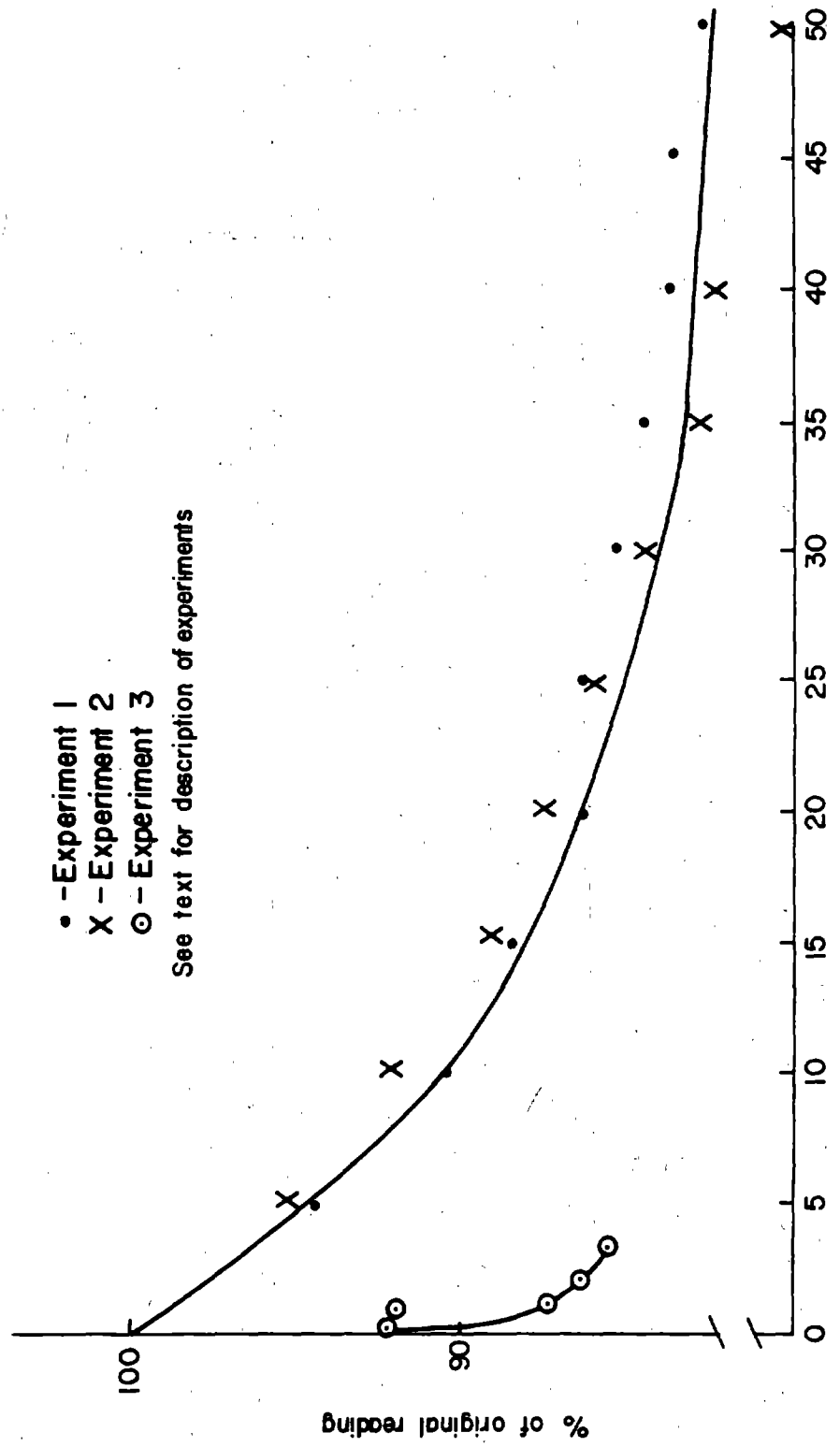

Figure 1-13 Change in Capacitance With Time, of Soil-Filled Test Container.

with the forming of a residue on the electrodes and the existence of a voltage between the electrodes led to the conclusion that electrochemical reactions at the electrodes were responsible for the observed time variation with brass and nickel sample holders. Platinum, however, is reputedly quite inert. Both platinum and stainless steel sample holders gave the same time varying results when they were filled with clays. These results were independent of connection with the bridge. Possible explanations for this phenomenon will be discussed in Chapter 6.

The next chapter deals with electrode polarization. An understanding of this concept aided in interpreting the results of the preliminary investigation and the planning of subsequent investigations.

CHAPTER 4

ELECTRODE POLARIZATION

Introduction

Due to the work of many electrochemists, electrode polarization is now fairly well understood. Many details are not clear, however, and some concepts are controversial. Basically, the explanation is as follows.

When an electrode is inserted into a solution a potential is set up between the electrode and some of the ions in the solution. These ions are attracted to the electrode, but, owing to their finite radius, can approach no closer than a few angstroms. These ions, together with the charge they induce in the electrodes, constitute the "diffuse double layer." Maxwell's laws can be applied to this system, taking into account the facts that the charge is discrete, the ion layer is diffuse, the dielectric constant of the solution varies, etc. When all the parameters are known or can be reliably estimated, the analysis yields results that are in fair agreement with experiment. This kind of agreement has been achieved only for pure solutions where impurities are constantly removed via

a mercury-drop electrode. The addition of just a little impurity (for example, a small amount of gelatin (20)) changes things considerably. One of the best references for the detailed theory of electrode polarization is Bockris and Reddy (17).

A Model for Electrode Polarization

In view of the fact that this model is so difficult to handle analytically and of dubious value for the kind of solutions used in this work, a somewhat simpler model was developed, as discussed in the following. Ions are the main charge carriers in soil. These cannot penetrate the metal electrode so they accumulate at the surface of the electrode. There is also some conductance. The model for these effects is a capacitor in parallel with a resistor. So the sample holder containing soil is modelled by the circuit shown in Figure 1-14. The resistors and capacitors in this model are not fixed-value lumped elements. For the moment, let us assume that R_2 and C_2 are constants. Intuitively, we expect C_1 and R_1 to depend on frequency since these parameters depend on the motion of ions, which have considerable inertia. Schwan (21) used the model shown in the lower half of Figure 1-15. He claimed that the frequency dependence is as shown in the second pair of equations in Figure 1-15. The first pair of equations relates the constants of the two circuits of Figure 1-15. We can check Schwan's estimate of C_1 by

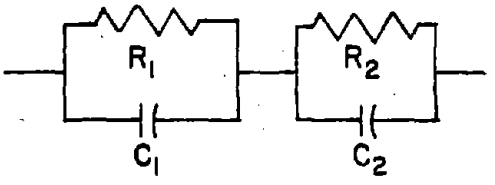

1 $R_1 + 1/j\omega C_1$ = electrode sheath impedance

2 $R_2 + 1/j\omega C_2$ = sample impedance

Figure 1-14. Circuit Model of Sample Holder Containing Soil.

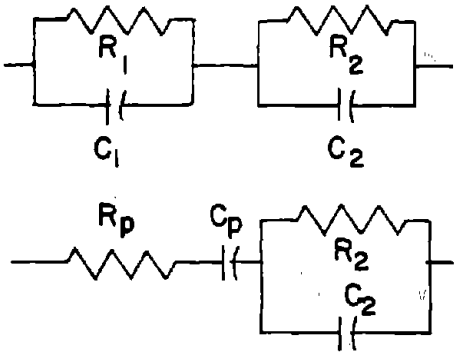

$C_1 = C_p/(1+\omega^2 C_p^2 R_p^2) = 2.5\ 10^6 f^{0.7}\ \mu F$

$R_1 = (1+\omega^2 C_p^2 R_p^2)/\omega^2 C_p^2 R_p^2 \approx 10^6 f^{-0.5}\ \Omega$

$R_p = 10^6 f^{-0.5}\ \Omega$

$C_p = .01$ (or .1) $f^{-0.3}\ \mu F$

Figure 1-15. Schwan's Circuit Model of Filled Sample Holder.

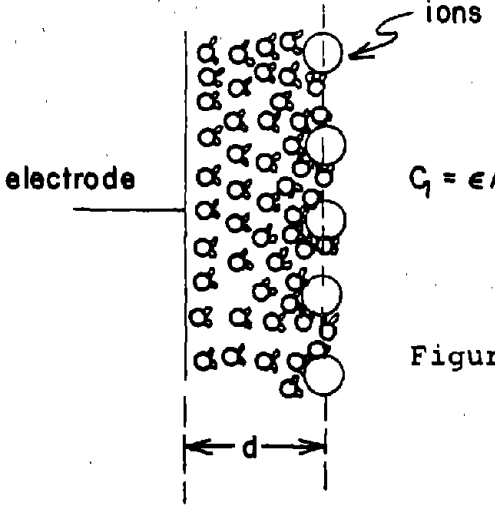

$C_1 = \epsilon A/d = 8.8 \times 10^{-12} \times 10 \times 10^{-4} / 8 \times 10^{-10}$
$= 1.1 \times 10^{-5}$ F

Figure 1-16. Calculation of C_1 Electrode Sheath Capacitance.

making an estimate of our own. C_1 of Figures 1-14 and 1-15 can be thought of as the capacitance of a parallel-plate capacitor. One plate is the metal electrode while the other is the ion sheath which covers the electrode. So $C_1 = \varepsilon A/d$, A being the area of each plate. We will calculate the capacitance on a unit area basis, thus A = 1 cm^2. The separation distance is d. This is about twice the hydrated radius of the ions, or about 8 angstroms. The dielectric is water, but the water is bound, and this reduces its relative dielectric constant to around 10 (17). So $C_1 \tilde{=} 11$ μF. (See Figure 1-16 for this detailed calculation.) A detailed theoretical calculation (17) yields $C_1 = 16\mu F$, independent of ion type and, within certain limits, of ion concentration. Now that the parameters are better understood, the equivalent circuit for electrode polarization may be analyzed. The detailed analysis is in Appendix III. The actual values measured are R and C, the equivalent parallel components of the circuit of Figure 1-14. Expressions for C and R are given in Figure 1-17. In Figure 1-18 R and C are sketched as functions of frequency.

This relationship can be tested by substituting into the equations for C and R reasonable values of R_2 and C_2 and plotting values of C and R versus ω. These should agree with the experimental values which have been given in Chapter 3. Looking at Figure 1-10, R_2 is about 260 Ω and C_2 about 60 pF. The area of the small electrode is about 10 cm^2, so C_1 is approximately $2 \times 10^{-4}\ f^{-.7}$F. Substituting these values into

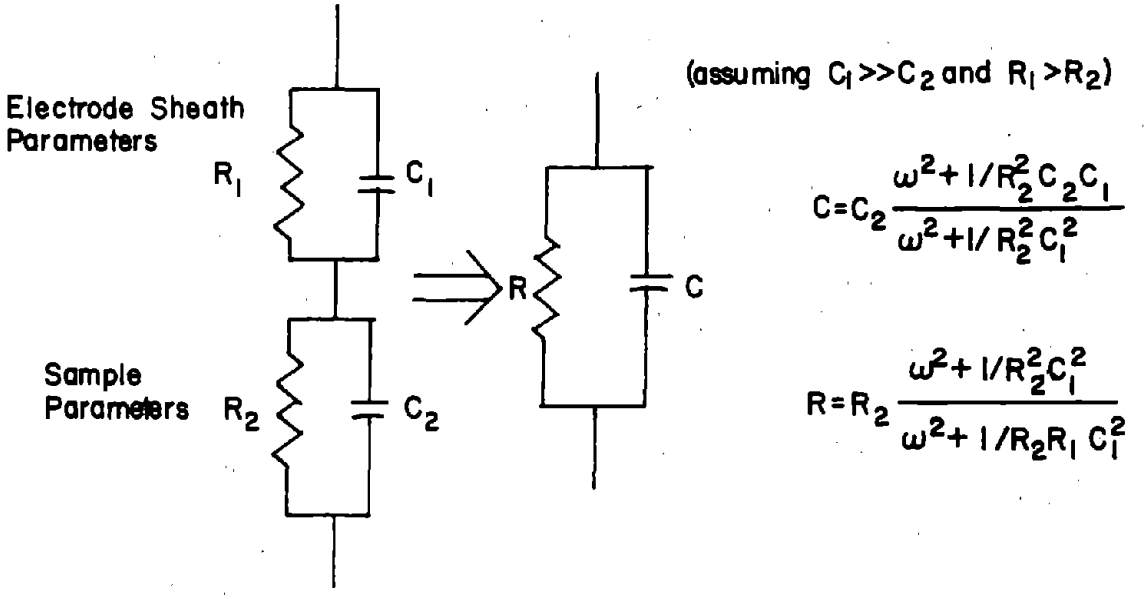

Figure 1-17. Equivalent Parallel R and C For Circuit of Figure 1-14 (Sample Holder Containing Soil).

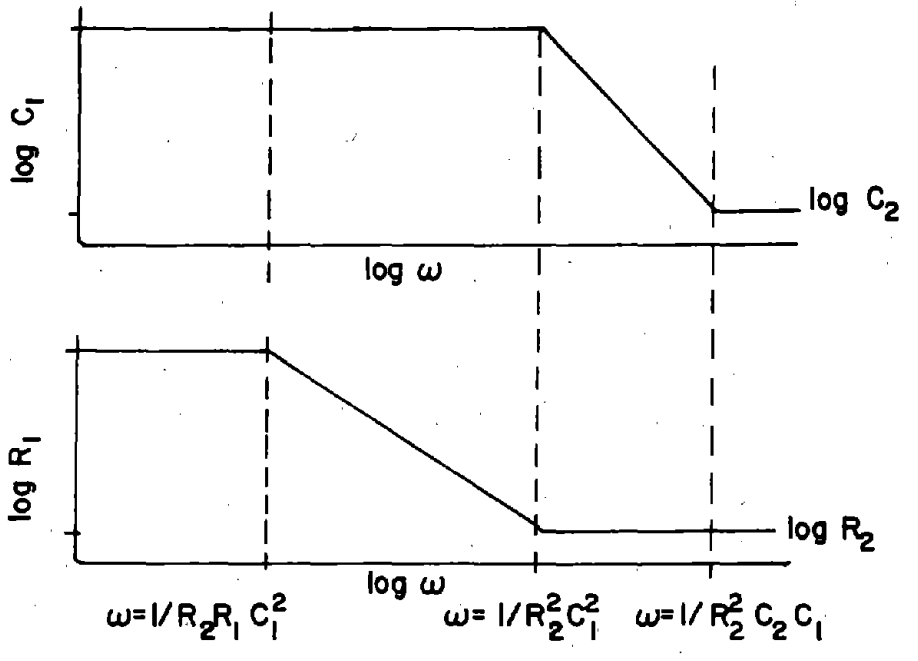

Figure 1-18. R and C of Figure 1-17 as Functions of Frequency.

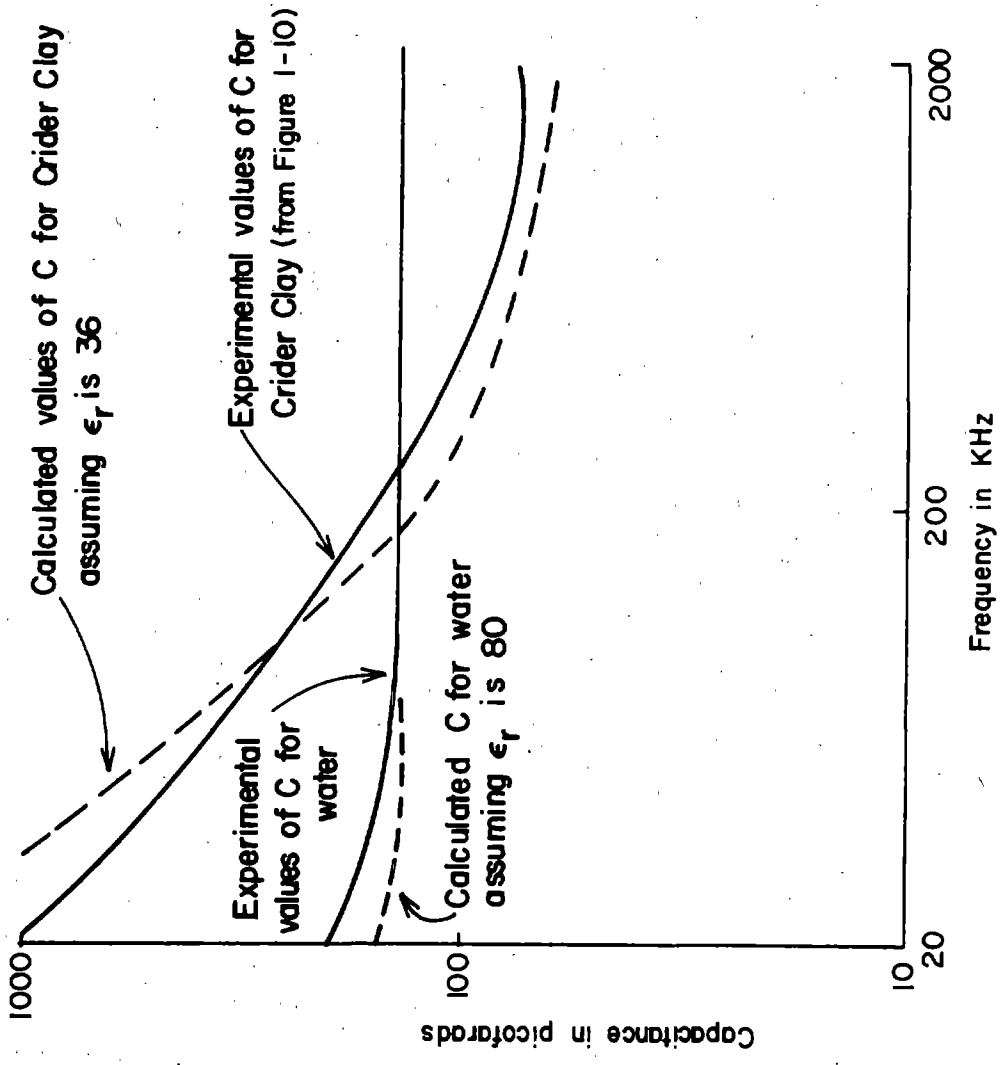

Figure 1-19. Comparison of Experimental and Theoretical Results for C of Figure 1-17.

the equation for C in Figure 1-17, the values plotted on Figure 1-19 are obtained. The agreement is fairly good, considering that C_1 is calculated from basic considerations. Were C_1 a little larger and slightly less dependent on frequency, the agreement would be nearly perfect.

Conclusions

The formula for C derived here allows one to estimate the effect of ion concentration in the soil sample. This concentration strongly influences the conductivity of a sample but should have little effect on its permittivity. Thus, the sample resistance is a function of ion concentration. As the equations of Figure 1-17 show, the overall capacitance, C, of the soil-filled sample holder is a function of the resistance of the soil inside. It appears from the equation for C in Figure 1-17, that each decade drop in the resistance, R_2, shifts the C vs. f curve about 1 1/2 decades in frequency.

CHAPTER 5
INVESTIGATION OF THE PROPERTIES OF SOME SOILS

In order to eliminate the effects of electrode polarization, measurements were obtained at frequencies greater than 2 MHz. In the beginning, a range of 5 to 40 MHz was used, but later it was necessary to use still higher frequencies.

Measurements in the 5 - 40 MHz Range

Apparatus and Measurement Procedure

The instrument used to perform the measurements was a 1606-B General Radio R-F Bridge. In addition to the bridge itself, various oscillators and detectors were required. A schematic diagram is shown in Figure 1-20.

The soil was placed in a coaxial capacitor, shown in Figure 1-21. The capacitor was made of nonmagnetic stainless steel, machined to the same dimensions as a section of General Radio 50-Ω transmission line: outer conductor, 1.587 cm OD, 1.429 cm ID; inner conductor, 0.621 cm DIA. The coaxial capacitor was 12.7 cm in length. At one end of the capacitor a

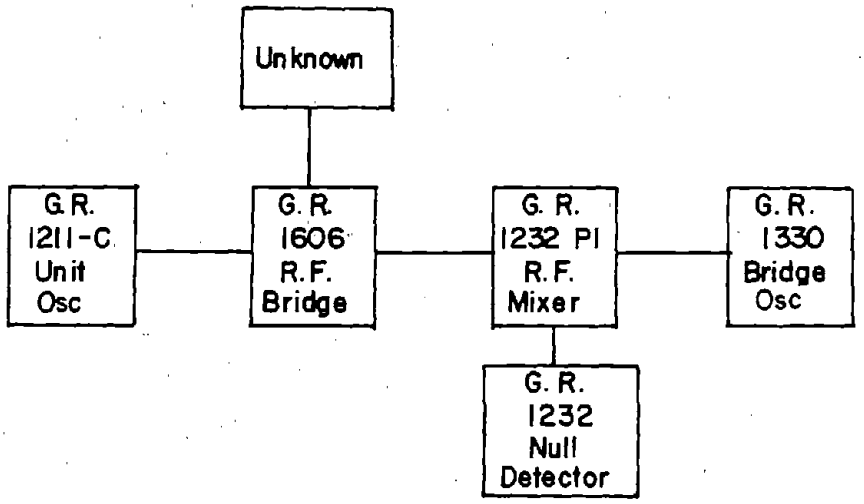

Figure 1-20. Block Diagram (5 - 40 MHz Range)

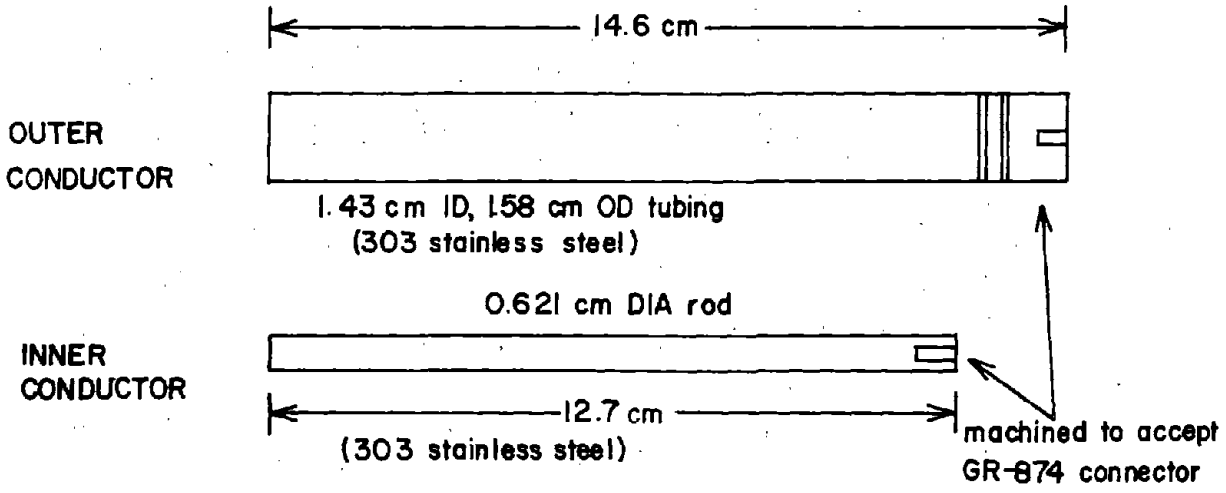

Figure 1-21. Sample Holder (5 - 40MHz Range)

General Radio 874 Locking Connector was attached, enabling the sample holder to be attached directly to the GR 1606-B R-F Bridge.

The procedure for performing the measurements was adapted from the manual for the 1606-B. The instrument has four adjustable dials; two are initial balance controls, and the other two indicate sample resistance and reactance. (The relationship between the measured reactance and the permittivity is stated in the next section.) Measurements were taken at 5 MHz, 10 MHz, 20 MHz, and 40 MHz. After the last measurement, the sample holder was disassembled and the contents emptied into a small container. By using the gravimetric method (see (22) for details of this method) the moisture content of the sample was obtained.

Calculations

The instrument measures the reactance and the resistance of the sample holder. The permittivity and conductivity can be calculated by using these quantities, and in this section the equations used to calculate the permittivity are set forth. Also, a test case using water was worked to show that the equations do indeed yield the permittivity.

Admittance. The first step is to convert the series resistance, R, and reactance, X, (impedance) to the equivalent parallel capacitance, C, and conductance, G, (admittance). The measured quantities are R and Xf where f is the frequency in MHz. The desired quantities are C and G. Let D denote -Xf.

$$1\text{-}4 \qquad R - j\frac{D}{f} = \frac{1}{G + j\omega C}$$

$$1\text{-}5 \qquad C = \frac{-D}{f^2R^2 + D^2}\,\frac{1}{2\pi\ 10^6};\quad G = \frac{Rf^2}{f^2R^2 + D^2}$$

In the above equations, the unit of R and X is ohms, that of C is farads, and that of G is mhos.

Fringing Capacitance Correction. In this sample holder there is a small amount of fringing capacitance which must be subtracted. A computer program was written to calculate the fringing capacitance, which was found to be independent of the dielectric constant and equal to about 0.38 pF. This value is simply subtracted from the calculated capacitance. Further details on this calculation are given in the second part of this chapter.

Permittivity Calculation. Next, it is necessary to find a relationship between permittivity and capacitance. If the capacitor could be treated simply as a lumped capacitor, permittivity could be calculated simply by dividing the measured capacitance by the capacitance of the empty sample holder. Even though this gives good results, for a more exact calculation it is necessary to take into account the distributed nature of the capacitance. The sample holder can be treated as a section of transmission line terminated in an open circuit. The input admittance of the sample holder is

$$1\text{-}6 \qquad Y_{IN} = Y_0\,\frac{Y_L + Y_0 \tanh \gamma\ell}{Y_0 + Y_L \tanh \gamma\ell}$$

where

Y_{IN} = input admittance,

Y_0 = characteristic admittance, $\sqrt{\frac{j\omega C_\ell + G_\ell}{j\omega L_\ell + R_\ell}}$,

Y_L = load admittance; for open circuit $Y_L = 0$,

γ = propagation constant, $\sqrt{(j\omega C_\ell + G_\ell)\ (j\omega L_\ell + R_\ell)}$,

C_ℓ = capacitance per unit length,

L_ℓ = inductance per unit length,

R_ℓ = resistance per unit length,

G_ℓ = conductance per unit length.

For an open circuit load,

1-7 $$Y_{IN} = Y_0 \tanh \gamma\ell$$

If $\tanh \gamma\ell \approx \gamma\ell$, then

1-8 $$Y_{IN} = Y_0 \gamma\ell = j\omega C + G.$$

One might reasonably ask whether $\gamma\ell$ is sufficiently small to warrant the assumption that $\tanh \gamma\ell \approx \gamma\ell$. Recall that

1-9 $$\gamma = \sqrt{(j\omega L_\ell + R_\ell)\ (j\omega C_\ell + G_\ell)}.$$

C_ℓ is determined by geometry and permittivity:

1-10 $$C_\ell = \frac{2\pi\epsilon}{\ell n\ b/a}$$

where

ϵ = permittivity,

b = dia. of outer conductor,

a = dia. of inner conductor.

Evaluating C,

1-11 $$C = \ell C_\ell = 0.667\epsilon_r \text{pF}.$$

We know that for an empty sample holder,

1-12 $$\gamma = j\omega \sqrt{LC} = j\ \omega/3 \times 10^8,$$

($\epsilon_r = 1$ for an empty sample holder)

1-13 $$LC = \frac{1}{9 \times 10^{16}},$$

1-14 $$L = 1.66 \times 10^{-7} \text{ Henry.}$$

G_ℓ is determined by the conductivity of the soil and geometry.

1-15 $$G_\ell = \frac{2\pi\sigma}{\ell n\ b/a}, \quad G = 7.57\sigma.$$

R is the series resistance of the transmission line. Since the sample holder is made of stainless steel there may be some reason to doubt that R is small. The resistance per unit length (R_ℓ) can be calculated by using the skin depth approximation. See Figure 1-22.

1-16 $$R_\ell = \frac{\rho}{A}$$

where

ρ = the resistivity of the material,

A = the cross sectional area.

1-17 $$A = \delta 2\pi a$$

where

a = the diameter of the inner conductor, 0.063 meter.

1-18 $$\delta = \left(\frac{2\rho}{\omega\mu}\right)^{\frac{1}{2}}$$

where

ω = the frequency in radians/second,

μ = the magnetic permeability, $4\pi \times 10^{-7}$ Henry meter,

ρ = resistivity, 0.72×10^{-6} ohm-meter.

So $R_\ell = 4.25 \times 10^{-6} \sqrt{f}$,

where

f = frequency in Hertz.

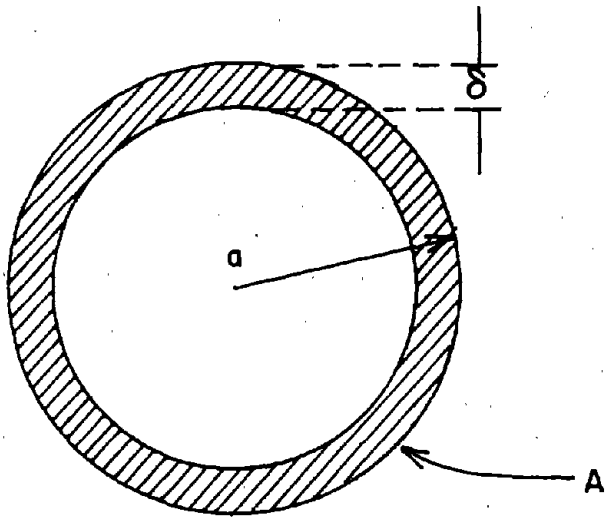

a = radius of solid conductor

δ = skin depth

A = cross-sectional area supporting conduction

Figure 1-22. Skin Depth of Conductor.

Comparing R_ℓ to ωL_ℓ

1-19 $$\omega L_\ell = f \times 1.045 \times 10^{-6},$$

1-20 $$R_\ell = \sqrt{f} \times 4.25 \times 10^{-6}.$$

Hence, $\omega L_\ell \approx 1.0$ while $R_\ell \approx 0.0042$ at approximately 1 MHz.

It can be concluded, therefore, that R is negligible compared to ωL. Thus $\gamma\ell$ can be expressed as

1-21 $$\gamma\ell = \sqrt{j\omega L\ (j\omega C + G)}.$$

Note that this is a complex number. Hence, when calculating $\tanh \gamma\ell$, the formula for complex arguments must be used.

1-22 $$\tanh(a + jb) = \frac{\sinh(a) + j\sin(b)}{\cosh(a) + j\cos(b)}.$$

Using this formula, $\tanh \gamma\ell$ can be expressed as a series expansion in terms of the real and imaginary parts of $\gamma\ell$. Finally, Y_{IN} can be expressed as a series expansion. Keeping two terms,

1-23 $$Y_{IN} = j\omega C \left[1 + \frac{\omega^2 LC}{3}\right] + G\left[1 + \frac{2\omega^2 L}{3}\left(C - \frac{LG^2}{5}\right)\right].$$

Measurements on Water. As a test of the correction formulae, measurements were performed on the sample holder using water as the dielectric. The results are summarized in Table 1-4.

Table 1-4. Measured Permittivity of Water.

Frequency in MHz	Relative Permittivity
Distilled Water, Conductivity = 0.003 Mho/meter	
5	80.2
10	79.5
20	78.0
40	75.5
0.005% NaCl Solution, Conductivity = 0.02 Mho/meter	
5	79.5
10	77.0
20	78.0
40	76.5
0.01% NaCl Solution, Conductivity = 0.03 Mho/meter	
5	81.3
10	81.3
20	81.5
40	75.0
0.02% NaCl Solution, Conductivity = 0.05 Mho/meter	
5	80.8
10	82.3
20	83.0
40	75.0
0.1% NaCl Solution, Conductivity = 0.2 Mho/meter	
5	88.5
10	80.4
20	93.0
40	88.2

Results

The complete results for the capacitance, resistance, permittivity, and conductivity of several different soils, for various moisture contents, and for the entire range of frequencies, are tabulated in Appendix I. Figures 1-23, 1-24, and 1-25 illustrate some representative data. The samples used to obtain the data were prepared according to the procedure outlined in Chapter 3. Due to the smaller size of the sample, only four to eight hours were required for the samples to come to thermal equilibrium. These results are discussed in Chapter 6.

Measurements in the 250 - 450 MHz Range

After the measurements on the laboratory-prepared samples were completed, it seemed logical to attempt to measure undisturbed samples from the field. Unfortunately, it was not practical to do this using the equipment for the 5 - 40 MHz range. In order to obtain the required minimum capacitance, it was necessary to use a sample holder which was 12.7 cm in length Soil samples of this length could not be forced into the sample holder without binding, compaction, and unreliable contact.

Good results could be obtained, however, for soil samples of one centimeter in length. Samples of this length were suitable for use in the 250 - 450 MHz range. In addition, it would be helpful to have information on the permittivity in this higher frequency range. For these reasons, it was decided to

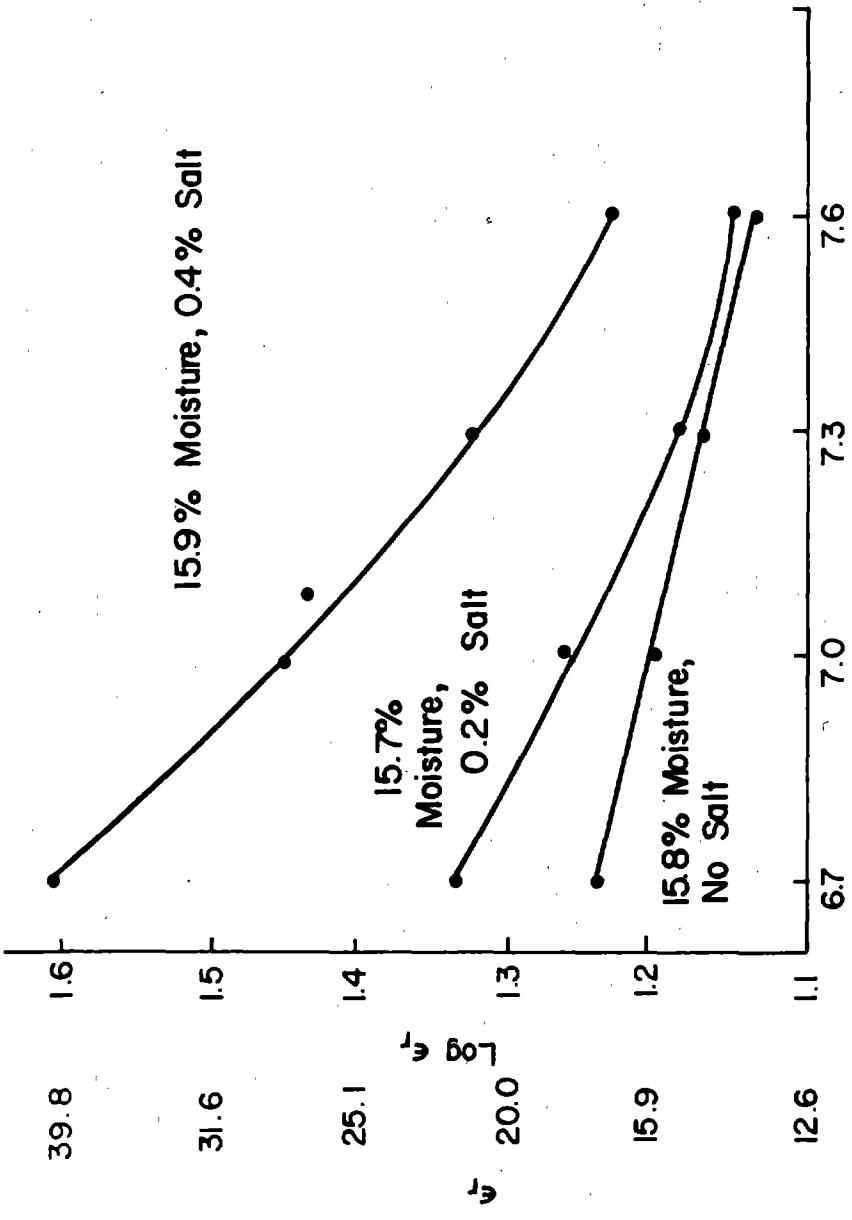

Figure 1-23. Log ϵ_r Vs. Frequency for Three Miami Silt Loam Samples.

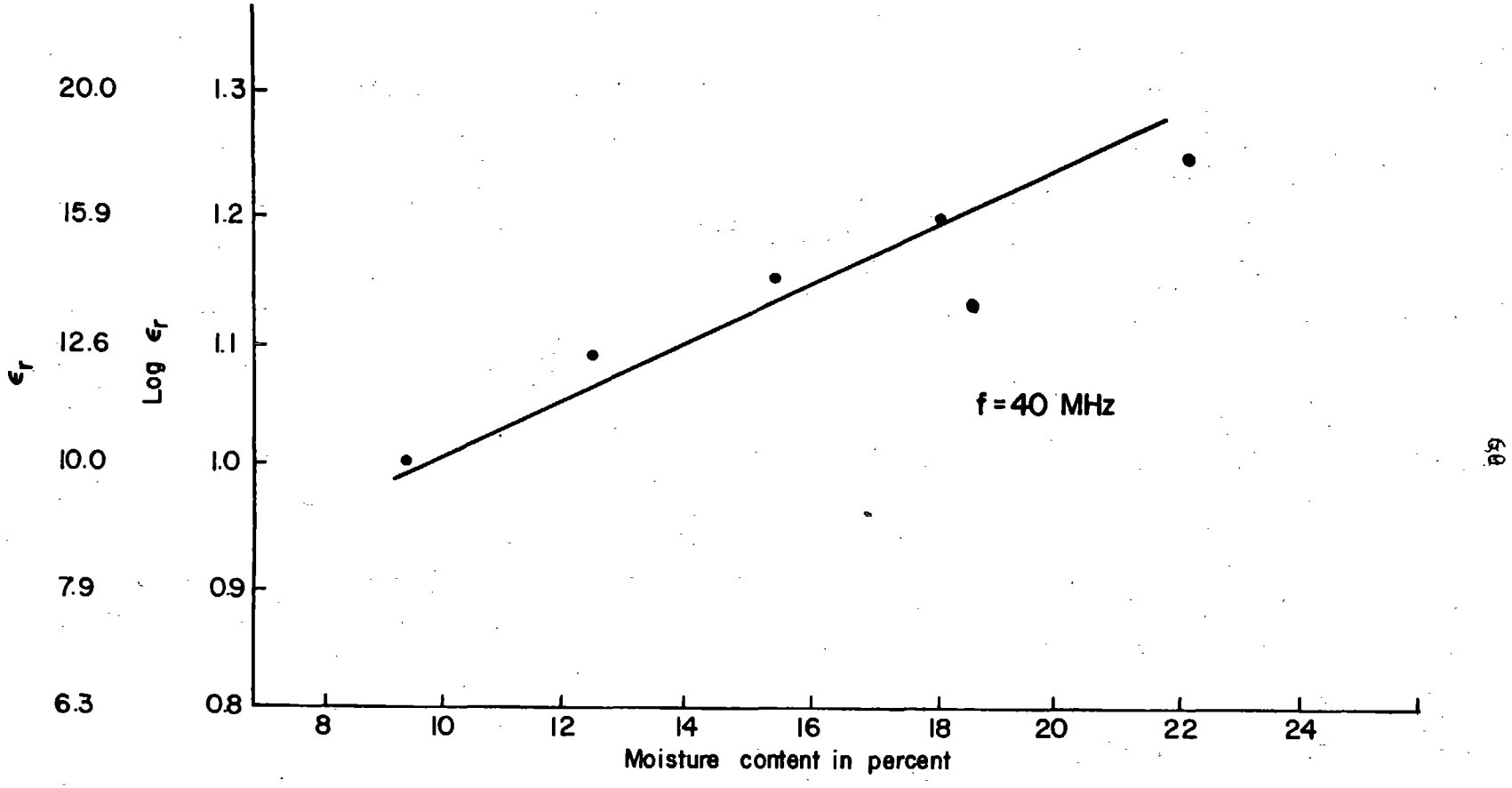

Figure 1-24. Log ϵ_r Vs. Moisture Content, 0.2% Salt Solution (Miami Silt Loam).

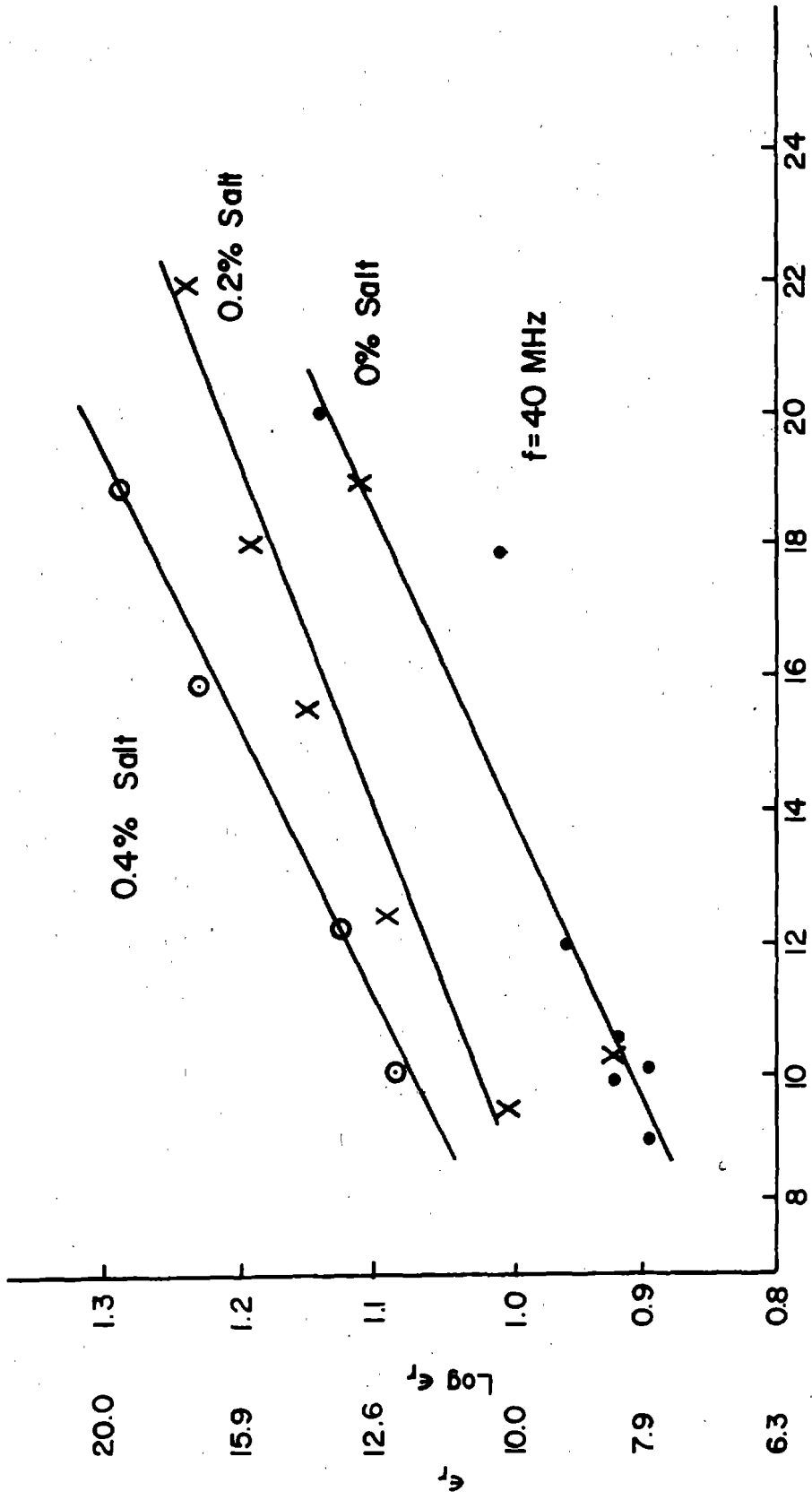

Figure 1-25. Effect of Salt on ε_r of Miami Silt Loam.

perform measurements on laboratory-prepared samples and field samples in the frequency range of 250 -450 MHz.

Apparatus and Measurement Procedure

A General Radio 1602-B Admittance Meter was used in this investigation. A block diagram of the instrument, together with its associated oscillators and detectors is shown in Figure 1-26. The Admittance Meter has a four-port junction at its center. Connected to the appropriate ports are an oscillator, a known conductance, a known susceptance, and the unknown. Three loops inside the junction are connected to the detector, which can be nulled by varying the coupling of these loops. When a null has been achieved, the coupling of the loops is related to the input admittance of the unknown port in a known fashion.

The Admittance Meter is a particularly easy instrument to use. The following procedure was adapted from the manual for the instrument. To begin, the source oscillator is set to the desired value, and the auxiliary oscillator is set to obtain maximum deflection on the detector. Occasionally, it is necessary to observe the mixer current. If the mixer current is too low the coupling loop on the auxiliary oscillator can be adjusted to give better results. After the susceptance stub is set according to the frequency, then the sample holder is attached to the "unknown" port. The three levers attached to the coupling loops are adjusted to obtain a null in the detector, and the positions of the levers are recorded.

Several points deserve attention. First, it is important

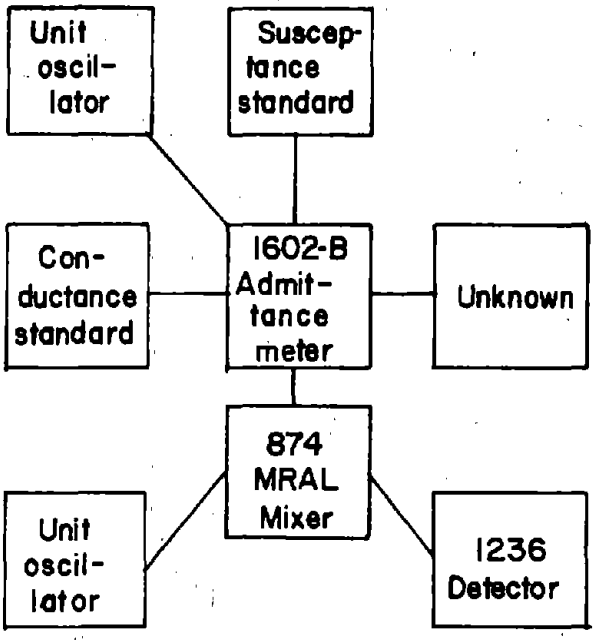

Figure 1-26. Block Diagram (250 - 450 MHz Range)

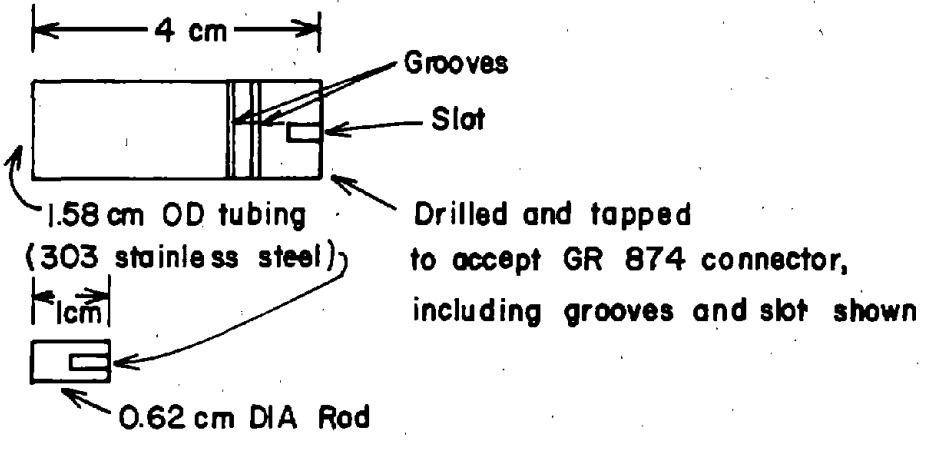

Figure 1-27. Sample Holder (250 - 450 MHz Range).

that the source oscillator be set as accurately as possible, and that the frequency of the oscillator be checked from time to time by means of a slotted line, unless the oscillator is known to be highly stable in frequency. Small errors in frequency cause errors in the final result. Secondly, the susceptance stub should be set according to the marks on the stub. The procedure given in the GR manual for setting the stub when the frequency is unknown leads to errors and should not be used.

Calculations

Five sets of calculations are performed on the data to obtain the permittivity: a line length correction, a finite sample length correction, a fringing capacitance correction, an optional electrode polarization correction, and a calculation of the permittivity from the sample input admittance.

Line Length Correction. The Admittance Meter measures the input admittance at the junction, but the sample is approximately 6 cm away from the junction. The equation which relates the input admittance at one point in a lossless line to the input admittance at another point is

$$Y_{IN\ 1} = Y_0 \frac{Y_{IN\ 2} - j\ Y_0 \tan \beta \ell}{Y_0 - j\ Y_{IN\ 2} \tan \beta \ell}, \tag{1-24}$$

where

$Y_{IN\ 1}$ = input admittance at the desired point,

$Y_{IN\ 2}$ = input admittance at the known point,

Y_0 = characteristic admittance of the line,

β = phase constant,

ℓ = distance between point 1 and point 2.

Note that Y_0 and β are characteristics of the transmission line and, therefore, known. $Y_{IN\ 2}$ is measured by the Admittance Meter.

In order to use the formula it is necessary to determine ℓ, which is the distance between the junction and the sample. This can be accomplished by attaching a known admittance to the "unknown" port. The known admittances used in this investigation were GR W03 (open circuit) and GR WN3 (short circuit) terminations. The use of these terminations not only simplifies the formulae but also provides a check on the error.

The simplified formulae for line length corrections are

(short circuit) $Y_{IN\ 2} = Y_0/\tan \beta\ell$,

(open circuit) $Y_{IN\ 2} = Y_0 \tan \beta\ell$.

Note that the product of the measured input admittances for short circuit and open circuit is just Y_0^2. Table 1-5 shows the data collected using WN3 and W03 terminations as well as the calculated value of ℓ and the estimated error. Knowing ℓ, one can calculate the input admittance at the sample holder by using Equation 1-24.

Finite Length of the Sample Holder. In the section on measurements in the 5 - 40 MHz range, equations were derived to relate the input admittance to the capacitance and conductance per unit length of the sample holder filled with soil. The relationships were

$$1\text{-}25 \qquad C = \frac{\text{Im}\ [Y_{IN}]}{\left(1 + \frac{\omega^2 LC}{3}\right)}$$

Table 1-5. Line Length Correction for 250-450 MHz Measurements

Frequency in MHz	Measured Admittance W03	WN3	Calculated Length (Meters)	Estimated Error
250	j 10.5	-j 39.0	0.0593	1.18%
300	j 13.0	-j 31.4	0.05895	1.02%
350	j 15.8	-j 25.5	0.0589	0.36%
450	j 23.3	-j 17.0	0.0595	0.56%

$$1\text{-}26 \qquad G = \frac{\mathrm{Re}\ [Y_{IN}]}{\left(1 + \frac{2\omega^2 L}{3}\ \left[C - \frac{LG^2}{5}\right]\right)}$$

These relations are also useful in the present calculations.

Fringing Capacitance. The correction for fringing capacitance mentioned in the section on measurements in the 5 - 40 MHz range is explained in more detail here. To begin, let us consider what fringing capacitance is and how it might affect the results. Looking at the sample holder, one can see that it is a coaxial capacitor. Because the capacitance per unit length of coaxial capacitors is well known, and since the length of the sample holder is also known, one might be tempted to conclude that the capacitance of the sample holder is just its length times the capacitance per unit length. This, however, is not the case. In fact, the capacitance of the sample holder is greater and the excess is termed the fringing capacitance. The reason for the discrepancy is that the formula for the capacitance per unit length was derived for an infinitely long capacitor. Since the sample holder is finite in length the uniformity of the infinite capacitor is gone. At the edge of the capacitor there are fringing fields which give rise to the fringing capacitance. See Figure 1-28. The calculation of the fringing capacitance consists of calculating the capacitance of the entire sample holder and comparing it to the length of the sample holder multiplied by the capacitance per unit length calculated for the case of an infinite capacitor. The calculation of the actual capacitance is accomplished by using the following relationships.

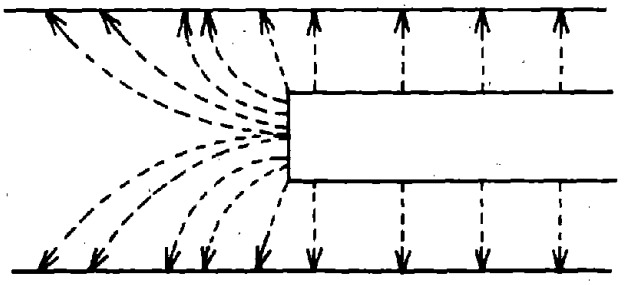

Electric field intensity vector (----------+)

Figure 1-28. Fringing Field.

1-27 $$C = \frac{q}{\Delta\phi}$$

where

C = capacitance,

q = charge on the electrode,

$\Delta\phi$ = voltage difference between electrodes.

Gauss' law yields

1-28 $$\oint \varepsilon \vec{E} \cdot \vec{dS} = q$$

where

$\vec{E}$ = electric field intensity,

$\vec{dS}$ = incremental surface area,

S = any surface which encloses q.

Recall that

1-29 $$\vec{E} = -\nabla\phi.$$

Finally, ϕ satisfies the Laplace equation in charge-free regions:

1-30 $$\nabla^2\phi = 0.$$

Using a computer one can solve the Laplace equation by means of finite difference methods. (See, for example, Ramo, Whinnery, and Van Duzer (23).) The Laplace equation becomes a difference equation which can be expressed as

1-31 $$\phi_{i,j} = \frac{\phi_{i+1,j} + \phi_{i-1,j} + \phi_{i,j+1} + \phi_{i,j-1}}{4}$$

This difference equation is solved for different assumed values of permittivity in the sample holder. The potential found in this way is substituted into Equation 1-29 and the fringing

capacitance calculated. The result found was that the fringing capacitance was equal to about 0.38 pF, independent of the permittivity of the soil in the sample holder. One of the programs used to calculate the fringing capacitance is given in Appendix 4.

Electrode Polarization Correction. This correction can be considered optional since it produced only small changes in the data. Recall the formula for measured capacitance derived in Chapter 4 and given in Figure 1-17,

$$C = C_2 \frac{\omega^2 + \dfrac{1}{R_2^2 C_2 C_1}}{\omega^2 + \dfrac{1}{R_2^2 C_1^2}}.$$

One can solve for C_2,

1-32 $$C_2 = C - \frac{C_1 - C}{\omega^2 R_2^2 C_1^2}.$$

For $C_1 >> C$,

1-33 $$C_2 = C - \frac{1}{\omega^2 R_2^2 C_1}.$$

Calculation of the Permittivity. Once the capacitance of the sample holder filled with soil has been found, the permittivity can be found simply by dividing the sample holder capacitance by the capacitance in air, 0.667 pF.

1-34 $$\epsilon_r = C_2 / 0.667 \times 10^{-12}$$

Test of Formulae. To insure the correctness of the formulae used to calculate the permittivity and to correct for

various effects, measurements were performed on materials with known dielectric constants: water, methyl alcohol, and plexiglas. The results are listed in Table 1-6. A computer program, written to obtain the permittivity can be found in Appendix IV.

Table 1-6 Measured Permittivity of Water, Methanol, and Methyl Methacrylate.

Relative permittivity of water (250 MHz, 20° C)

Sample Holder	Measured Permittivity	Generally Accepted Value for Permittivity
#1	80.5	80.3
#2	79.6	80.3
#3	80.5	80.3

Relative permittivity of methanol (250 MHz, 20° C, Sample Holder #1)

Measured Permittivity	Generally Accepted Value for Permittivity
32.2	32.2

Relative permittivity of methyl methacrylate (Sample Holder #1)

Frequency in MHz	Measured Permittivity	Generally Accepted Range of Values for Permittivity
250	2.58	2.2 - 3.2
300	2.52	2.2 - 3.2
350	2.41	2.2 - 3.2
450	2.39	2.2 - 3.2

Sample Preparation

In this investigation three different kinds of soil samples were prepared: laboratory-prepared samples, laboratory-prepared samples with salt, and samples from the field. The laboratory-prepared samples were prepared according to the procedure outlined in Chapter 3. When salt was required it was added to the soil before the ice was mixed with the soil. The salt content is expressed as a percent soil solution, e.g., a twelve gram soil sample with three grams of water added and 0.03 gram of salt would be a sample with 25% moisture content, and a 1% salt soil solution. In other words, the soil is wetted with a 1% salt solution.

As the name implies, field samples were taken directly from the field, specifically, three pits dug on the Purdue University Horticulture Farm. To obtain a sample, one removed approximately three inches of soil from one face of the pit and inserted the outer conductor of the sample holder into the side of the pit. Then the outer conductor, together with the soil inside it, was removed, packed in water-proof bags, and taken immediately to the laboratory. In the laboratory a hole was drilled in the center of the plug of soil, and the center conductor was carefully inserted, then tamped in to insure good contact with the electrodes. Finally, a special tool was inserted to remove excess soil so that the soil sample was precisely one cm in length. A rubber stopper was placed on the end of the outer conductor to prevent evaporation. Then, the measurements were performed immediately, using the Admittance Meter.

Unfortunately, the very wet conditions which prevailed during the investigation forced modification of the procedure. One pit remained flooded for the entire season and was not used. Samples from the other two pits were at or near field capacity of moisture. Although these data were useful, the decision was made to test a greater range of moisture content. The procedure, therefore, was modified.

A three-inch diameter brass pipe was inserted a few inches into the face of the pit. This was taken to the Laboratory where the soil plug was removed and sliced into 1.5 cm thick slabs. These were placed on a pressure plate and dried to the appropriate moisture content. (This is a standard technique. See, for example, (24).) Once the slab was at the desired moisture content, the outer conductor was inserted into it, and the procedure thereafter was identical to the one explained previously.

The results are tabulated in the third section of Appendix I. Figures 1-29 to 1-34 illustrate the relationship between moisture content and the logarithm of permittivity. Figure 1-35 shows the frequency dependence of the permittivity. Some properties of the soils used in this investigation are summarized in Appendix II.

RESULTS

Several observations can be made about the data.

1. The log of the permittivity increased approximately linearly with increasing moisture content.
2. The salt content does not seem to affect the results.
3. In this frequency range the permittivity has very little dependence on frequency, although the clay soil seems to exhibit more dependency than the others.

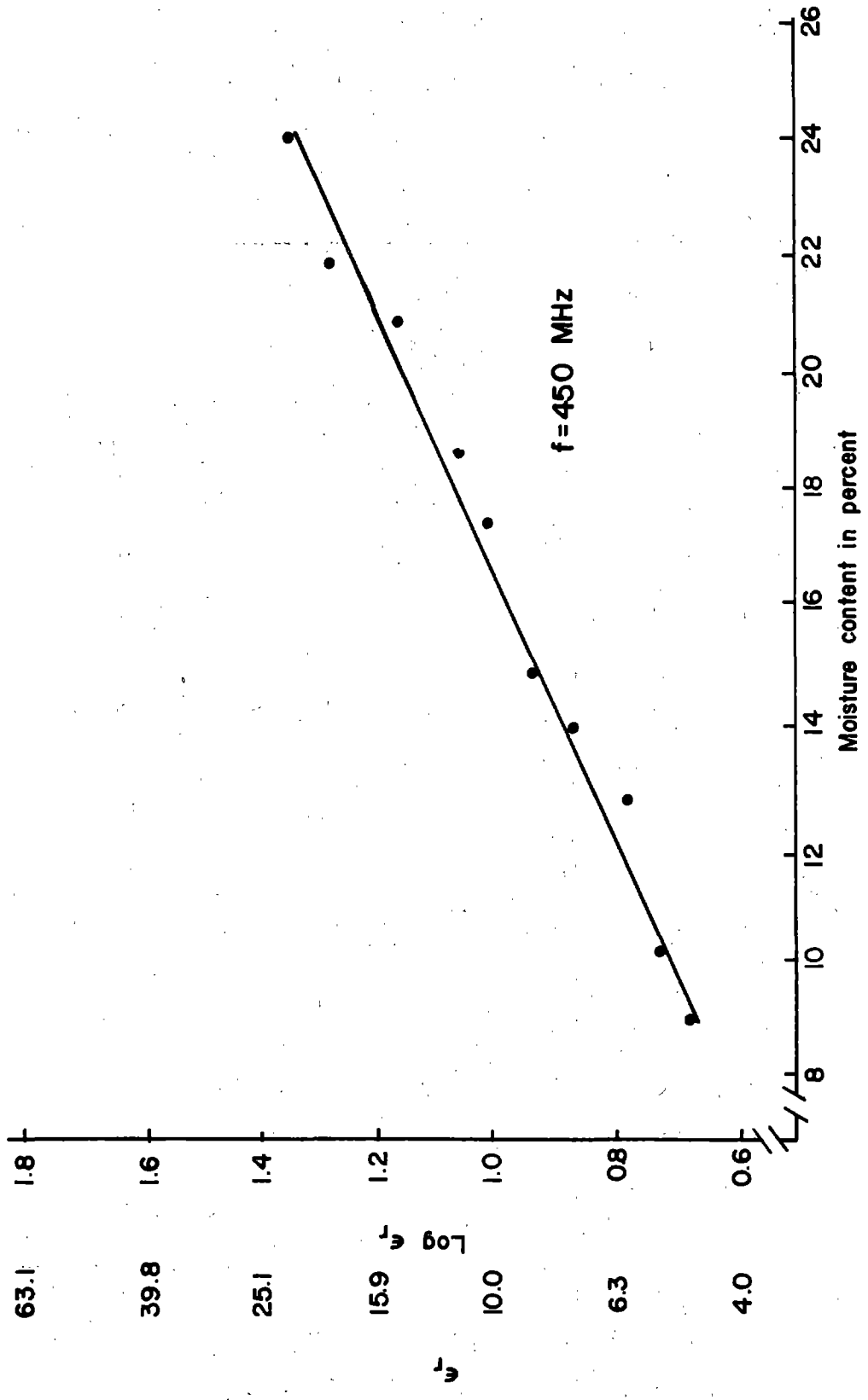

Figure 1-29. ϵ_r Vs. Moisture Content for Miami Silt Loam, Laboratory Prepared.

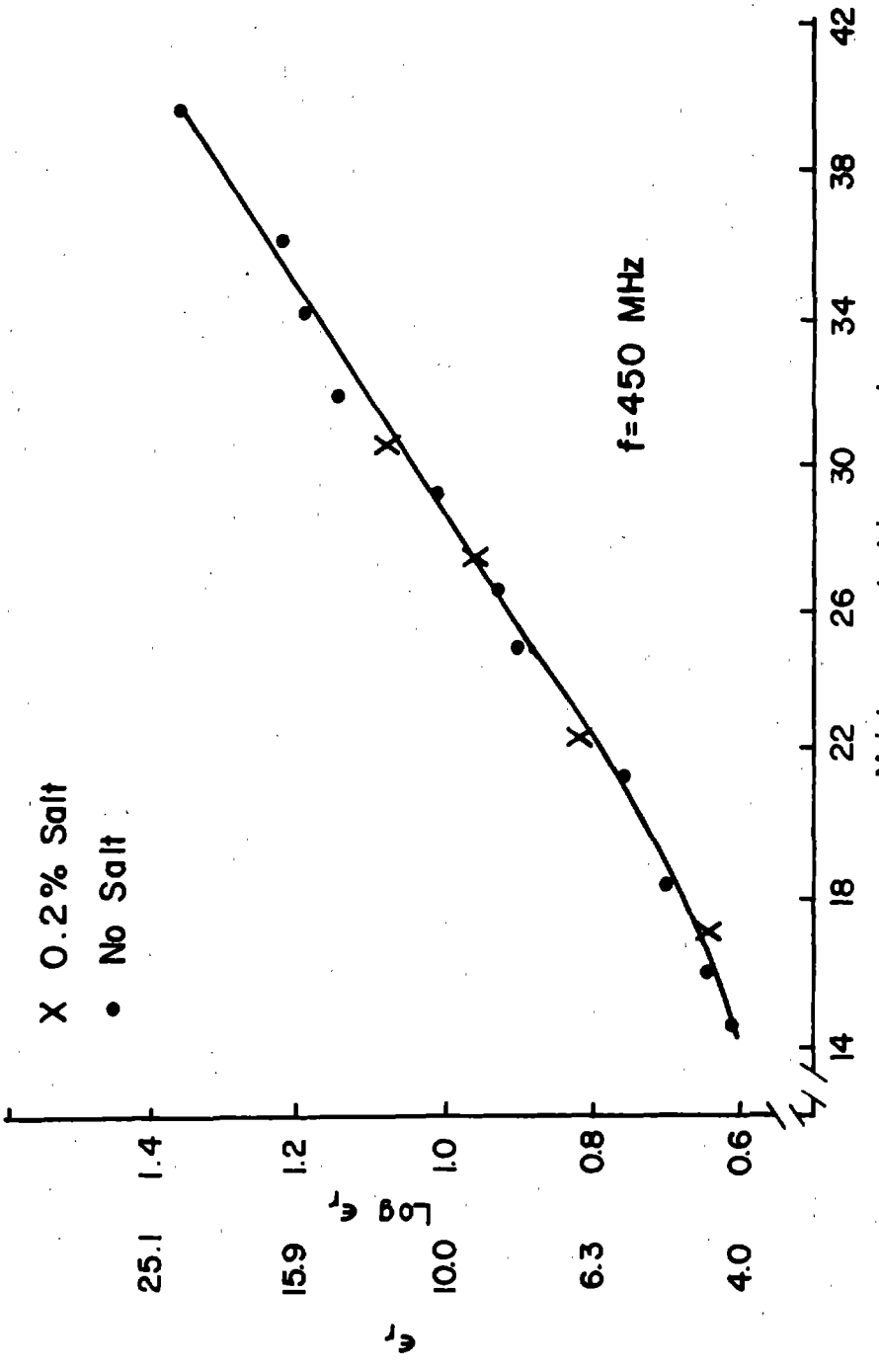

Figure 1-30. ϵ_r Vs. Moisture Content for Crider Clay, Laboratory Prepared.

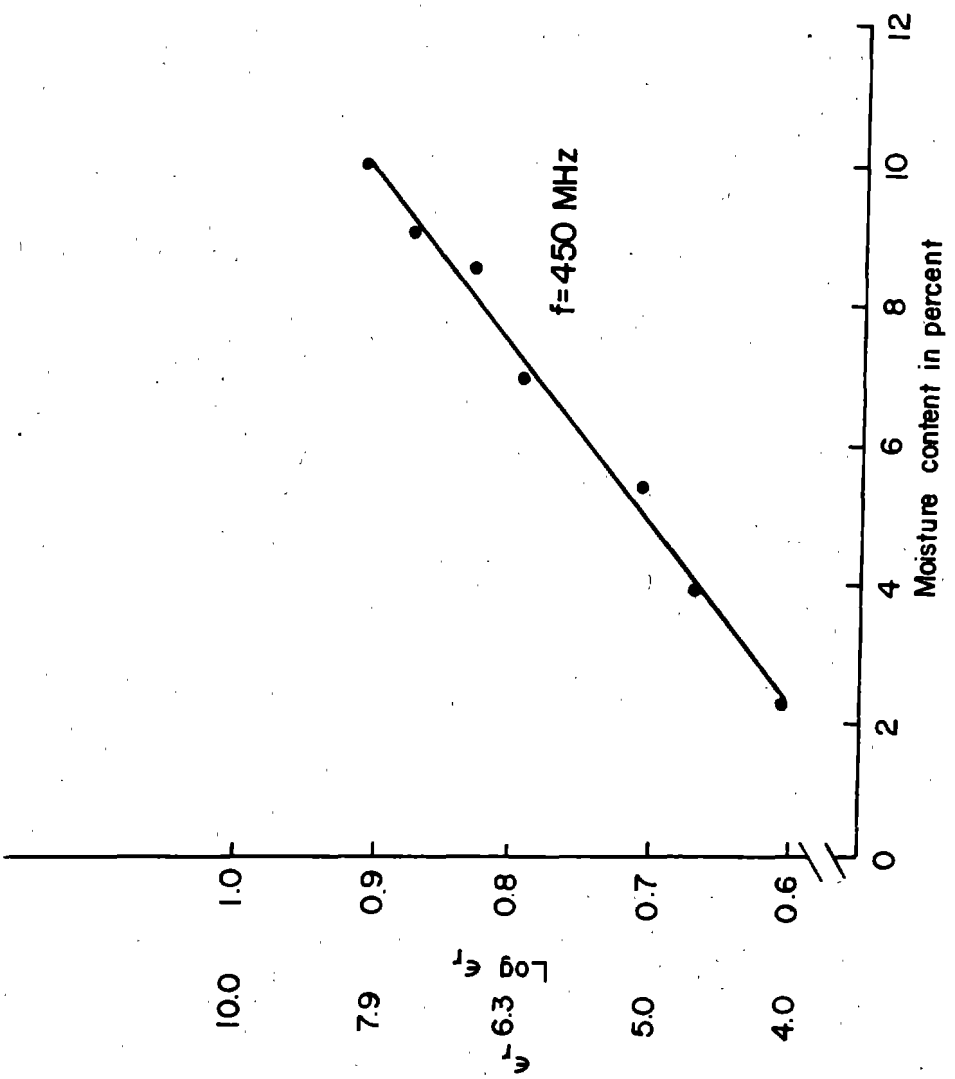

Figure 1-31. ϵ_r Vs. Moisture Content for Chelsea Sand, Laboratory Prepared.

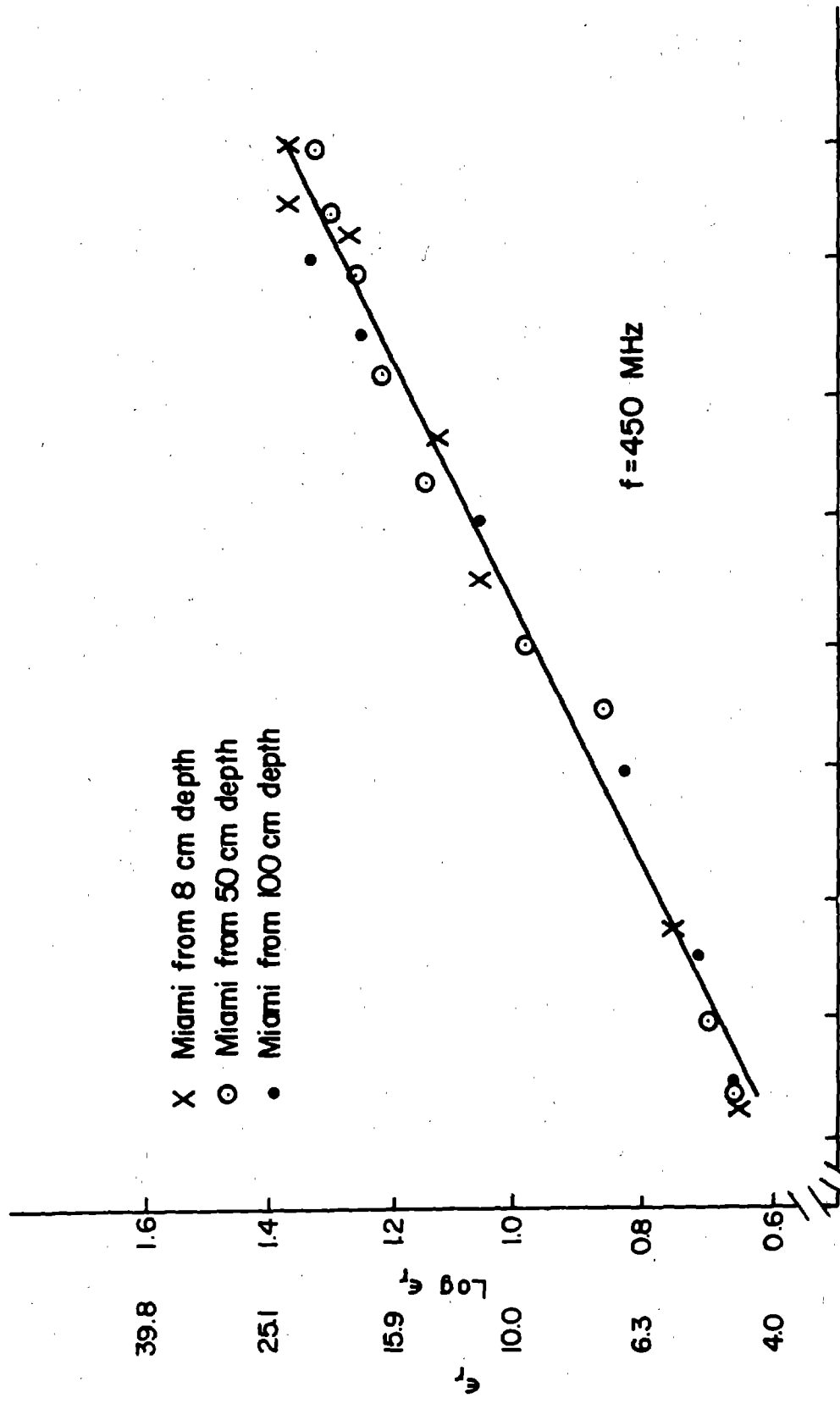

Figure 1-32. ϵ_r Vs. Moisture Content for Miami Silt Loam Taken from Field Pit.

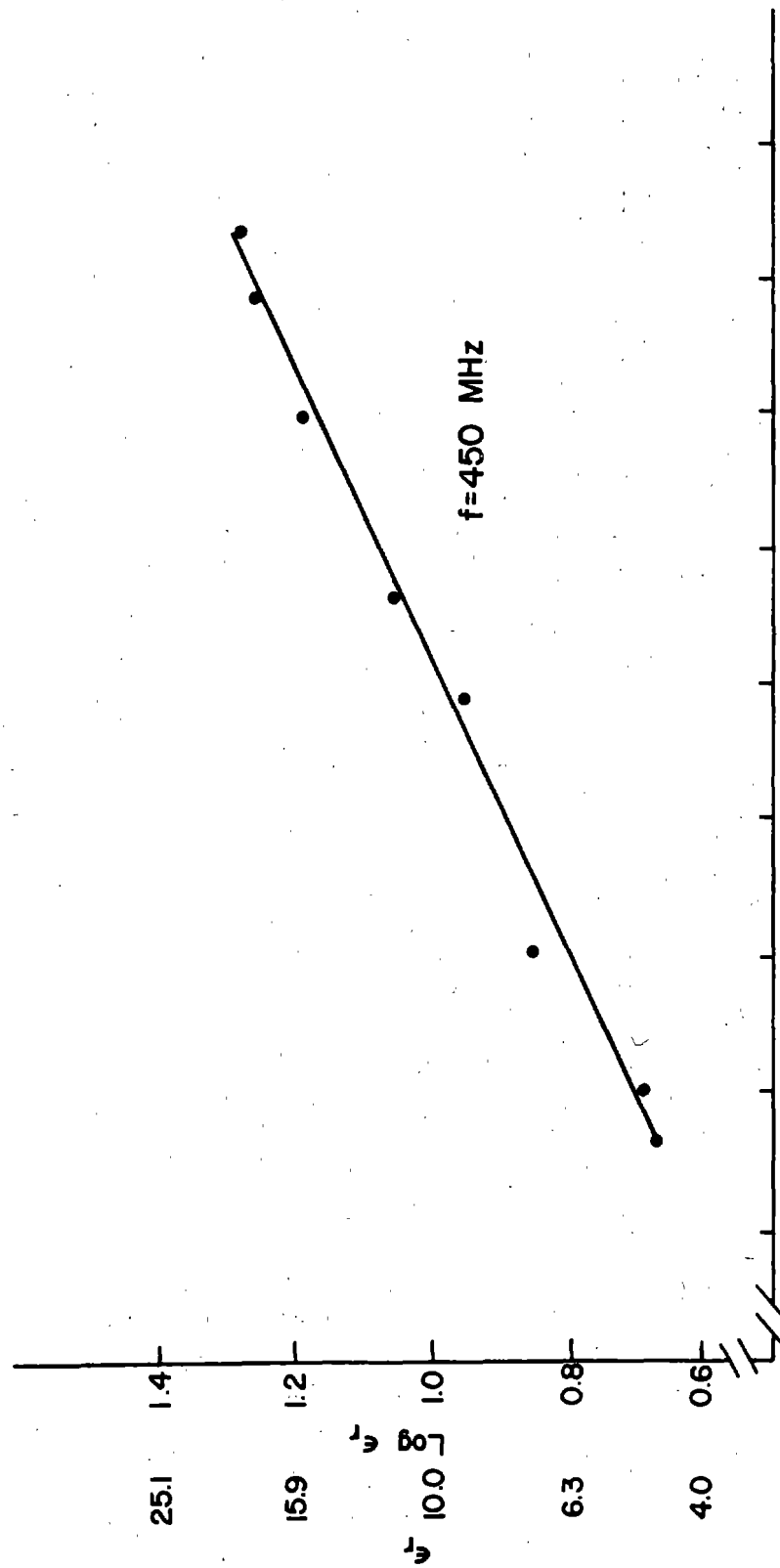

Figure 1-33. ϵ_r Vs. Moisture Content for Crosby Silt Loam Taken from Field Pit.

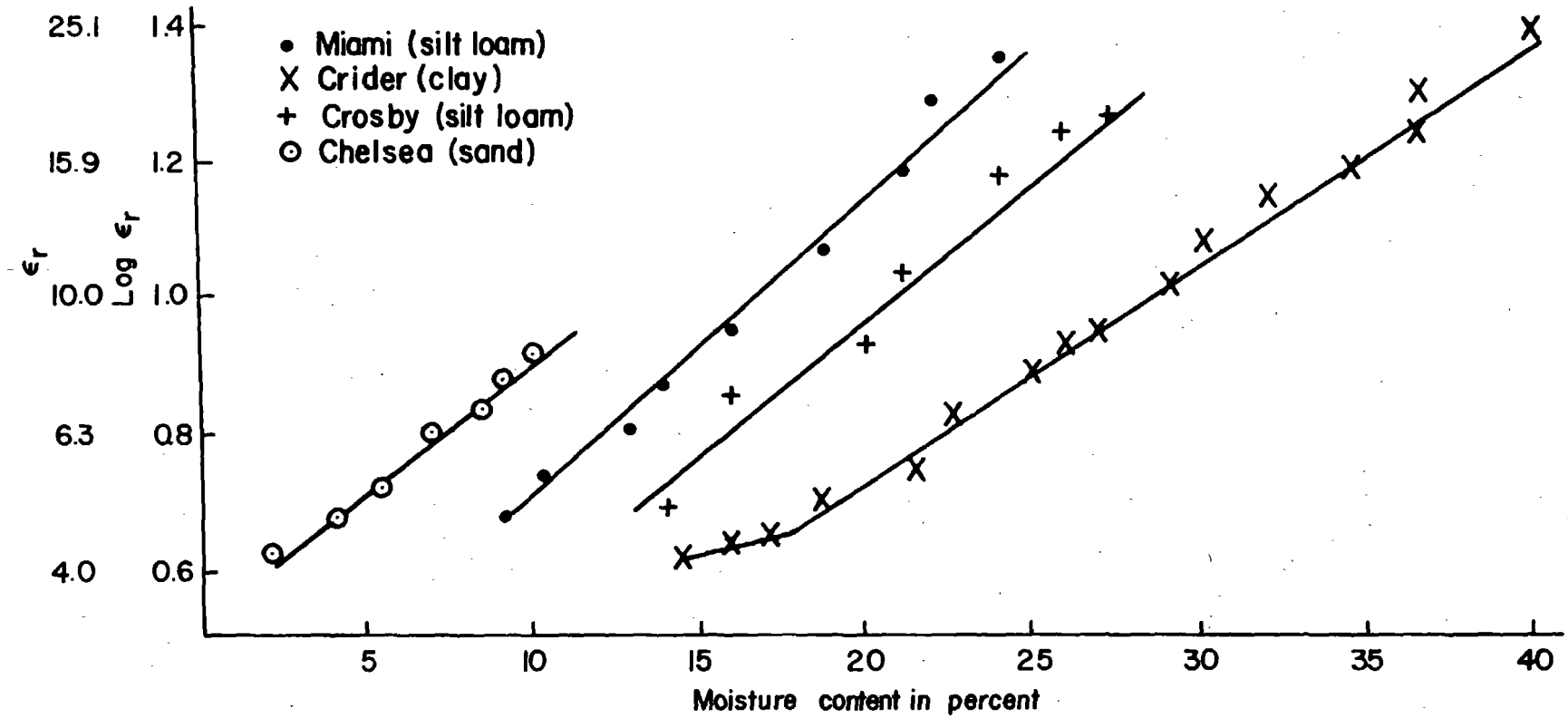

Figure 1-34. Permittivity of All Soils Measured Vs. Moisture Content at a Frequency of 450 MHz.

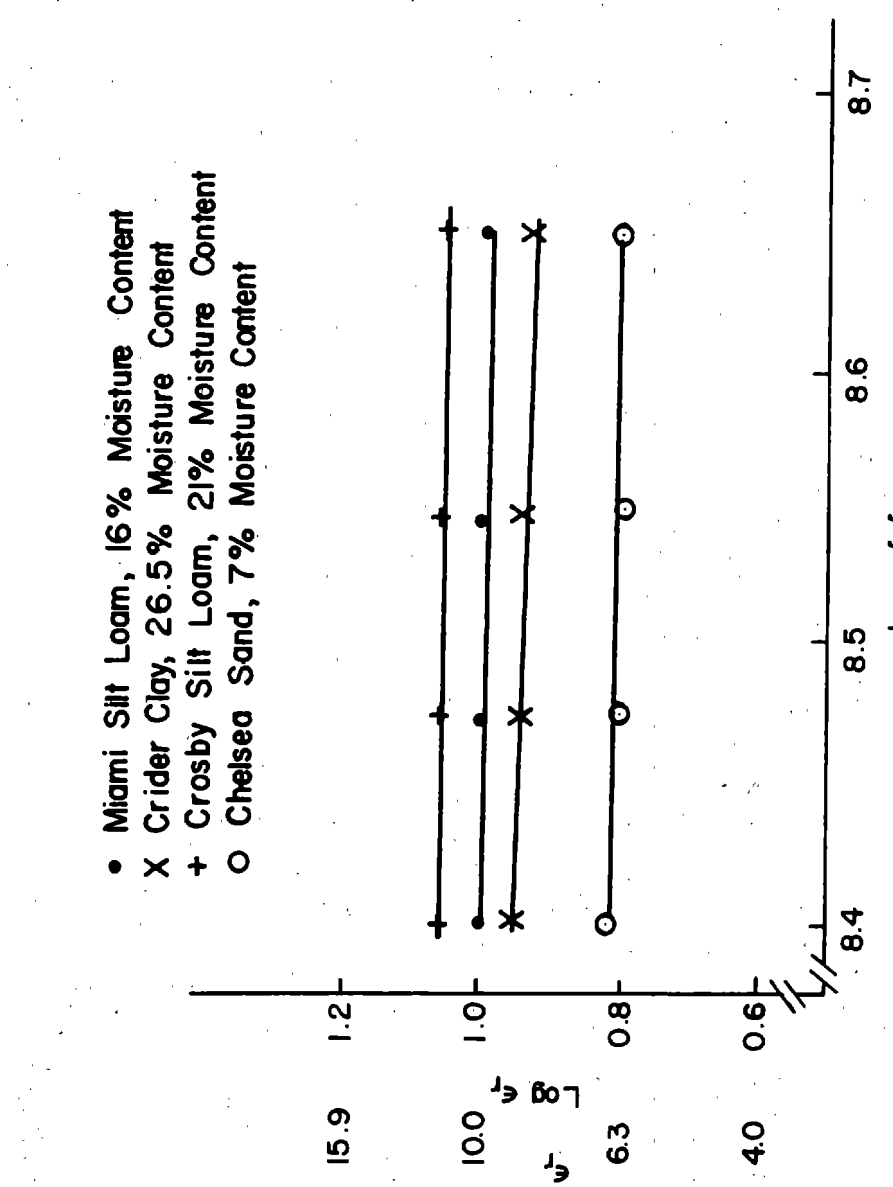

Figure 1-35. Typical Frequency Dependence of ϵ_r For Several Soils. (Frequency Range: 250-450 MHz.)

CHAPTER 6

DISCUSSION OF RESULTS

In this chapter results from the investigation of permittivity of some soils in three frequency ranges are discussed.

Measurements in the 0.02 - 2 MHz Range

The procedures used to obtain the results discussed in this section can be found in Chapter 3. The data are tabulated in Appendix I. The apparent dielectric constants can be obtained from the capacitance by dividing the capacitance listed in the table by the capacitance of the empty sample holder, 1.65 pF. This has not been done because the results are not of practical value to the present investigation.

Several aspects of the data are worth noting. The apparent dielectric constants are very high for almost all the soils tested. In addition, the apparent dielectric constants are strongly dependent on frequency. Furthermore, the conductivity also has an effect on the apparent dielectric constant. These phenomena are not consistent with the assumptions that the apparent dielectric constant is, in fact, the actual

dielectric constant, and that the dielectric constant of a soil sample can be calculated from the dielectric constants of the constituent soil and water by some simple mixing rule, e.g., $\varepsilon_r = \varepsilon_{water}$ (fraction of water)+ ε_{soil} (fraction of soil). In Chapter 4 it was shown that the theory of electrode polarization not only qualitatively explains the phenomena, but also makes quantitative predictions which are close to experimental results.

Because the model of electrode polarization gives results which agree reasonably well with experimental results, one might ask if the theory could be used to correct for electrode polarization effects in the data from the first part of Appendix I. Unfortunately, as shown below, the answer is no. An approximate correction formula has been derived for the case where electrode polarization is a minor effort. (See Chapter 5, Equation 1-33.)

$$\varepsilon_{AC} \simeq \varepsilon_{AP} - \frac{1}{\omega^2 R_2^2 C_1 C_0}$$

where

ε_{AC} = actual dielectric constant

ε_{AP} = apparent dielectric constant (measured)

ω = angular frequency

R_2 = resistance of sample in ohms

C_1 = electrode capacitance in farads, due to an ion sheath on the electrode

C_0 = capacitance in farads, of empty sample holder

If C_1 were equal to 10^{-6}F, C_0 equal to 1.7×10^{-12}F, R_2 equal to 1280 Ω, ω equal to $2\pi \times 10^5$ radians/second, and the actual dielectric constant equal to ten, the above formula would predict an apparent dielectric constant of 100. Suppose the dielectric constant actually measured was 110. This is within 10% of the predicted value, which is reasonably good agreement. If one calculates the ε_{AC} by using the measured value $\varepsilon_{AP} = 110$, one obtains 20 which is 100% greater than the actual value. The basic problem here is that the difference between two large nearly equal numbers always has fewer significant digits than the two original numbers.

Estimating the electrode capacitance is very difficult, since it is proportional to the surface area of the electrode in contact with the sample. Due to surface irregularities, the area of the electrode can be an order of magnitude larger than a perfectly smooth surface of the same dimensions. Even neglecting the problem of estimating the surface area of the electrode, one is still faced with the problem of estimating the amount of surface area which is actually in contact with the soil samples. Although careful packing of the soil is helpful, some variation of the actual contact area is unavoidable. Finally, the electrode capacitance itself has some frequency dependence which complicates the situation. The conclusion is that, where electrode polarization has a large influence on the data obtained, it is probably not feasible to correct for electrode

polarization. At higher frequencies, where ε_{AP} and ε_{AC} are not greatly different, correction is feasible but not particularly helpful.

An interesting phenomenon encountered in the course of this investigation was the time dependence of the data, described in Chapter 3. Even after the possibility of a chemical reaction at the electrode was eliminated, the capacitance of clay and muck soil decreased with time. One possible explanation is that some of the moisture is adsorbed into the surface of the soil particles and, therefore, the permittivity of the sample is reduced since adsorbed water has a lower dielectric constant. Another possibility is that as moisture is adsorbed into the surfaces, less moisture is available to support ionic conduction. This would result in a decrease in sample conductivity with a consequent decrease in the effect of electrode polarization. Hence, the apparent dielectric constant would decline.

Actually, these two explanations are not mutually exclusive and, in fact, there is some evidence that both processes occur. Wiebe (15), whose investigation was cited in Chapter 2, noted a decline in measured dielectric constant with time. His measurements were performed at a frequency high enough to preclude any electrode polarization effects. On the other hand, decrease in conductivity of laboratory samples with time has been noted by other authors (25), and the model in Chapter 4 shows that this would decrease the apparent permittivity. This effect should not be present, of course, with soil in the field.

This preliminary study served to explain several studies published in the literature. For example, the very high apparent dielectric constants measured by Anderson (8) must have been the result of electrode polarization. Likewise, the strong influence of salt content noted by Thorne and Russell (11) can be traced to electrode polarization, which illustrates the futility of insulating electrodes, as Wallihan and Thorne and Russell (10, 11) did in order to overcome the effects of soil conductivity. The insulation merely reduces the electrode capacitance somewhat, which increases the range of frequency over which electrode polarization has an important effect.

Measurements in the 5 - 40 MHz Range

The procedures used to obtain the data discussed in this section are given in Chapter 5. The data are tabulated in the second section of Appendix I.

In an attempt to overcome the effects of electrode polarization, the frequency of measurement was increased to a range of 5 - 40 MHz. Unfortunately, the attempt was only partly successful. As can be seen from the frequency dependence curves of Figure 1-23, the dielectric constant is markedly less dependent on frequency, and the values of permittivity are much more reasonable than for the frequency range of 20 - 2000 kHz, as shown in Figure 1-19. The addition of salt, however, still has an effect on the results, albeit a small effect. This gives one an opportunity to assess a prediction made in Chapter

4, where it was claimed that a one decade decrease in R_2 should result in the C vs. frequency curve being shifted one-and-a-half decades to the right. R_2, the "sample resistance," is inversely proportional to σ, the sample conductivity, while C is proportional to the dielectric constant, ϵ_r. Hence, an increase of one decade in σ should result in a one-and-one-half decade shift in ϵ_r. Table 1-7 shows the correspondence between this prediction and the data collected. The agreement is reasonable. A number of other observations could be made in this section concerning the permittivity, but it seems best to defer those remarks until the next section where electrode polarization does not confuse the issue.

Measurements in the 250 - 450 MHz Range

The data discussed in this section were collected according to the procedure outlined in Chapter 5 and are tabulated in the third section of Appendix I.

In this frequency range electrode polarization has a negligible effect. This can be seen from the fact that the addition of salt does not affect the permittivity and that the dielectric constant is not strongly dependent on frequency.

Considering the frequency dependence in more detail, one notes that the changes in log ϵ with respect to frequency, Δ Log $\epsilon/\Delta f$, tend to be higher for soils higher in clay content but, for any given soil, Δ Log $\epsilon/\Delta f$ is independent of moisture content. Likewise, the change in conductivity increases for increasing clay content, but $\Delta\sigma/\Delta f$ is approximately independent

Table 1-7. Comparison of Predicted with Actual Frequency Shift of C vs. Frequency Curve Due to Change in Conductivity.

Samples Compared	Predicted Frequency Shift in Decades	Actual Frequency Shift in Decades
9.9% M.C., 0% Salt		
10.0% M.C., 0.4% Salt	0.606	0.66
12.4% M.C., 0% Salt		
12.3% M.C., 0.4% Salt	0.925	1.00
15.8% M.C., 0% Salt		
15.9% M.C., 0.4% Salt	0.72	0.87
19.0% M.C., 0.2% Salt		
18.9% M.C., 0.4% Salt	1.11	1.08

Note: The above data are for Miami Silt Loam in the 5-40 MHz range. M.C. refers to moisture content.

of moisture content. The conductivity, however, is increasing faster with respect to frequency in this range than in the 5 - 40 Mhz range.

Now let us turn our attention toward the behavior of the dielectric constant as a function of moisture content. The most striking feature of Figures 29 to 34 is the linearity of the graphs over most of their range. This is strange since a simple mixing rule, for example, $\varepsilon_r = \varepsilon_{water}$ (fraction water) + ε_{soil} (fraction soil), would lead one to expect the curves to be straight lines on a linear scale, not a logarithmic one. Also, note from Figure 1-34, that the curves for different soils have different intercepts (projected) on the abscissa axis. The significance of this observation can be better appreciated by looking at Table 1-8 where the permittivity of each soil at its wilting point is tabulated. It is possible to conclude from this table and Figure 1-34, that the intercepts are correlated with the wilting point moisture, implying that the permittivity is a logarithmic function of the available moisture content. The logarithm of relative permittivity vs. available moisture content is plotted for several soils in Figure 1-36, bearing out the above conclusion.

To explain these observations one can begin with the concept of available moisture. In Chapter 1 available moisture was defined as the amount of moisture in excess of the wilting point moisture. The availability of water to plants and the permittivity of water are both related to the same physical phenomenon, the adsorption of water. Water becomes "bound"

Table 1-8. Permittivity of soils at the wilting point.

Soil	Relative Permittivity
Chelsea (sand)	4.05
Crider (clay)	5.07
Crosby (silt loam)	4.91
Miami (silt loam	4.58

f=450 MHz

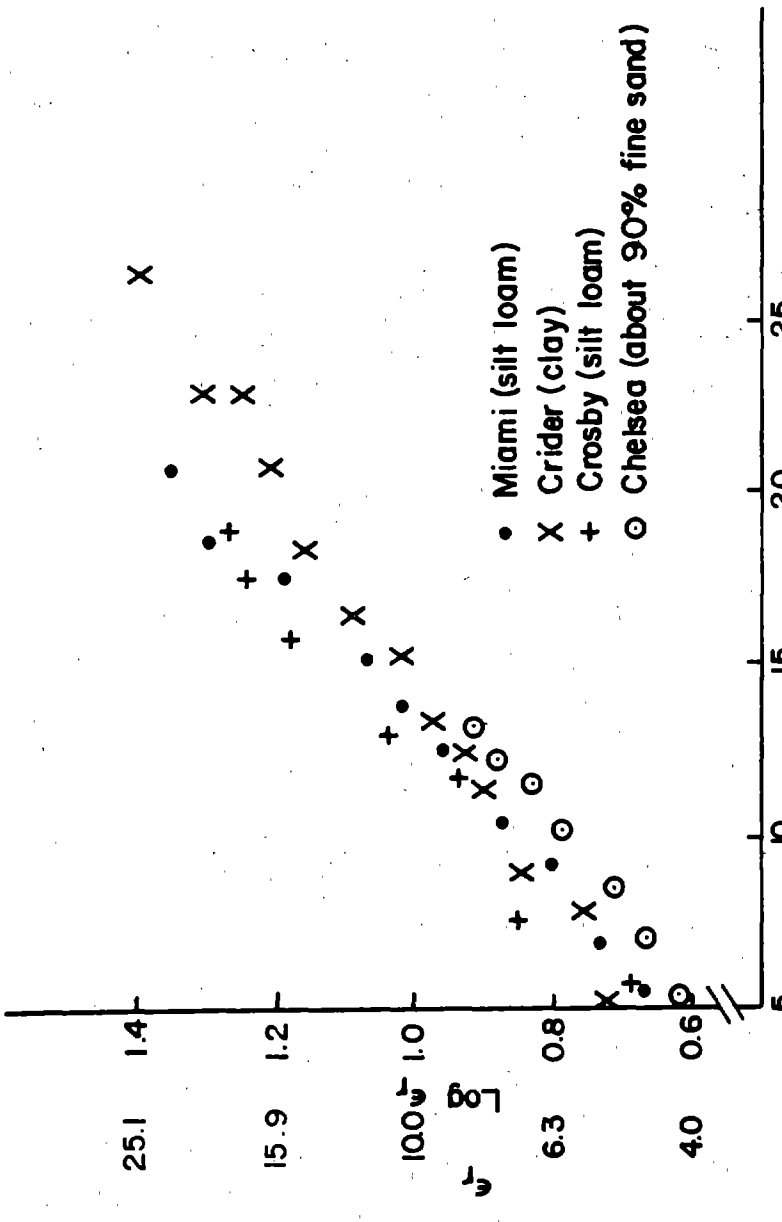

Figure 1-36. Permittivity Vs. Available Moisture Content. This figure has been adapted from Figure 1-34 by adjusting the abscissa to show available moisture content rather than **total moisture content.**

to the surface of the soil particles and this binding makes it difficult for the roots to extract moisture. The rotation of water dipoles by an alternating electric field is also hindered by the binding of the water to the surface. Since the high dielectric constant of water is due to the ability of its dipoles to rotate in response to an applied electric field, the dielectric constant of "bound" water is much less than that of free water. As a first approximation, soil moisture can be thought of as consisting of two kinds of water, free (with a relative permittivity of about 80) and bound (with a relative permittivity of 5 to 10). The data from this investigation are consistent with this explanation, because moisture below the wilting point seems to have much less effect on the permittivity.

Examining the data in more detail, one can arrive at further conclusions. For example, one may ask why the logarithm of permittivity is proportional to the available moisture content instead of the permittivity itself being proportional to the moisture content. A possible answer is that all the available water is not equally available. Assuming a distribution of permittivities corresponding to a distribution of binding forces, one can obtain an approximately logarithmic relationship as illustrated in Figure 1-37.

The top illustration in Figure 1-37 shows a hypothetical graph of the dielectric constant of water vs. distance from the surface of a soil particle. This can be used to obtain a hypothetical permittivity vs. moisture curve. Consider a reasonable simple mixing rule,

Figure 1-37. Effect of Transition Region.

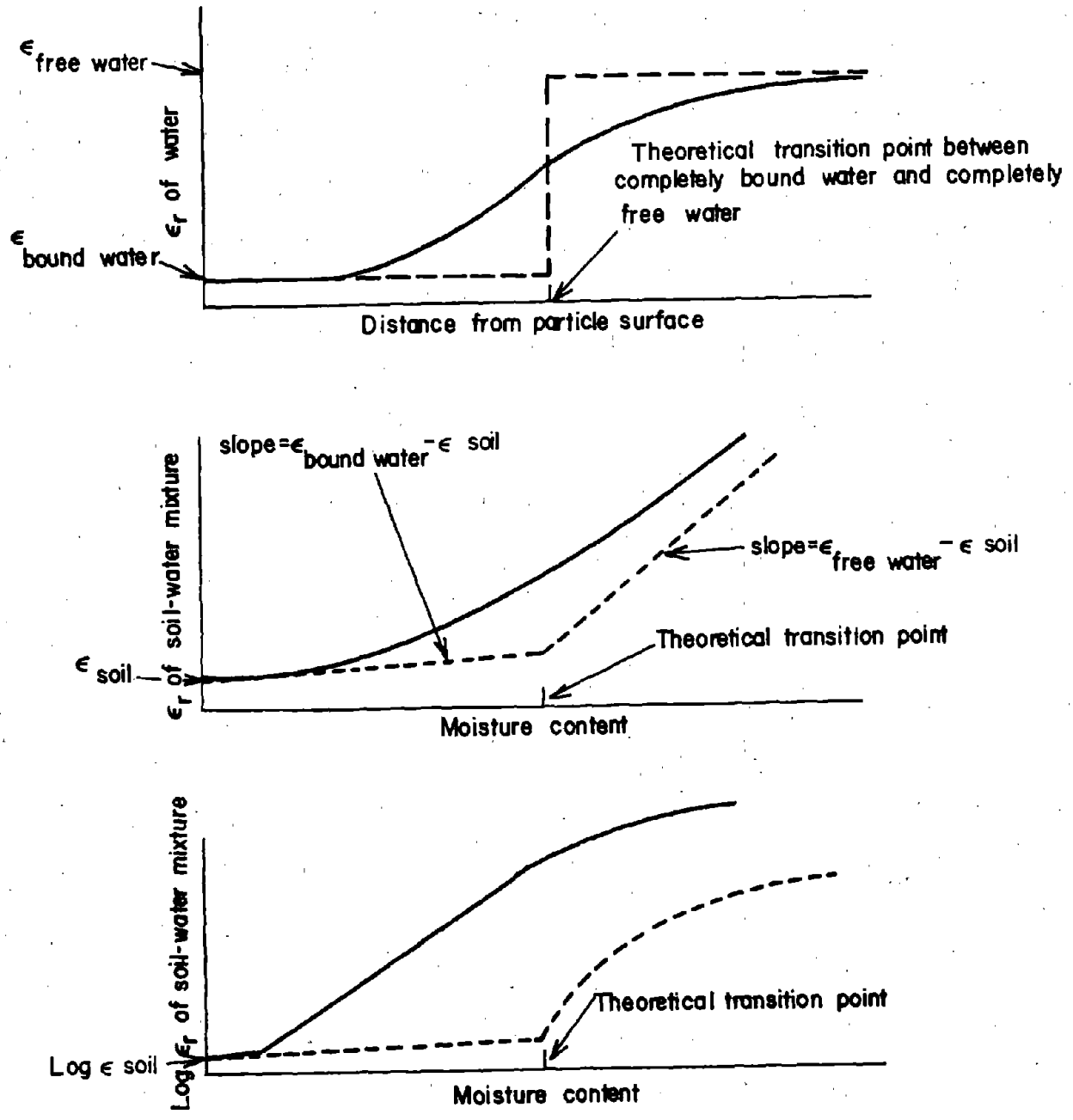

Note: The dashed curves are hypothetical curves drawn under the assumption that the water present is either completely bound to the soil particles (ϵ_r = 5÷10), or completely free (ϵ_r = 80). The solid curves are hypothetical curves drawn under the assumption that over a small range of distances from the soil particles the water molecules are only partially bound and the relative permittivity of this water gradually increases from about 10 to 80 as the distance from the soil particle increases.

$$\varepsilon_{mixture}=\varepsilon_r=\varepsilon_{soil}\ (\text{fraction soil})+\varepsilon_{water}\ (\text{fraction water}).$$

Because (fraction soil) = 1 - (fraction water),

$$\varepsilon_r=(\varepsilon_{water}-\varepsilon_{soil})\ (\text{fraction water})+\varepsilon_{soil}.$$

Hence, the slope of the relative permittivity vs. moisture content curve is simply the difference between the permittivity of the water and that of the soil. By using this relationship, one can construct the relative permittivity (ε_r) vs. moisture content curve graphically as shown in the second illustration of Figure 1-37. Finally, the third graph shows the permittivity vs. moisture content curve using a logarithmic permittivity scale. Superimposed on each graph is a curve (dotted line) showing the same quantities under the assumption that only free and bound water exists with no transition region. The figure shows that the addition of the transition region gives curves which are similar to the experimental curves.

At this point, the reader is reminded that the models set forth here are merely presented as reasonable explanations to be used as a means of generating new predictions and, possibly, stimulating new research. In this spirit, let us consider the frequency dependence of the permittivity. The frequency dependence for ordinary free water is well known. It is constant up to the "relaxation frequency" where it rapidly declines to a relatively small value. This relaxation frequency is above any frequencies used in the present work. One might hypothesize that for bound water the relaxation frequency is simply shifted to a lower frequency. This is a reasonable assumption since ice behaves this way. If this is the case, then one might conclude that the water in the transition region is

undergoing relaxation in our frequency range of measurement. This suggests a slight decline in the dielectric constant with frequency which should be more noticeable for small moisture contents. The decline should also be a little greater for clays, because in both cases a greater percentage of the total moisture is in the transition range. This is borne out by Figures 1-10 and 1-12.

The conductivity data can also be interpreted in this same light. The conductivity can be considered as being composed of two components: one due to ionic conduction, the other due to dielectric loss. As is well known, the theory of dipole relaxation shows that dielectric loss reaches a peak at the relaxation frequency. For ordinary free water, the dielectric loss begins to increase around 500 MHz. Since water in the transition region is nearing its relaxation frequency, it should show increasing loss at a somewhat lower frequency than does free water. This should be reflected in an increasing $\Delta\sigma/\Delta f$, with increasing frequency which, in fact, does increase, as shown by the data in the Appendices. Of course, the conductivity increases for increasing moisture, because this favors increased ionic conduction.

Our main interest in performing these measurements is to arrive at an assessment of the usefulnes of permittivity as an indicator of soil moisture. From these measurements one can conclude that the permittivity is a good indicator of soil moisture provided that some information about the soil is available. Even in the absence of any knowledge about the soil,

Figure 1-36 shows that the relative permittivity gives a useful estimate of the available moisture content. For the soil high in clay content (Crider) the correlation is least satisfactory.

It is also of interest to note that the laboratory samples were very similar to the Miami samples taken from the field, differing only in conductivity. It is not surprising that the conductivities of the field samples were greater, since pore structure, which is absent in the laboratory prepared samples, increases ionic conduction.

As a final point, let us consider the larger than expected permittivities for small available moisture contents in clay. There are at least two possible explanations. The first possibility is that the transition region is constructed in such a way that the permittivity at the wilting point is higher for clays. The second possibility is that soil particle surface admittance (discussed in Chapter 2) still has some small effect even at our highest frequencies. According to Schwartz' theory, (14), spherical particles 0.02 micrometer in diameter could have some effect up to 500 MHz. For needle-shaped particles the effect could be enhanced. In either case it would seem that performing the measurements at even higher frequencies than 450 MHz would give better results. A higher frequency would lessen the effect of surface admittance and also would "relax" more of the dipoles. It seems possible, therefore, that one could find a range of frequencies for which a better correlation exists between available moisture content and permittivity.

CHAPTER 7

CONCLUSIONS

The results of a number of previous investigations on the relationship between the electrical permittivity and the moisture content of soils have been accounted for herein, by the theory of electrode polarization. Hence, the negative conclusions reached about dielectric methods, based on these earlier studies, can be disregarded.

When the effects of electrode polarization can be neglected, it seems that an acceptable relationship exists between available moisture content and electrical permittivity. A model has been developed which is based on concepts originated by soil scientists. The model appears to explain the main features of the data and is consistent with the observations. In addition, the model predicts an even better correlation between available moisture content and permittivity at still higher frequencies than those used in the present work.

PART II

Electrical Methods for Determining Soil Permittivity Profiles

CHAPTER 1

STATEMENT OF THE PROBLEM

Objectives

The ultimate goal of this investigation is to explore the feasibility of electrical methods for determining the soil moisture profile, defined as the soil moisture content as a function of depth in the soil. In the previous part of this report, a satisfactory relationship was obtained between the available moisture content and the electrical permittivity for several different soils. Thus the problem reduced to determining the permittivity as a function of depth in the soil.

One possible method for measuring the permittivity profile is similar to conventional techniques of determining the soil moisture profile. A hole could be dug or augered and an electrical probe inserted to measure the permittivity at various depths. This might offer certain advantages in cost and convenience over conventional methods, but electrical methods hold out the promise of still greater advantages.

Since electromagnetic radiation does penetrate the earth and also is partially reflected by changes in the electrical properties of the soil, it seems possible that information on the permittivity could be recovered without actual physical contact with the soil below the surface. If a method could be found for accomplishing this it would offer significant advantages over presently available schemes in speed and convenience.

In this part of the report, various remote sensing techniques for determining soil moisture content are explored. They are termed remote sensing techniques because actual contact with the object being measured is not required. To begin, some factors which influence the choice of methods are identified.

Factors Which Influence the Choice of Methods

Electrical methods rest on the assumption that the electromagnetic radiation penetrates the soil to a sufficient depth. In addition to this, particular techniques make assumptions about the electrical properties of the soil and other aspects of the problem. To discuss these assumptions and requirements more intelligently, one should consider the various factors which influence the choice of methods: electrical properties of the soil, distribution of the permittivity in the soil, temperature, penetration of electromagnetic radiation, resolution of measurements, and the kinds of data that can be collected.

Magnetic Permeability

Some ores have high electrical permeabilities, but study by Lukshin et.al. (1) revealed that all the common soils tested had relative permeabilities of about one. Hence permeability can be assumed to be equal to its vacuum value everywhere, independent of all variables.

For many years the Electrical Conductivity of the soil has been studied to determine its suitability as an indicator of soil moisture. The studies have established (see (26), for example) that conductivity is not a reliable indicator because the ions in the soil strongly influence the conductivity. The quantity of ions in the soil vary from place to place and time to time.

Frequently, the conductivity is sufficiently large that the conduction current isn't negligible compared to the displacement current. Although the conductivity of soil varies with frequency, it is approximately bounded by zero below and one mho/meter above. Actually, most soils have conductivities of less than one-tenth mho/meter.

Electrical Permittivity

Permittivity is related to the available moisture content of the soil. It appears to decline slightly with increasing frequency between 1 MHz and 1 GHz.

In Chapter II of Part 1 studies were cited which demonstrated that clays have a very high dielectric constant due to their "surface admittance." In the frequency range where surface admittance is important, permittivity is not a reliable

indicator of soil moisture. Surface admittance is the dominant effect below 10 kHz. Above 2 GHz the permittivity declines due to the inability of the water dipoles to reorient themselves in response to the rapidly oscillating field. Approximate limits on the relative permittivity of soil are three and fifty.

Temperature also has some effect on permittivity. This is worth noting since temperature can vary with depth independent of moisture content. Thus permittivity variations could be attributed erroneously to moisture content variations.

Studies by Schofield (27) revealed maximum variations of 10°F between soil temperatures to a depth of four feet. Other studies have found differences up to 18°F. Using the formula given in Part I, Chapter 2, one can show that this leads to relative permittivity variations of five percent. If this error is unacceptable it should be possible to correct the data by using information about the temperature profile.

Distribution of Electrical Permittivity in the Soil

In general, the soil cannot be assumed to consist of layers of constant permittivity. The moisture content is usually a continuous function of depth, although a sand lens or some similar structure occasionally gives rise to a rapid change in moisture content.

For most agricultural soils it is reasonable to assume that the permittivity profile does not change much in the

horizontal direction, but there are exceptions. The properties of alluvial soils and soils with depressions frequently change rapidly in short distances along the surface, but such areas could be avoided if desired, since they are easily identified.

On the other hand, it is unrealistic to assume complete horizontal stratification. If horizontal stratification is implicit in a model, then the method must be checked to insure that satisfactory results can be obtained by using information from a limited area, as is done later in this chapter.

Penetration of Electromagnetic Radiation

The electrical properties of the soil govern the depth of penetration of electromagnetic radiation. One measure of penetration is skin depth, the depth at which the electric field is 36.8% of its value at the surface. The usual simplified formula for calculating skin depth cannot be used for soil since the displacement current density is not negligible compared to the conduction current density in this case, or vice versa. A correct formula for skin depth can be derived from the Helmholtz equation,

$$2\text{-}1 \quad \nabla^2 E - j\omega\mu\,(j\omega\epsilon + \sigma)\,E = 0.$$

For a plane wave traveling in the +z direction,

$$2\text{-}2 \quad E = Ae^{-j\sqrt{-j\omega\mu\ (j\omega\varepsilon + \sigma)}\ z}.$$

The skin depth, δ, is just the reciprocal of the real part of the exponent,

$$2\text{-}3 \quad \delta = \frac{1}{\text{REAl}\ [j\ \sqrt{-j\omega\mu\ (j\omega\varepsilon + \sigma)}]}.$$

Algebra yields

$$2\text{-}4 \quad \delta = \frac{\sqrt{2}}{\sqrt{\omega\mu}\ \sqrt{-\omega\varepsilon + \sqrt{(\omega\varepsilon)^2 + \sigma^2}}},$$

where

ω = angular frequency in radians per second

$\mu = \mu_r\ \mu_o$

μ_o = permeability of vacuum ($4\pi \times 10^{-7}$ henry/meter).

μ_r is the relative permeability, which is dimensionless.

$\varepsilon = \varepsilon_r\ \varepsilon_o$

ε_o = permittivity of vacuum ($1/36\pi \times 10^{-9}$ farad/meter). ε_r is the relative permittivity, which is dimensionless.

σ = conductivity in mhos/meter.

For ε_r equal to thirty-six and σ equal to two-tenths of a mho/meter, the skin depth is 1.12 meters at 1 MHz, 0.35 meter at 10 MHz, 0.2 meter at 100 MHz, and 0.16 meter at 1 GHz.

Resclution

Resolution refers to the ability of a system to distinguish objects wiich are close together. In the context of the

present discussion, the objects to be resolved might be layers of high permittivity separated by a layer of lower permittivity. A measure of the resolution of a system is the least thickness of the intermediate layer for which the system can distinguish the two high permittivity layers. For a thinner intermediate layer, the two high permittivity layers would appear to be a single layer.

Even if the soil is not layered, resolution has an effect. Low resolution systems tend to smooth out abrupt transitions and blur fine detail. In some cases this is a disadvantage, but occasionally the lack of resolution eliminates troublesome, and unimportant effects of thin layers and inhomogeneities.

Generally, the resolution of systems is governed by the wavelength of the radiation. The limit of resolution is usually considered to be about half the wavelength. In soils, the wavelength is about 1/2 to 1/7 the wavelength in vacuum. At 300 MHz these assumptions lead to a resolution of about 8 to 25 centimeters. The resolution of each particular system is discussed in the section on that system since the special characteristics of each system govern its resolution.

Information Available

The data for the moisture measurement system must consist of measurements made of the electromagnetic fields at or above the surface of the earth. This constraint rules out, for example, methods which involve transmittance measurements since there is no practical way to make these <u>in situ</u>.

General Approach to the Problem

Assumptions

To facilitate analysis it is assumed that the area to be measured is flat and infinite in extent. A coordinate system is defined as shown in Figure 2-1. The permeability is assumed to be equal everywhere to its value in a vacuum. The permittivity may vary arbitrarily with depth, but it is assumed constant on any plane parallel to the plane $z = 0$. The same assumption is made with regard to conductivity. The displacement current density is not assumed to be much greater than the conduction current density. Sufficient penetration is assumed and the effect of temperature is neglected.

The Problem

Simply stated, the problem is to determine the permittivity profile, given the electromagnetic fields at or above the surface. One way to approach the problem is to relate the known surface field to the unknown permittivity profile by means of Maxwell's equations. This involves three steps. First, Maxwell's equations can be written for this particular situation and a "formal" solution can be obtained. Since the permittivity is unknown the "formal" solution will contain an unknown function. But the formal solution will contain useful information about the electromagnetic fields in the earth. Next, the formal solution must be related to something that can be measured: data taken at or above the surface. Finally, a relationship must be established between the formal solution and the permittivity variations.

Within the framework of this general approach there are a number of techniques to calculate the permittivity profile. The presently available methods for measuring the electrical permittivity of the earth as a function of depth, have been considered with considerable care by one of the present authors (F.V.S.) and the results are contained in unpublished form. The two methods which seem to be best adapted to the problem at hand are Becher's method and Slichter's method. In the next two chapters these methods are considered.

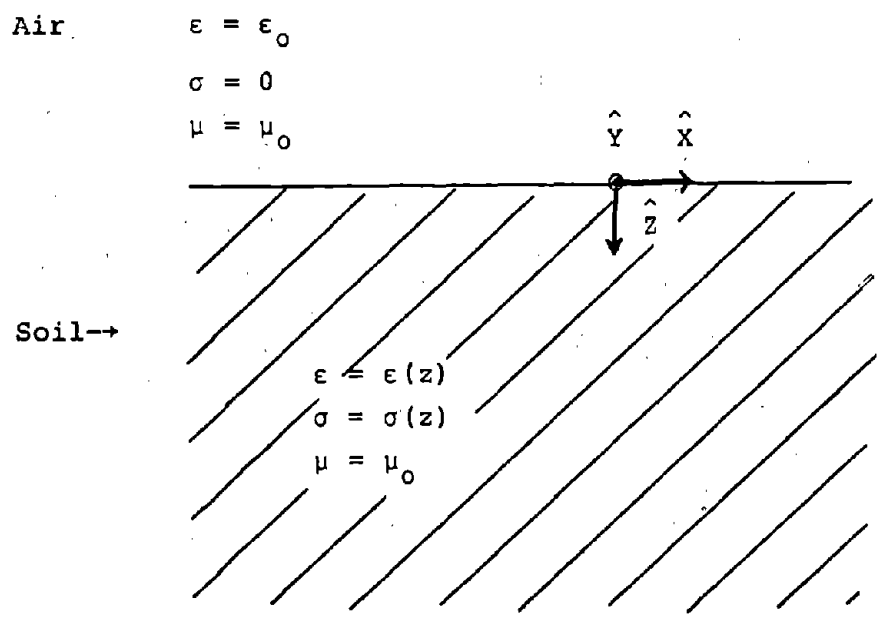

Figure 2-1. Model of Physical Situation.

CHAPTER 2

MARCHENKO-SHARPE-BECHER METHOD

This method seemed to be especially well suited for determining the permittivity profile of the soil, since it was developed for geoelectric exploration. The technique uses reflected electromagnetic waves as data. In this chapter, the Marchenko-Sharpe-Becher method is presented and its suitability for determining soil moisture profiles is assessed. Actually, it turns out that the method is not applicable to the present problem, although at first it appears to be, so it is only outlined here. The mathematical presentation is sketchy; only enough detail is being included to make possible an understanding of the apparent inadequacy of the method.

Presentation of the Method

The foundation of this method is Marchenko's work on the inverse scattering problem (28). Sharpe (29) adapted Marchenko's results to the problem of nonuniform transmission line synthesis. Sharpe also showed that a particular representation of the data greatly simplified the process of

obtaining a solution. Finally, Becher (30) used an analogy between plane wave propagation theory and transmission line theory to apply Sharpe's results to the geoelectric exploration problem. Some extensions of Sharpe's work were necessary to accomplish this.

Marchenko's Work

Marchenko's analysis deals with plane waves which originate at infinity, impinge upon a scattering potential V(x), and are reflected back to infinity. For the case of electromagnetic waves, one can easily see that Maxwell's equations, applied to this situation, lead to a wave equation. Marchenko was concerned with quantum mechanical scattering, so he dealt with the Schrödinger equation, also a wave equation. Since Marchenko's work has general application, the equations presented will not be specialized to electromagnetic terms, but left in the form used by Marchenko, except to express the phaser as $e^{j\lambda x}$ rather than $e^{-i\lambda x}$.

Although Marchenko dealt with quantum scattering, his development follows the general approach outlined in Chapter 1 of Part II. The basic equation is

$$2\text{-}5 \qquad \frac{d^2Y}{dx^2} + \lambda^2 Y = V(x)Y,$$

where

Y is a function of x (e.g. electrical field intensity),

λ is a separation constant,

V(x) is an unknown potential, and

x is a distance.

The objective of the analysis is to determine V(x) from knowledge of the asymptotic properties of Y. For convenience, Equation 2-5 with the boundary condition,

$$2\text{-}6 \qquad e^{-j\lambda x}\, Y(x,\lambda) = 1 \text{ as } x \to \infty$$

can be transformed into an integral equation,

$$2\text{-}7 \qquad Y(x,\lambda) = e^{j\lambda x} + \int_x^\infty \frac{\sin\,(t-\lambda)}{\lambda}\, V(t)\, Y(t,\lambda)\, dt.$$

This is a type of Volterra equation, and the form of a particular solution is well known. If one postulates that

$$2\text{-}8 \qquad \int_x^\infty t|V(t)|dt < \infty$$

it can be shown, using a theorem of Titchmarsh, that one can obtain a particular solution in the form

$$2\text{-}9 \qquad Y_p\,(x,\lambda) = e^{j\lambda x} + \int_x^\infty K(x,t)e^{j\lambda t}dt,$$

where K(x,t) is called the kernel.

The relationship between K(x,t) and V(t) is discussed later in the chapter. The first step of the general approach outlined in Chapter 1 is complete; a formal solution has been obtained. Now it is necessary to relate this formal solution to something which can be measured. To begin, note that a particular solution, Y_p, was found above. The general solution, G(x,λ), is a superposition of the waves propagating in opposite directions.

$$2\text{-}10 \qquad G(x,\lambda) = Y_p(x,\lambda)C + Y_p(x,-\lambda)D.$$

This can be expressed as

$$2\text{-}11 \quad G(x,\lambda) = \frac{1}{2j\lambda} \left[Y_p(x,-\lambda) - Y_p(x,\lambda)\, S(-\lambda)\right] Y_p^*(-\lambda),$$

where * denotes complex conjugation, and

$$S(\lambda) = Y_p^*(-\lambda)\, [Y_p^*(\lambda)]^{-1}.$$

$S(\lambda)$ is called the scattering datum and has the property that $1 - S(\lambda)$ is a Fourier transform of a function, $F_s(t)$,

$$2\text{-}12 \quad 1 - S(\lambda) = \int_{-\infty}^{\infty} F_s(t) e^{-j\lambda t} dt.$$

Starting with this information, Marchenko was able to relate the kernel, $K(x,t)$, to the scattering datum, $S(\lambda)$, by means of Parseval's equation. The relationship obtained is termed the fundamental equation,

$$2\text{-}13 \quad F_s(x+y) + K(x,y) + \int_x^{\infty} K(x,t)\, F_s(t+y) dt = 0, \quad 0 < x < y.$$

Now the formal solution must be related to the potential, $V(x)$. This can be done by substituting the formal solution, Equation 2-9, into the integral equation, Equation 2-7.

$$2\text{-}14 \quad \int_x^{\infty} K(x,t) e^{j\lambda t} dt = \int_x^{\infty} \frac{\sin \lambda (s-x)}{\lambda} V(s)\, e^{j\lambda s} ds$$

$$+ \int_x^{\infty} V(s) ds \int_s^{\infty} \frac{\sin \lambda (s-x)}{\lambda} e^{j\lambda u} K(s,u) du.$$

Denote the first term of the right hand side by A, the second by B. Using trigonometric relationships, one can show that

$$2\text{-}15 \quad \frac{\sin \lambda (s-x)}{\lambda} e^{j\lambda s} = \frac{1}{2} \int_x^{2s-x} e^{j\lambda t} dt,$$

$$\frac{\sin \lambda (s-x)}{\lambda} e^{j\lambda u} = \int_{x+u-s}^{u+s-x} e^{j\lambda t} dt.$$

Substituting these relations into integrals A and B and interchanging the order of integration, one obtains

$$2\text{-}16 \qquad A = \int_x^\infty e^{j\lambda t}\left[\frac{1}{2}\int_{\frac{x+t}{2}}^\infty V(s)\,ds\right]dt,$$

$$2\text{-}17 \qquad B = \int_x^\infty e^{j\lambda t}\left[\frac{1}{2}\int_x^{\frac{x+t}{2}} V(s)\,ds\int_{t+x-s}^{t+s-x} K(s,u)\,du + \frac{1}{2}\int_{\frac{x+t}{2}}^\infty V(s)\,ds\int_s^{t+s-x} K(s,u)\,du\right]dt.$$

Substituting the expression into Equation 2-14 and using the uniqueness of the Fourier integral representation,

$$2\text{-}18 \qquad K(x,t) = \frac{1}{2}\int_{\frac{x+t}{2}}^\infty V(s)\,ds + \frac{1}{2}\int_x^{\frac{x+t}{2}} V(s)\,ds \int_{t+x-s}^{t+s-x} K(s,u)\,du + \frac{1}{2}\int_{\frac{x+t}{2}}^\infty V(s)\,ds \int_s^{t+s-x} K(s,u)\,du, \quad 0 < x \leq t.$$

Now let t = x and Equation 2-18 reduces to the following equation,

$$2\text{-}19 \qquad K(x,x) = \frac{1}{2}\int_x^\infty V(s)\,ds.$$

To summarize Marchenko's work, let us recall that he has provided a relationship, Equations 2-12 and 2-13, between part of the formal solution, K(x,t), and a known quantity, S(λ), and a relationship, Equation 2-19, between the kernel, K(x,x), and the desired quantity, V(x). Note, however, that in order to calculate V(x), one must first solve an integral equation, Equation 2-13.

Sharpe's Work

Sharpe dealt with the problem of constucting the characteristic impedance of a transmission line in such a way as to

produce a specified input admittance. By normalizing certain variables in the transmission line equations, he showed that these equations can be put in the form of a Schrödinger equation. Thus, Sharpe's problem is identical to Marchenko's from a mathematical viewpoint. Marchenko's results, therefore, apply to Sharpe's problem also. Recall that Marchenko's solution required solving an integral equation. Sharpe sought to overcome this difficulty by representing the specified input admittance as a rational function of frequency. By using contour integration, he was able to reduce the integral equation to an algebraic equation. The details are outlined below.

Sharpe began with the transmission line equations for a lossless line;

$$2\text{-}20 \qquad \frac{dV}{dz} = j\omega L(z) I(z),$$

$$2\text{-}21 \qquad \frac{dI}{dz} = j\omega C(z) V(z),$$

where

V is the voltage across the line,

I is the current, in the line conductors,

L(z) is the inductance per unit length of the line,

C(z) is the capacitance per unit length,

ω is the angular frequency of the voltage and current,

z is the distance from the input of the line.

Define a local characteristic impedence, $Z_o(z)$, and a local phase coefficient, $\beta(z)$,

$$2\text{-}22 \qquad Z_o(z) = \sqrt{L(z)/C(z)},$$

2-23 $\beta(z) = \sqrt{L(z)C(z)}$.

Now normalize the distance, voltage, and current, respectively.

2-24 $x = \frac{1}{\omega} \int_0^z \beta(t)dt$

2-25 $u(z) = V/\sqrt{Z_0(z)}$

2-26 $v(z) = I\sqrt{Z_0(z)}$

Substituting these normalized functions into Equations 2-20 and 2-21 gives

2-27 $\frac{du(x)}{dx} + p(x)u(x) - j\omega v(x) = 0,$

2-28 $\frac{dv(x)}{dx} - p(x)v(x) - j\omega u(x) = 0,$

where $p(x) = \frac{1}{2} \frac{d}{dx} \ln Z_0 z(x)$.

Eliminating $v(x)$ in Equation 2-27 and $u(x)$ in Equation 2-28, one obtains the Schrödinger equations.

2-29 $\frac{d^2u(x)}{dx^2} + [\omega^2 - P(x)] \; u(x) = 0,$

2-30 $\frac{d^2v(x)}{dx^2} + [\omega^2 - Q(x)] \; v(x) = 0,$

where $P(x) = p^2(x) - \frac{dp(x)}{dx}$, $Q(x) = p^2(x) + \frac{dp(x)}{dx}$.

Note that $P(x)$ and $Q(x)$ are subject to the same restrictions as Marchenko's potential, $V(x)$. See Equation 2-8.

Sharpe thus established the connection between transmission line theory and Marchenko's work. To see this, note the analogy between Equation 2-29 or 2-30 and Marchenko's equation (2-5).

Since Marchenko's results apply to this case, one can write the solution to Equation 2-9 by analogy to Equation 2-9,

$$2\text{-}31 \qquad u(x,\omega) = e^{j\omega x} + \int_x^\infty A(x,t)e^{j\omega t}dt,$$

where

A(x,t) is the kernel, analogous to K(x,t) in Equation 2-9. The next step is to determine A(x,t) in terms of known quantities. Under the assumptions that he imposed, Sharpe showed that the problem of determining the kernel from known quantities, was reduced to that of solving a linear system of algebraic equations.

Marchenko's fundamental equation, 2-13, is the key equation in the process of determining the kernel. To reduce this integral equation to an algebraic system, Sharpe first related the input admittance to Marchenko's datum, which is analogous to a reflection coefficient. The normalized admittance of the transmission line is

$$2\text{-}32 \qquad y(x,\omega) = \frac{v(x,\omega)}{u(x,\omega)}.$$

The normalized admittance is

$$2\text{-}33 \qquad Y(\omega) = y(0,\omega).$$

Under the condition that the line becomes sufficiently uniform as x approaches infinity, outgoing wave solutions which are asymptotically exponential exist and $Y(\lambda) = v(0,\lambda)/u(0,\lambda)$ is a positive real function. λ is the complex frequency, $\lambda = \omega - j\xi$.

It is possible to prove that $u(0,\omega)$ and $v(0,\omega)$ are rational functions of ω with only simple poles and that, knowing any one of the quantities $Y(\lambda)$, $u(\lambda)$, or $v(\lambda)$ allows one to determine the other two uniquely. So, knowing $Y(\lambda)$ allows one to determine $u(0,\omega)$. Once $u(0,\omega)$ is known, Marchenko's theory can be used to obtain $F_s(t)$ and $A(x,t)$ from Equations 2-11, 2-12, and 2-13. Note that $u(0,-\omega)/u(0,\omega)$ is analogous to $S(\lambda)$ in Equation 2-12. Now perform the inverse Fourier transform on both sides of Equation 2-12. Then

$$2\text{-}34 \qquad F_s(t) = \frac{1}{2\pi}\int_{-\infty}^{\infty} 1 - \frac{u(0,-\omega)}{u(0,\omega)}\; e^{j\omega t} d\omega.$$

In order to obtain the kernel, $A(x,y)$, one can then solve an equation analogous to Marchenko's fundamental equation, 2-13.

$$2\text{-}35 \qquad F_s(x+y) + A(x,y) + \int_x^{\infty} A(x,t)\; F_s(t+y)\,dt = 0.$$

Consider this calculation in more detail. Recall that $u(0,\omega)$ is a rational function, with only simple poles, and so $1 - \frac{u(0,-\omega)}{u(0,\omega)}$ can be presented as

$$2\text{-}36 \qquad 1 - \frac{u(0,-\omega)}{u(0,\omega)} = \sum_{\nu=1}^{n} \frac{\rho_\nu}{\omega-\kappa_\nu} + \sum_{\nu=1}^{n} \frac{\sigma_\nu}{\omega-\mu_\nu},$$

where

κ_ν is a complex pole whose imaginary part is greater than zero,

μ_ν is a complex pole whose imaginary part is less than zero,

ρ_ν and σ_ν are complex residues.

Contour integration over the entire upper half plane gives

$$2\text{-}37 \qquad F_s(t) = j\sum_{\nu=1}^{n} \rho_\nu e^{j\kappa_\nu t}.$$

Substituting into equation 2-35 and performing the integration,

$$2\text{-}38 \qquad A(x,t) = \sum_{\nu=1}^{n} f_\nu(x) e^{j\kappa_\nu t},$$

where f_ν is found from the system

$$2\text{-}39 \qquad -\rho_\nu \sum_{\mu=1}^{n} f_\mu \frac{e^{j[\kappa_\mu + \kappa_\nu]x}}{\kappa_\mu + \kappa_\nu} + f_\nu(x) + j\rho_\nu e^{j\kappa_\nu x} = 0.$$

Thus the integral equation reduces to a linear system of algebraic equations. Once $A(x,t)$ is determined, one can use Equation 2-31 to determine $u(x,\omega)$.

$$2\text{-}31 \qquad u(x,\omega) = e^{j\omega x} + \int_x^\infty A(x,t) e^{j\omega t} dt$$

This expression can be substituted into Equation 2-29 to yield $P(x)$.

$$2\text{-}29 \qquad \frac{d^2u(x)}{dx^2} + [\omega^2 - P(x)]u(x) = 0.$$

Upon substituting Equations 2-31 and 2-38 into Equation 2-29, one obtains,

$$2\text{-}40 \qquad -\omega^2 e^{j\omega x} + \frac{d^2}{dx^2} \int_x^\infty \sum_{\nu=1}^{n} f_\nu(x) e^{j(\kappa + \omega)t} dt + [\omega^2 - P(x)]$$

$$[e^{j\omega x} + \int_x^\infty \sum_{\nu=1}^{n} f_\nu(x) e^{j(\kappa + \omega)t} dt] = 0.$$

Simplifying, using standard formulae for differentiation and integration, one obtains,

$$2\text{-}41 \qquad P(x) = -2 \frac{d}{dx} \sum_{\nu=1}^{n} f_\nu(x) e^{j\kappa_\nu x}.$$

$P(x)$ is related to $Z_0(x)$, the desired quantity. To see this, recall that

2-42 $$P(x)\ (\frac{1}{2}\frac{d}{dx}\ \ln Z_o(x))^2 - \frac{1}{2}\frac{d^2}{dx^2}\ \ln Z_o(x).$$

It is possible to show that

2-43 $$Z_o(x) = Z_o(\infty)\ \frac{\det[I-R(x)]}{\det[I-R(x)]}$$

where

I is the identity matrix,

R is a matrix whose elements are $R_{\nu\mu} = \rho_\nu \frac{e^{j(\kappa_\nu + \kappa_\mu)x}}{\kappa_\nu + \kappa_\mu}$,

$Z_0(\infty) = \lim Z_0(x)$, $x \to \infty$.

Becher's Work

Becher applied Sharpe's results to geoelectric exploration, that is, the use of electromagnetic waves to determine the electromagnetic properties of the earth. By exploiting an analogy between plane wave propagation theory and transmission line theory, Becher was able to put the equations for a plane wave in the same form as Sharpe's Equations 2-20 and 2-21.

2-44 $$\frac{dE_x(z)}{dz} = j\omega\mu_o Hy(z),\ \frac{dEx(z)}{dz} = j\omega\mu_o Hy(z),$$

2-45 $$\frac{dH_y(z)}{dz} = -j\omega\varepsilon(z)E_x(z),$$

where

E_x is the electric field intensity in the x direction,

H_y is the magnetic field strength in the y direction,

μ_0 is the permeability of vacuum,

$\varepsilon(z)$ is the permittivity of the earth,

ω is the angular frequency,

x,y, and z are defined in Figure 2-1.

In addition to plane waves, Becher also treated the case of a man-made source (a current distribution) and derived equations for this situation as well. Becher also made several extensions of Sharpe's work. First, he showed that the lossy line (R-L line), where $\sigma >> \omega\varepsilon$, can be cast in the form of Equations 2-20, and 2-21, which were derived for the lossless line (L-C line), where $\omega\varepsilon >> \sigma$. Becher then proceeded to derive a transformation between these cases. For the R-L line,

$$2\text{-}46 \quad \frac{dE(z,\omega)}{dz} = -j\omega\mu_0 H_z(z,\omega)$$

$$\frac{dH(z,\omega)}{dz} = -\sigma(z)E(z,\omega),$$

where

$\sigma(z)$ is the conductivity of the earth.

If

$$2\text{-}47 \quad \mu_0 = L \text{ and } j\omega = \gamma^2,$$

then

$$2\text{-}48 \quad j\omega\mu_0 H(z,\omega) = -j\gamma L\,[j\gamma H(z,-j\gamma^2)].$$

Define

$$2\text{-}49 \quad \tilde{H}(z,\gamma) \equiv j\gamma H(z,-j\gamma^2),$$
$$\tilde{E}(z,\gamma) \equiv E(z,-j\gamma^2)$$

The result is

$$2\text{-}50 \quad \frac{d\tilde{E}(z,\gamma)}{dz} = -j\gamma L\,\tilde{H}(z,\gamma),$$

and

$$2\text{-}51 \quad \frac{d\hat{H}(z,\gamma)}{dz} = -j\gamma C(z)\,\hat{E}(z,\gamma),$$

where C represents σ and γ represents the transformed angular frequency. Equations 2-50 and 2-51 are in the form of the lossless transmission line equations.

A second extension of Sharpe's work due to Becher concerns distance normalization. Sharpe dealt with lossless transmission lines where the speed of propagation changes only slightly over distances which are small compared to the wavelength. Hence, his normalized distance, x, is approximately proportional to the true distance, z.

$$2\text{-}52 \quad x = \frac{1}{\omega}\int_0^z \beta(t)dt \approx \frac{1}{\omega}\int_0^z \beta dt \approx \frac{\beta}{\omega}z.$$

For the geoelectric problem, however, this is no longer true. Becher derived a differential equation relating x and z and proceeded to solve it. By substituting the results into Sharpe's equations, Becher was able to express the variation of permittivity as a function of true distance.

Requirements For Using Becher's Method

The source of electromagnetic energy, the data collection process, and the medium whose permittivity variations are being measured, must each satisfy certain requirements. First, consider the requirements for the source. Becher considered two cases, a plane wave source, and a line source. In the first case, the plane waves were assumed to originate from natural

electromagnetic disturbances due to fluctuations in ionospheric currents. In general, these plane waves are very low frequency: usually the lowest frequency is less than one Hz. If plane waves are not available, one must use a line source. In either case, the source must have a fairly broad bandwidth. The bandwidth depends on the expected change in the permittivity as a function of depth, and can be estimated by exploiting the fact that the relationship between the reflection coefficient, $\Gamma(2\beta)$, and the log of the characteristic impedance is in the form of a Fourier transform.

2-53 $$\Gamma(2\beta) = \frac{1}{2}\int_{-\infty}^{\infty} e^{-j2\beta z}\frac{d}{dz}\,[\ln Z(z)]dz.$$

If $Z(z)$ is considered to be the impulse response and $\Gamma(2\beta)$ is considered to be the bandwidth, then the product of the bandwidth, B, and the impulse response, R, of $\frac{d\ln Z(z)}{dz}$ is

2-54 $$BR>2.$$

B and R are both measured in the radius of gyration sense. For an example worked by Becher, the required bandwidth is three decades.

The data required by the method are the surface electric and magnetic fields. For the case of a plane wave source, it is sufficient to measure the electric field intensity vector and magnetic field strength vector perpendicular to it at a single point. Note that both vectors are in the plane of the surface. When a line source is used, however, it becomes necessary to measure the fields over the entire surface. In general,

it is possible to choose a current distribution which gives azimuthal symmetry. In this case, one needs to measure only the magnetic and electric fields along a line passing through the point where the permittivity profile is desired. For a line source, the data are the input admittances

$$2\text{-}55 \quad Y(0,\omega) = \int_0^\infty H_y(y,0,\omega)\,dy \Big/ \int_0^\infty E_x(y,0,\omega)\,dy$$

for all frequencies. (The coordinates are defined in Figure 2-1.) As a practical matter, one can truncate the integration at some finite value of y. This point will be explored in more detail in Chapter 3 of Part II.

The Marchenko-Sharpe-Becher method is not entirely general, because it does not apply to an arbitrary permittivity variation. Certain restrictions are placed on the medium. To begin, it is assumed that σ and ε are constant on any plane parallel to the surface and that σ and ε for large z, (displacement perpendicular to the surface), approach constants faster than $1/z^2$. In addition, this technique requires that either $\sigma >> \omega\varepsilon$ or $\omega\varepsilon >> \sigma$, and that ε or σ (dependent upon which is the variable of interest) be constant with respect to the frequency, that is, that the medium be nondispersive.

Conclusions

As noted in Chapter 1 of Part II, the data collected in Part I show that soil cannot be regarded as nondispersive except possibly over a small range between a few megahertz and a few gigahertz. In this range, however, $\omega\varepsilon$ and σ are of com-

parable magnitude so that neither $\omega\varepsilon >> \sigma$ nor $\sigma >> \omega\varepsilon$ holds. Furthermore, over this range the conductivity is changing with respect to frequency.

These facts imply that the Marchenko-Sharpe-Becher method cannot be applied to the moisture profile problem. Two basic improvements are required: the general lossy case should be included in the scope of the method and knowledge of the surface fields at only a single frequency should be necessary. Both of these extensions appear to involve considerable changes in the development. A method which incorporates these improvements was developed thirty-five years before the Marchenko-Sharpe-Becher method, and this technique, due to Slichter, will be presented in the next chapter.

CHAPTER 3

SLICHTER'S METHOD

Slichter's method (31) uses an antenna on the surface of the earth to radiate waves into the ground. Information collected at the surface is then used to characterize the electrical permittivity and conductivity profile of the earth, vertically downward. It is believed that this method can be applied to the problem of soil moisture measurement. Consequently, it is discussed in considerably more detail than was the Marchenko-Sharpe-Becher method.

Presentation of the Method

A circular current sheet is located on the planar interface between two semi-infinite half-spaces, in which the electrical permittivity and conductivity vary only with depth, as shown in Figure 2-2. For reasons of convenience in analysis, this ϕ-directed surface current density, $I(\rho)$, is chosen such that

$$I(\rho) = \rho/a, \qquad 0 < \rho < a,$$

$$I(\rho) = 1/2, \qquad \rho = a,$$

$$I(\rho) = 0, \qquad \rho > a,$$

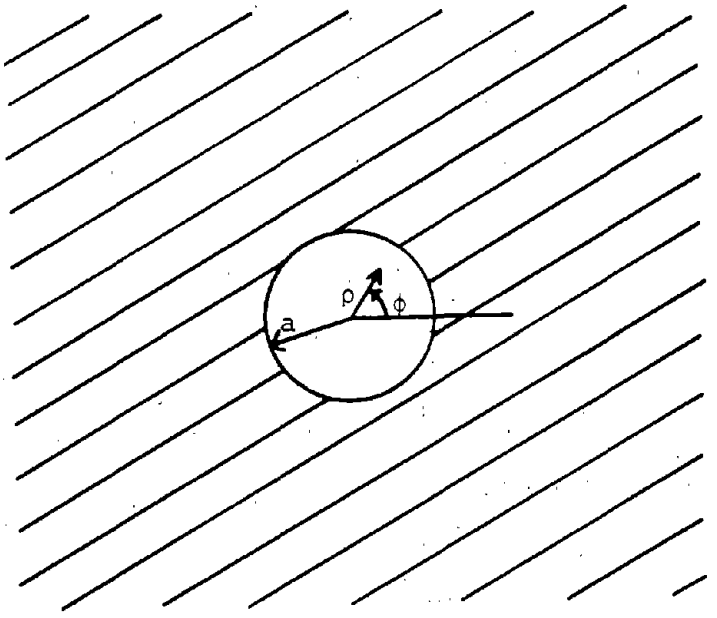

Top View

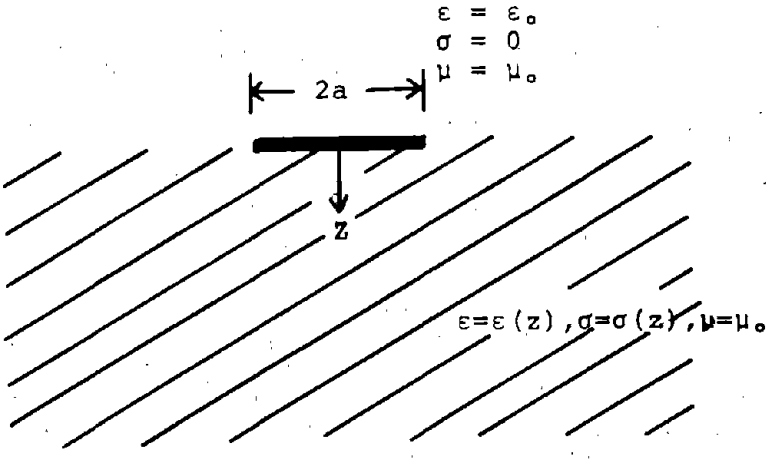

Side View

Figure 2-2. Current source on the earth.

where a is the radius of the disc of current, as shown in Figure 2-2. This current density varies sinusoidally in time with angular frequency ω. The problem is to determine the permittivity, $\varepsilon(z)$, and the conductivity, $\sigma(z)$, from measurements made at the surface, $z = 0$.

The first step is to formulate the problem in terms of Maxwell's equations and then obtain a formal solution. Maxwell's equations deal with the electromagnetic field: E, the electric field strength, and B, the magnetic induction, which are due to the current distribution on the plane, $z = 0$. Subscripts on these variables refer to the direction of these vector quantities. Symmetry implies that B_ϕ is everywhere zero. Likewise, E_ρ and E_z are everywhere zero, as can be seen from the following Maxwell equation, in cylindrical coordinates (ρ,ϕ,z).

$$2\text{-}56 \qquad (\sigma + j\omega\varepsilon)\vec{E} = \frac{1}{\rho}\left(\frac{\partial H_z}{\partial \phi} - \frac{\partial H_\phi}{\partial z}\right)\vec{\rho} + \left(\frac{\partial H_\rho}{\partial z} - \frac{\partial H_z}{\partial \rho}\right)\vec{\phi} + \frac{1}{\rho}\left(\frac{\partial (\rho H_\phi)}{\partial \rho} - \frac{\partial H_\rho}{\partial \phi}\right)\vec{z},$$

where H is the magnetic field strength. Recall that $H = B/\mu$, where μ is the permeability, and that symmetry implies that $\frac{\partial}{\partial \phi}$ operating on any vector is zero. Since B_ϕ is zero, so also is H_ϕ. Hence

$$2\text{-}57 \qquad (\sigma + j\omega\varepsilon)\vec{E} = \left(\frac{\partial H_\rho}{\partial z} - \frac{\partial H_z}{\partial \rho}\ \vec{\phi}.\right)$$

Maxwell's equations then can be written, using the customary phasor notation.

$$2\text{-}58 \quad \frac{\partial}{\partial z}\left(\frac{B}{\mu}\right)_\rho - \frac{\partial}{\partial \rho}\left(\frac{B}{\mu}\right)_z = (\sigma + j\omega\epsilon)E_\phi$$

$$2\text{-}59 \quad \frac{\partial E_\phi}{\partial z} = j\omega B_\rho$$

$$2\text{-}60 \quad \frac{\partial E_\phi}{\partial \rho} + E_\phi/\rho = -j\omega B_z$$

$$2\text{-}61 \quad \nabla \cdot \vec{B} = 0$$

$$2\text{-}62 \quad \nabla \cdot \epsilon\vec{E} = \rho_c,$$

where ρ_c is the volume charge density. The boundary conditions at $z = 0$ are

$$2\text{-}63 \quad (E_\phi)_{+z} = (E_\phi)_{-z},$$

$$2\text{-}64 \quad (B_z)_{+z} = (B_z)_{-z},$$

$$2\text{-}65 \quad (B_\rho)_{+z} = (B_\rho)_{-z} + \mu_o I(\rho),$$

where $I(\rho)$ is the ϕ - directed surface current density flowing in the surface $z = 0$.

From this point on, the electric field strength in the ϕ direction will be denoted by E. This should not cause any confusion since the ϕ component is the only nonzero component of the electric field strength.

Substituting Equations 2-59 and 2-60 into 2-58, yields

$$2\text{-}66 \quad \frac{\partial^2 E}{\partial z^2} + \frac{\partial^2 E}{\partial \rho^2} + \frac{1}{\rho}\frac{\partial E}{\partial \rho} - \frac{E}{\rho^2} = j\omega\mu[\sigma + j\omega\epsilon]E.$$

By separating variables, ($E = R(\rho)\ Z(z)$) one obtains the Bessel equation

$$2\text{-}67 \quad \frac{d^2R}{d\rho^2} + \frac{1}{\rho}\frac{dR}{d\rho} + (\lambda^2 - 1/\rho^2)R = 0,$$

where λ is the separation constant, and the equation

$$2\text{-}68 \quad \frac{d^2Z}{dz^2} - (\lambda^2 + j\omega\mu\sigma - \omega^2\mu\varepsilon)Z = 0.$$

Above the surface, $z < 0$, where $\varepsilon = \varepsilon_o$ and $\sigma = 0$, this last equation simplifies to

$$2\text{-}69 \quad \frac{d^2Z}{dz^2} - (\lambda^2 - \frac{\omega^2}{c^2})Z = 0,$$

$$2\text{-}70 \quad Z = D(\lambda) \exp\left(\pm\sqrt{\lambda^2 - k_o^2}\, z\right),$$

where $k_o = \omega/c$, and c is the speed of light.

Returning to Equation 2-67, it is clear that $R = J_1(\lambda\rho)$, since E and B remain finite at $\rho = 0$. Let the solution to Equation 2-68, which vanishes at $z \to +\infty$, be denoted by $Z_1(z,\lambda)$. Now recall that the electric field, which is the solution to Equation 2-66, is a product solution. In order to satisfy the boundary conditions, this product must be integrated with respect to the separation constant, λ.

$$2\text{-}71 \quad E_+ = E(z) = \int_o^\infty J_1(\lambda\rho)\, F_1(\lambda)\, Z_1(z,\lambda)\, d\lambda, \quad z > 0$$

$$2\text{-}72 \quad E_- = E(z) = \int_o^\infty J_1(\lambda\rho)\, F_2(\lambda) \exp\left(\sqrt{\lambda^2 - k_o^2}\, z\right) d\lambda, \quad z < 0,$$

where F_1 and F_2 are functions chosen such that the integrals converge and satisfy the boundary conditions. The first of these conditions requires that the plus sign be used in $\exp\left(\pm\sqrt{\lambda^2 - k_o^2}\, z\right)$ for $z < 0$, since $\lambda^2 > k_o^2$ for $\lambda \to \infty$. Since $E_+ = E_-$ at $z = 0$ for all λ, it is clear that

2-73 $F_2(\lambda) = F_1(\lambda)\ Z_1(0,\lambda)$.

Now the boundary condition on the magnetic induction can be used to determine F_1, by using Equations 2-65 and 2-59:

2-74 $(B_\rho)_{+z} - (B_\rho)_{-z} = \mu_o I(\rho)$,

2-75 $\left(\frac{\partial E_+}{\partial z}\right)_{+0} - \left(\frac{\partial E_-}{\partial z}\right)_{-0} = j\omega\mu_o I(\rho)$.

Substituting 2-71, 2-72, and 2-73 into 2-75 yields

2-76 $$\int_0^\infty J_1(\lambda\rho)\ F_1(\lambda)\left\{\frac{\partial Z_1(0,\lambda)}{\partial z} - Z_1(0,\lambda)\ \sqrt{\lambda^2 - k_o^2}\right\} d\lambda = j\omega\mu_o I(\rho).$$

Our particular choice of $I(\rho)$ makes it especially easy to determine F_1 since a well-known integral is

2-77 $$a\int_0^\infty J_1(\lambda\rho)\ J_2(\lambda a)d\lambda = \begin{cases} \rho/a, & 0<\rho/a<1 \\ 1/2, & \rho/a = 1 \\ 0, & \rho/a>1. \end{cases}$$

By using Equations 2-55, 2-76, and 2-77, one can conclude that in our case

2-78 $$ja\omega\mu_o J_2(\lambda a) = F_1(\lambda)\left\{\frac{\partial Z_1(0,\lambda)}{\partial z} - Z_1(0,\lambda)\ \sqrt{\lambda^2 - k_o^2}\right\},$$

for all λ.

Now the solution for E_+ can be written

2-79 $$E_+ = ja\ \omega\mu_o \int_0^\infty \frac{J_2(\lambda a)J_1(\lambda\rho)Z_1(z,\lambda)d\lambda}{\frac{\partial Z_1(0,\lambda)}{\partial z} - \sqrt{\lambda^2 - k_o^2}\ Z_1(0,\lambda)}.$$

Provided that the integrals converge uniformly, B_z and B_ρ for $z>0$ are given by

$$2\text{-}80 \quad B_\rho(z,\rho) = \frac{1}{j\omega}\frac{\partial E_\phi}{\partial z} = a\mu_o\int_o^\infty \frac{J_2(a\lambda)J_1(\rho\lambda)\frac{\partial}{\partial z}Z_1(z,\lambda)}{\frac{\partial Z_1(0,\lambda)}{\partial z} - \sqrt{\lambda^2 - k_o^2}Z_1(0,\lambda)}\,d\lambda,$$

$$2\text{-}81 \quad B_z(z,\rho) = -\frac{1}{j\omega}\left[\frac{\partial E_\phi}{\partial \rho} + \frac{E_\phi}{\rho}\right] = -a\mu_o\int_o^\infty \frac{\lambda J_2(a\lambda)J_o(\rho\lambda)Z_1(z,\lambda)}{\frac{\partial Z_1(0,\lambda)}{\partial z} - \sqrt{\lambda^2 - k_o^2}Z_1(0,\lambda)}\,d\lambda.$$

Slichter (31) shows that indeed these integrals in Equations 2-79, 2-80, and 2-81 do converge uniformly, if

$$\lim_{z\to\infty} \varepsilon(z) < \varepsilon_2 \text{ (a constant)}$$

and

$$\lim_{z\to\infty} \sigma(z) = \sigma_2 \text{ (a constant)}.$$

From the physical considerations of the present problem, these are acceptable restraints, since the electromagnetic field will penetrate, effectively, no more than a few meters into the earth, and no exceptionally large values of ε or of σ normally occur at such depths.

A formal solution for the electromagnetic fields has been found, but it involves an unknown function, $Z_1(z,\lambda)$. This function must be related to some quantity which can be measured. Fortunately, one can relate Z_1 to the magnetic fields at the surface. To begin, write B_ρ and B_z for $z = 0$ in the forms

$$2\text{-}82 \quad B_\rho(0,\rho) = \int_o^\infty J_1(\lambda\rho)\, k_\rho(\lambda)\,d\lambda,$$

$$2\text{-}83 \quad B_z(0,\rho) = \int_o^\infty J_o(\lambda\rho)\, k_z(\lambda)\,d\lambda,$$

where

$$2\text{-}84 \quad k_\rho(\lambda) = a\mu_o J_2(\lambda a)\, \frac{\partial Z_1(0,\lambda)}{\partial z} \Big/ \left(\frac{\partial Z_1(0,\lambda)}{\partial z} - \sqrt{\lambda^2 - k_o^2}\, Z_1(0,\lambda)\right)$$

$$2\text{-}85 \quad k_z(\lambda) = -a\mu_o \lambda J_2(\lambda a)\, Z_1(0,\lambda) \Big/ \left(\frac{\partial Z_1(0,\lambda)}{\partial z} - \sqrt{\lambda^2 - k_o^2}\, Z_1(0,\lambda)\right).$$

The objective is to invert these equations for the magnetic fields in order to obtain expressions for k_ρ and k_z in terms of the surface magnetic fields. Now the Fourier-Bessel theorem states that

$$2\text{-}86 \quad F(r) = \int_o^\infty J_\nu(\mu r)\,\mu d\mu \int_o^\infty F(R) J_\nu(\mu R)\, R dR,$$

provided $\int_o^\infty F(R) R^{1/2} dR$ is absolutely convergent.

B_ρ is everywhere finite and vanishes at infinity at least as rapidly as $1/\rho^2$. Therefore, $\int_o^\infty B_\rho \rho^{1/2} d\rho$ is absolutely convergent. B_z is everywhere finite, but vanishes at infinity as $1/\rho$ in the lossless case. However, loss does in fact occur, hence an attenuation factor proportional to $e^{-\alpha\rho}$ must be included in the expression for B_z. So, asymptotically, B_z can be expressed as $Be^{-\alpha\rho}/\rho$, where B is a constant. Therefore, $\int_o^\infty B_z \rho^{1/2} d\rho$ is absolutely convergent.

Expressing B_ρ and B_z in terms of their real and imaginary parts and, substituting into the Fourier-Bessel theorem, one obtains

$$2\text{-}87 \quad B'_\rho(0,\rho) = \int_o^\infty J_1(\lambda\rho)\lambda d\lambda \int_o^\infty B'_\rho(0,\xi) J_1(\lambda\xi)\xi d\xi,$$

$$2\text{-}88 \quad B''_\rho(0,\rho) = \int_o^\infty J_1(\lambda\rho)\lambda d\lambda \int_o^\infty B''_\rho(0,\xi) J_1(\lambda\xi)\xi d\xi,$$

$$2\text{-}89 \quad B'_z(0,\rho) = \int_o^\infty J_o(\lambda\rho)\lambda d\lambda \int_o^\infty B'_z(0,\xi) J_o(\lambda\xi)\xi d\xi,$$

$$2\text{-}90 \quad B''_z(0,\rho) = \int_0^\infty J_0(\lambda\rho)\,\lambda d\lambda \int_0^\infty B''_z(0,\xi) J_0(\lambda\xi)\,\xi d\xi,$$

where $B_\rho = B'_\rho + jB''_\rho$ and $B_z = B'_z + jB''_z$.

By comparison of Equations 2-87 through 2-90 with Equations 2-82 and 2-83, one can see that, since Equations 2-87 through 2-90 must be valid for all values of ρ,

$$2\text{-}91 \quad k'_\rho(\lambda) = \lambda \int_0^\infty B'_\rho(0,\rho) J_1(\lambda\rho)\,\rho d\rho,$$

$$2\text{-}92 \quad k''_\rho(\lambda) = \lambda \int_0^\infty B''_\rho(0,\rho) J_1(\lambda\rho)\,\rho d\rho,$$

$$2\text{-}93 \quad k'_z(\lambda) = \lambda \int_0^\infty B'_z(0,\rho) J_0(\lambda\rho)\,\rho d\rho,$$

$$2\text{-}94 \quad k''_z(\lambda) = \lambda \int_0^\infty B''_z(0,\rho) J_0(\lambda\rho)\,\rho d\rho,$$

where

$$k_\rho = k'_\rho + jk''_\rho,$$

$$k_z = k'_z + jk''_z.$$

Now define the quantity

$$2\text{-}95 \quad K(\lambda,0) \equiv \frac{k_\rho(\lambda)}{k_z(\lambda)}$$

and note from Equations 2-84, 2-85, and 2-95 that

$$2\text{-}96 \quad K(\lambda,0) = \left[\frac{-\frac{\partial Z_1(z,\lambda)}{\partial z}}{\lambda Z_1(z,\lambda)} \right]_{z=0}.$$

Furthermore, it now is shown that $K(\lambda,0)$ can be expressed in terms of measurable quantities, the surface fields. By using Equations 2-91 through 2-94 and Equation 2-95, one can write

$$2\text{-}97 \quad K(\lambda,0) = \frac{\int_0^\infty B'_\rho(0,\rho)J_1(\lambda\rho)\rho d\rho + j\int_0^\infty B''_\rho(0,\rho)J_1(\lambda\rho)\rho d\rho}{\int_0^\infty B'_z(0,\rho)J_0(\lambda\rho)\rho d\rho + j\int_0^\infty B''_z(0,\rho)J_0(\lambda\rho)\rho d\rho} .$$

Now a relationship must be found between Z_1 and the desired quantities, $\varepsilon(z)$ and $\sigma(z)$. This relationship will take the form of a MacLaurin series expansion. As was indicated in the General Approach given in Chapter 1 of Part II, the starting point for finding the relationship is the substitution of Z_1 into Maxwell's equations. Recall Equation 2-68, whose solution is Z_1, for $z > 0$.

$$2\text{-}98 \quad \frac{\partial^2}{\partial z^2} Z_1 - (\lambda^2 + j\omega\mu\sigma - \omega^2\mu\varepsilon) Z_1 = 0.$$

For large λ,

$$2\text{-}99 \quad Z_1(z,\lambda) \approx c(\lambda)e^{-\lambda z}.$$

Therefore, we may write

$$2\text{-}100 \quad \lim_{\lambda\to\infty} K(\lambda) \equiv -\lim_{\lambda\to\infty} \frac{\frac{\partial Z_1(0,\lambda)}{\partial z}}{\lambda Z_1(0,\lambda)} = 1.$$

Hence, for large values of λ, one can write

$$2\text{-}101 \quad K(\lambda) \approx \sum_{n=0}^{\infty} a_n \lambda^{-n}, \quad (z = 0),$$

where a_n are constants, and $a_0 = 1$.

Substitute

$$2\text{-}102 \quad Y(z,\lambda) \equiv \frac{-\frac{\partial}{\partial z} Z_1(z,\lambda)}{Z_1(z,\lambda)} \equiv \lambda K(\lambda,z)$$

into Equation 2-98 to obtain

2-103 $$\frac{\partial v}{\partial z} - v^2 + (\lambda^2 + j\omega\mu\sigma - \omega^2\mu\varepsilon) = 0.$$

For large λ, the asymptotic expression for v is

2-104 $$v(z,\lambda) = \lambda \sum_{n=0}^{\infty} \alpha_n(z)\lambda^{-n},$$

where $\alpha_n(z)$ is a function of z. It is clear from Equations 2-101 and 2-102 that

2-105 $$\lim_{z\to 0} v(z,\lambda) \to \lambda K(\lambda),$$

for all λ, so

2-106 $$\lim_{z\to 0} \alpha_n(z) \to a_n.$$

Now it is possible to show that, for all z,

2-107 $$\alpha_o = 1.$$

The argument to prove this is as follows. From Equation 2-104 we see that, for all z,

2-108 $$\lim_{\lambda\to\infty} v(z,\lambda) = \lambda\alpha_o.$$

Now, from Equation 2-68, with ε, μ, and σ bounded for all z, and for finite ω, we have

2-109 $$\frac{\partial^2 Z_1}{\partial z^2} - [\lambda^2 + f(z)]Z_1 = 0,$$

where now f(z) is bounded for all z. Hence

2-110 $$\lim_{\lambda\to\infty} Z_1(z) = Ae^{\pm\lambda z},$$

where A is an arbitrary constant and the plus sign in the exponent must be discarded because $Z_1(z)$ must be finite for all positive values of z. Then, from Equations 2-102, 2-108, and 2-110, it can be seen that

$$2\text{-}111 \qquad \alpha_0 = \lim_{\lambda\to\infty} \frac{v(z,\lambda)}{\lambda} = -\lim_{\lambda\to\infty} \frac{\frac{\partial}{\partial z} Z_1(z,\lambda)}{\lambda Z_1(z,\lambda)} = 1,$$

for all z.

To find expressions for the other α_n, we proceed as follows. Substitute the series expansion for v into the Riccati equation which v satisfies, Equation 2-103:

$$2\text{-}112 \qquad \lambda\sum_{n=0}^{\infty} \frac{d\alpha}{dz}\lambda^{-n} - \lambda^2\sum_{n=0}^{\infty} \sum_{r=0}^{n} \alpha_r\alpha_{n-r}\lambda^{-n} + \lambda^2 - \omega^2\mu\varepsilon + j\omega\mu\sigma = 0.$$

Algebraic simplification yields

$$2\text{-}113 \qquad \sum_{n=-1}^{\infty} \lambda^{-n} \left[- \frac{d\alpha_{n+1}}{dz} + \sum_{r=0}^{n+2} \alpha_r\alpha_{n+2-r} \right] = j\omega\mu\sigma - \omega^2\mu\varepsilon.$$

Note that the right-hand side is independent of λ, hence the left is also. Therefore,

$$2\text{-}114 \qquad n \neq 0, \quad \frac{d\alpha_{n+1}}{dz} = \sum_{r=0}^{n+2} \alpha_r\, \alpha_{n+2-r},$$

$$2\text{-}115 \qquad n = -1, \quad \frac{d\alpha_0}{dz} = 0 \Leftarrow 2\alpha_0\alpha_1 \rightarrow \alpha_1 = 0,$$

$$2\text{-}116 \qquad n = 0, \quad 2\alpha_2 = j\omega\mu\sigma - \omega^2\mu\varepsilon.$$

Given $\alpha_2(z)$, a complex function of z, $\sigma(z)$ and $\varepsilon(z)$ can be calculated assuming that ω and μ are constant and known.

Now, assume that $\sigma(z)$ and $\varepsilon(z)$ are sufficiently smooth so that all derivatives of interest exist. Granting this, Equation 2-116 shows that all derivatives of interest also exist for $\alpha_2(z)$. So $\alpha_2(z)$ can be expanded in a MacLaurin series.

$$2\text{-}117 \quad \alpha_2(z) = \alpha_2(0) + \frac{d\alpha_2}{dz}\bigg|_0 z + \frac{d^2\alpha_2}{dz^2}\bigg|_0 \frac{z^2}{2!} + \cdots$$

The coefficients of this series can be determined from Equation 2-114. Since

$$2\text{-}118 \quad \alpha_n(z) \to a_n, \text{ as } z \to 0,$$

$$2\text{-}119 \quad \alpha_0(0) = a_0 = 1,$$

$$2\text{-}120 \quad \frac{d\alpha_2(0)}{dz} = 2\alpha_3(0) = 2a_3$$

$$2\text{-}121 \quad \frac{d^2\alpha_2(0)}{dz^2} = 2\frac{d\alpha_3(0)}{dz} = 4a_4 + 2a_2^2$$

$$2\text{-}122 \quad \frac{d^3\alpha_2(0)}{dz^3} = \frac{d^2}{dz^2}\left(2\alpha_0(0)\alpha_3 + \alpha_1\alpha_2 + \alpha_2\alpha_1\right)$$

Evaluating the derivatives using Equation 2-114,

$$2\text{-}123 \quad \frac{d^3\alpha_2(0)}{dz^3} = 8a_5 + 16a_3a_2.$$

$$2\text{-}124 \quad \frac{d^4\alpha_2(0)}{dz^4} = 16a_6 + 48a_4a_2 + 40a_3^2 + 16a_2^3$$

To recapitulate, Equation 2-116 shows that

$$2\text{-}125 \quad \varepsilon(z) = \frac{2}{-\omega^2\mu}\,\mathrm{Re}[\pm\alpha_2(z)].$$

Now $\alpha_2(z)$ can be expressed as a MacLaurin series and the coefficients of this series can be related to the kernel, $K(\lambda)$.

It is worth noting at this point that $K(\lambda)$ can be determined from knowledge of only one component of the surface magnetic field instead of both, as was done in Equation 2-95. To see this, recall that

$$2\text{-}126 \qquad K(\lambda) = \frac{\dfrac{-\partial Z_1(0,\lambda)}{\partial z}}{\lambda Z_1(0,\lambda)}$$

Recall also, from Equation 2-85, that

$$2\text{-}127 \qquad k_z = -a\mu_o J_2(\lambda a)\ \lambda Z_1(0,\lambda) \Big/ \left[\frac{\partial}{\partial z} Z_1(0,\lambda) - Z_1(0,\lambda)(\lambda^2 - k_o^2)^{1/2}\right]$$

Solving algebraically for $[-\partial Z_1(0,\lambda)/\partial z]/[\lambda Z_1(0,\lambda)]$ in Equation 2-127, yields

$$2\text{-}128 \qquad K(\lambda) = -\frac{\dfrac{\partial}{\partial z} Z_1(0,\lambda)}{\lambda Z_1(0,\lambda)} = \frac{a\mu_o J_2(\lambda\alpha)}{k_z(\lambda)} - \frac{(\lambda^2 - k_o^2)^{1/2}}{\lambda}\ .$$

One can summarize the steps involved in the calculation of $\varepsilon(z)$ as follows:

(1) Create the current density given in Equation 2-55 and measure the magnitude and phase angle of the resulting z component of the magnetic field at the surface.

(2) Using Equations 2-93 and 2-94, calculate $k_z(\lambda)$.

(3) Using Equation 2-128, calculate $K(\lambda)$.

(4) Approximate $K(\lambda)$ by a power series. If λ^{-1} is taken as the variable, any of the many techniques for polynomial approximation may be used. The reader is referred to any standard text in numerical anaylsis.

(5) Using the coefficients, $\{a_i\}$ calculated in step 4, calculate the coefficients of the MacLaurin series, 2-117, using Equations 2-114 and 2-115, as shown in this section.

(6) Calculate $\alpha_2(z)$ using the MacLaurin series, Equation 2-117.

(7) Calculate $\varepsilon(z)$ using Equation 2-125.

Requirements for Using Slichter's Method

The specifications for the source of electromagnetic waves are very explicitly stated in Equation 2-55. The current distribution used in Equation 2-55, however, was chosen for mathematical convenience and does not seem to represent a fundamental limitation. Note that the source radiates at a single frequency.

The requirements on the data collection are more stringent than those on the source. One must measure the magnetic fields on the surface of the earth. It is shown earlier in this chapter, however, that it is sufficient to measure only the z - component of the magnetic field. It is necessary, though, to measure both the magnitude and the phase of this component with respect to the source.

One may ask how practical these requirements are. First, consider the measurement of phase. When Slichter developed the method in 1933, the measurement of phase at high frequencies was a very difficult task. Since then, techniques have been developed to perform this type of measurement. For this particular case, it might be simplest to perform the measurement in two steps. First, the magnitude as a function of the radial distance could be measured and, secondly, the magnetic wave could be mixed with a wave of known amplitude and phase with respect to the source. The phase of the magnetic field could then be deduced by using the known information: both magnitudes, the magnitude of the sum, and the phase of the reference.

Another requirement of Slichter's method is that the data on the magnetic field must be collected on the surface of the earth along a line extending from the point where the permittivity profile is desired, radially outward to infinity. These data are used in Equation 2-128 in the process of calculating the kernel, which require the calculation

$$2\text{-}129 \quad k_z = \lambda \int_0^\infty B_z(0,\rho) J_o(\lambda\rho)\, \rho d\rho.$$

Obviously this requirement of making measurements of B_z to infinity, is impossible. As was noted in Chapter 1 of Part II, the earth is seldom homogeneous in directions parallel to the surface of the earth for long distances. It is also clear, however, that the integral in Equation 2-129 converges rapidly, since both B_z and $J_o(\lambda\rho)$ decrease rapidly with increasing ρ. k_z should be calculable to a good approximation by using data collected within only a circle of radius ρ_m of the point where the moisture profile is desired:

$$2\text{-}130 \quad k_z \simeq \int_0^{\rho_m} B_z(0,\rho) J_o(\lambda\rho)\, \rho d\rho.$$

In order to obtain an indication of the required magnitude of ρ_m, an example was worked. The procedure consisted of choosing a permittivity profile, calculating the exact kernel, using this to calculate the resulting exact surface magnetic field, then attempting to recover the kernel by using Equation 2-130 for various values of ρ_m. Figures 2-3 to 2-6 show the results, which are discussed later.

Consider the steps of the calculation in more detail.

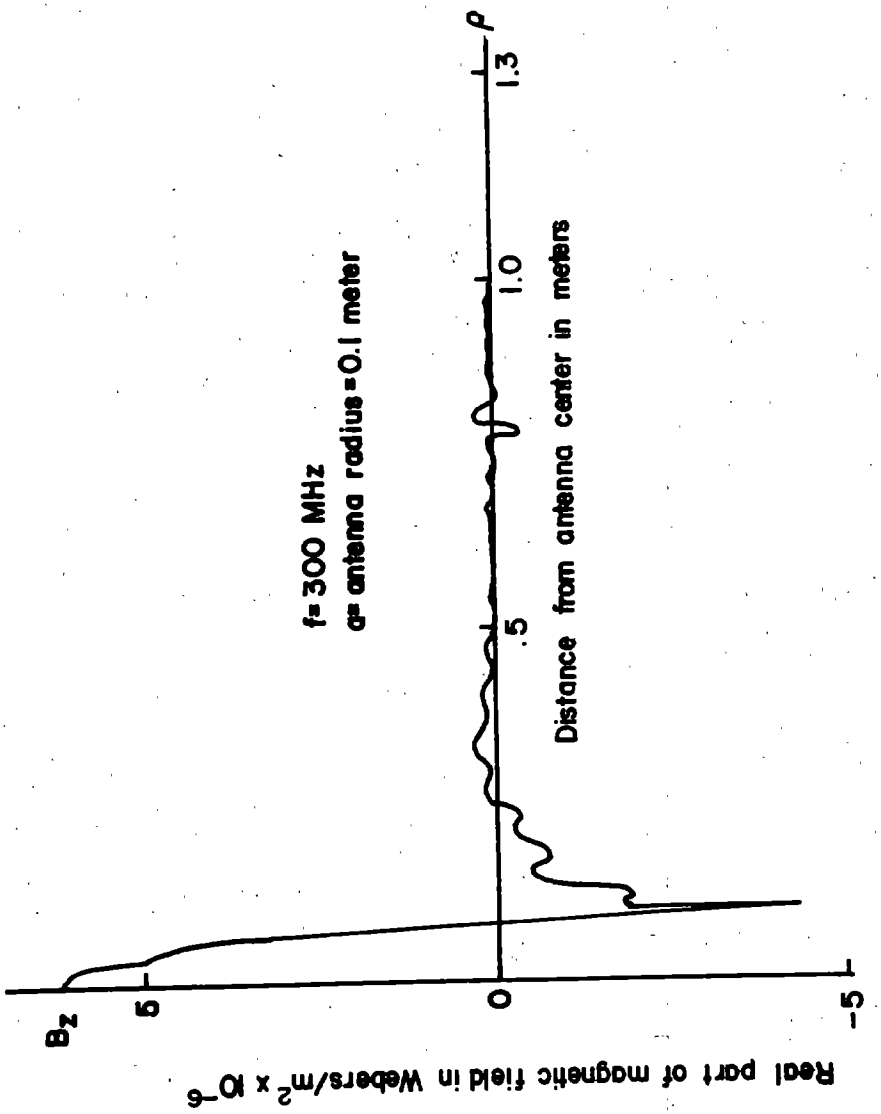

Figure 2-3. Real part of exact magnetic field. (B_z') as a function of distance from the center of the antenna.

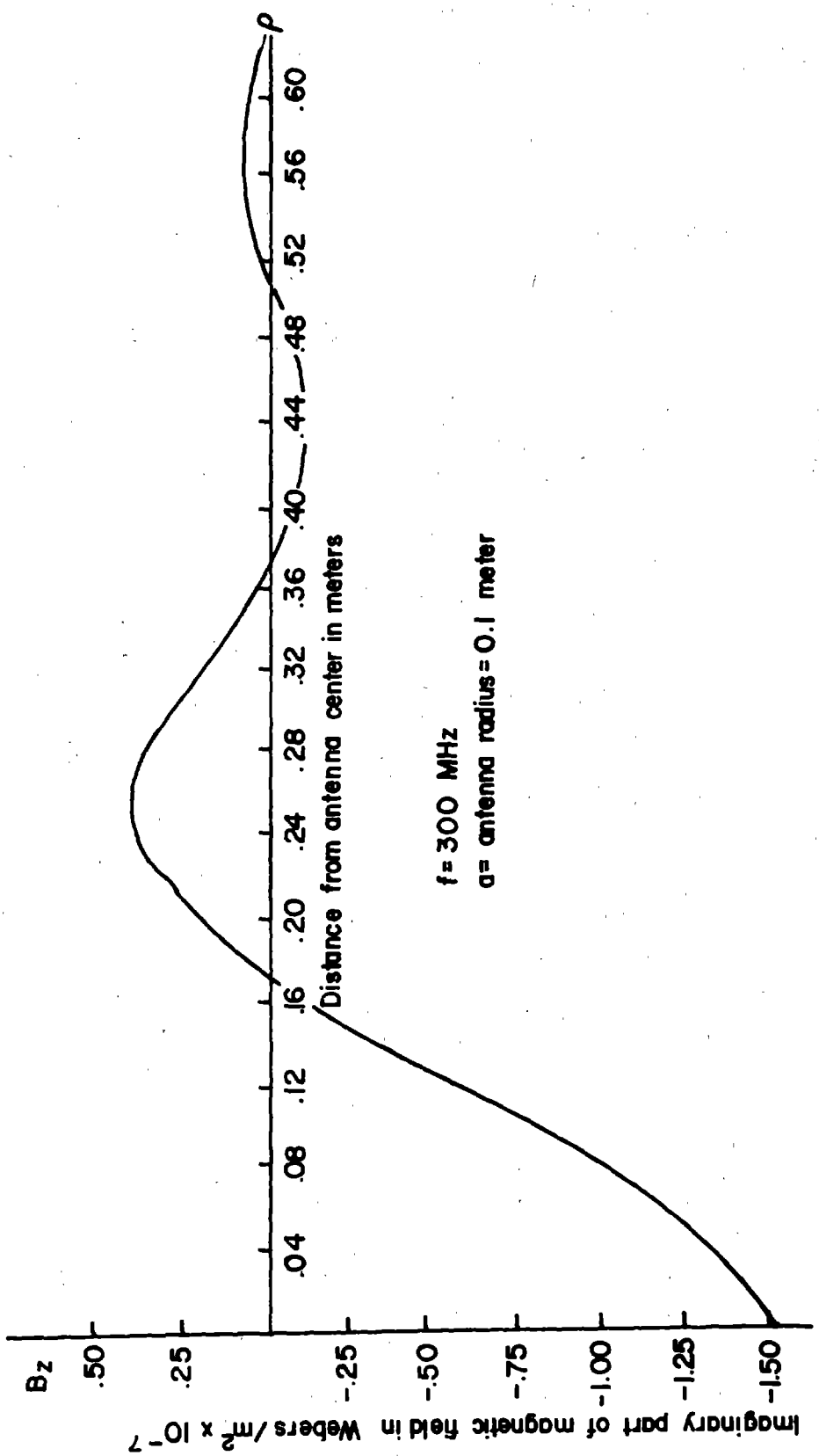

Figure 2-4. Imaginary part of exact magnetic field. (B_z") as a function of distance from the center of the antenna.

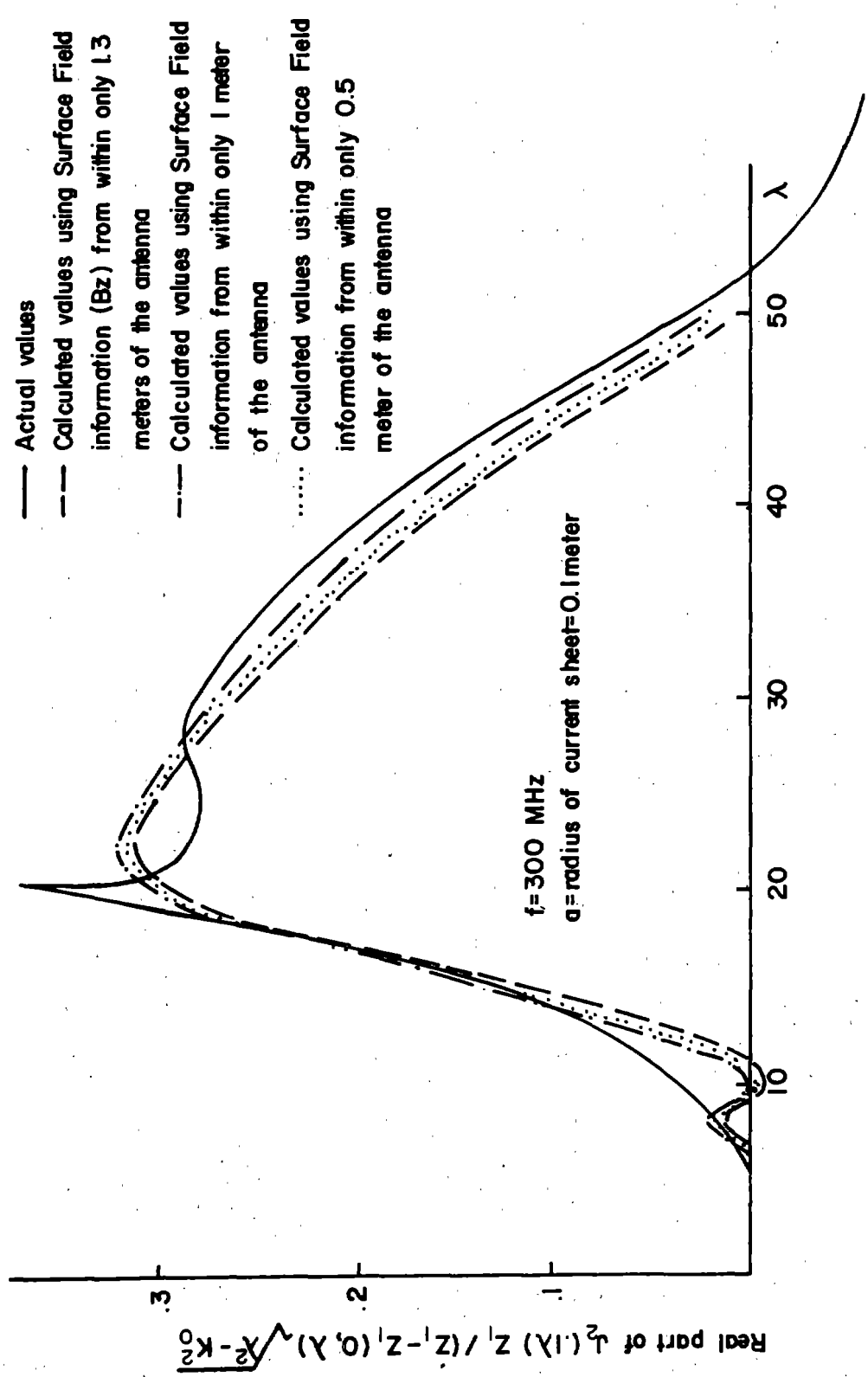

Figure 2-5. Real part of $J_2(.1\lambda)\ Z_1(0,\lambda)/\left(\frac{\partial Z_1(0,\lambda)}{\partial z} - Z_1(0,\lambda)\sqrt{\lambda^2-k_0^2}\right)$ versus the separation constant, λ. This is the real part of K_z, as given by Equation 2-85, divided by $(-a\ \mu_0\lambda)$.

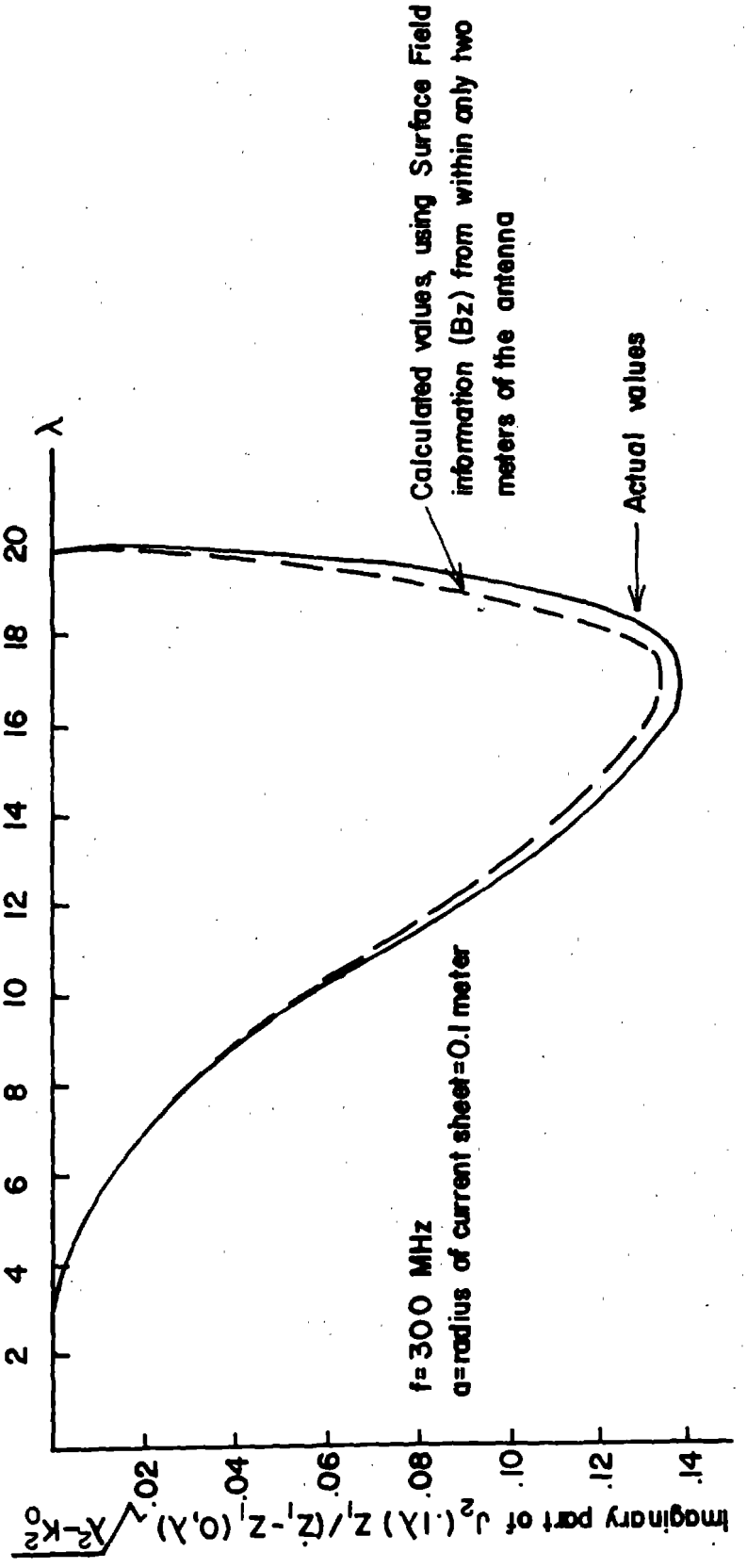

Figure 2-6. Imaginary part of $J_2(.1\lambda)\ Z_1(0,\lambda) \ / \ \frac{\partial Z_1(0,\lambda)}{\partial z} - Z_1(0,\lambda)\ \sqrt{\lambda^2 - k_0^2}$ versus the separation constant, λ. This is the imaginary part of k_z as given by Equation 2-85, divided by $(-a\mu_0\lambda)$.

(1) A constant electrical permittivity profile was chosen to faciliate calculation. The actual value chosen for ϵ_r was 4.5.

(2) k_z was calculated by using the equation below

2-131 $$k_z = a\mu\lambda J_2(\lambda a) Z_1(0,\lambda) / \left[\frac{\partial Z_1}{\partial z}(0,\lambda) - \sqrt{\lambda^2 - k_o^2} Z_1(0,\lambda)\right]$$

In this particular case Z_1 can be calculated easily from Equation 2-68, because it is being assumed that $\sigma = 0$ and that $\epsilon(z) = 4.5$, a constant. The function, k_z, can be calculated exactly for each value of λ.

(3) Using the calculated exact values, for k_z, the z - component of the surface magnetic field was calculated according to Equation 2-83.

2-83 $$B_z(0,\rho) = \int_0^\infty J_o(\lambda\rho) k_z(\lambda) d\lambda.$$

B_z, of course, could not be evaluated exactly, since the integral in Equation 2-83 is not tabulated. It will be seen, however, that for the particular k_z in this example the integral converges rapidly. This enables one to estimate the quantity by calculating successive integrals for increasing values of the upper limit and checking the agreement. The difference between successive integrals is defined as D.

$$D = \frac{\left| \int_0^{\lambda_n} J_o(\lambda\rho) k_z(\lambda) d\lambda - \int_0^{\lambda_{n+1}} J_o(\lambda\rho) k_z(\lambda) d\lambda \right|}{\left| \int_0^{\lambda_n} J_o(\lambda\rho)\ k_z(\lambda) d\lambda \right|}.$$

When this quantity became less than 0.005, the estimate of $B_z(0,\rho)$ was accepted. This limit of 1/2% for D is consistent with the accuracies expected from this method of measuring soil moisture. The field components are sketched in Figures 2-3 and 2-4.

(4) Then a quantity proportional to k_z was calculated just as it normally would be in a practical implementation of Slichter's method using Equation 2-130.

$$k_z \simeq \int_0^{\rho_m} B_z(0,\rho) J_0(\lambda\rho)\rho d\rho. \qquad 2\text{-}130$$

The values of ρ_m used were 0.5 meter, 1.0 meter, 1.3 meters, and 2.0 meters. The results are plotted in Figures 2-5 and 2-6.

The reader may well be curious concerning the significance of these results. As was explained previously, the calculation of k_z, and then $K(\lambda)$ is a key step in the calculation of the permittivity. So, if it were impossible to calculate the kernel, Slichter's method would not be practical. The primary physical limitation in calculating the kernel is the lack of homogeneity in any plane parallel to the surface. Hence it is essential to verify that the kernel can be calculated by using data from within a limited surface area. The results thus far indicate that this can be done.

Another key step in the calculation depends upon expanding $\epsilon(z)$ and $\sigma(z)$, the permittivity and conductivity, in MacLaurin series. Since $\epsilon(z)$ and $\sigma(z)$, are physical

quantities, it is clear that step and oscillatory discontinuities are not possible. While this satisfies the purely theoretical requirements for a MacLaurin expansion, practical constraints dictate stronger conditions. Specifically, $\varepsilon(z)$ and $\sigma(z)$ should be reasonably smooth functions of z, requiring few therms for an accurate expansion.

As it turns out, the inherent limitations in resolution of about one-half wavelength, or about 5 inches or 12 cm (a commonly accepted limit for resolution in instruments utilizing wave phenomena) help to achieve this result. Spatial variations in permittivity and conductivity which are significantly smaller than the wavelength have little effect on the the reflected wave and are indistinguishable at the surface from smooth transitions. This artificial smoothing, due to the finite resolution of the system, causes no difficulty to soil scientists who seldom require fine resolution.

Review of Slichter's Method

The calculation of permittivity using Slichter's method can be outlined as follows:

(1) Generate an electromagnetic field by using a magnetic dipole antenna with the current distribution:

$$I(\rho) = \begin{cases} \rho/a, & 0<\rho<a, \\ 1/2, & \rho=a, \\ 0, & \rho>a. \end{cases} \qquad 2\text{-}131$$

The frequency should be of the order of 300 MHz, as shown in Part I.

(2) Measure the magnitude and phase with respect to source, of the z - component of the magnetic field along any line extending radially away from the antenna. This must be done out to a distance of about one wavelength (approximately one meter) from the center of the antenna.

(3) Calculate the kernel using the equation below.

$$2\text{-}132 \quad K(\lambda) = \frac{a\mu_o J_2(\lambda a)}{\lambda \int_o^{\rho_m} B_z(0,\rho) J_o(\lambda\rho)\rho d\rho} - \frac{\sqrt{\lambda^2 - k_o^2}}{\lambda} .$$

(4) Expand the kernel as a power series.

$$2\text{-}133 \quad K(\lambda) \approx \sum_{n=0}^{\infty} a_n \lambda^{-n} .$$

(5) By exploiting the relations outlined in this chapter, calculate the coefficients of the MacLaurin series expansion of α_2.

$$2\text{-}134 \quad \alpha_2(0) = a_2,$$
$$\dot{\alpha}_2(0) = 2a_3,$$
$$\ddot{\alpha}_2(0) = 2a_4 + a_2^2,$$
etc.

(6) Calculate $\alpha_2(z)$.

$$2\text{-}135 \quad \alpha_2(z) = \alpha_2(0) + \dot{\alpha}_2(0)\, z + \frac{\ddot{\alpha}_2(0)}{2} z^2 \ldots$$

(7) Calculate the permittivity.

$$2\text{-}136 \quad \epsilon = -\frac{2}{\omega^2 c^2} \mathrm{Re}[\alpha_2(z)].$$

Conclusions

Slichter's method appears to be feasible, since its assumptions and requirements seem to be consistent with the properties of soil reported in Part I of this thesis. In addition, modern technology can satisfactorily perform the operations required.

More work is required to implement the method. It would be useful to calculate a number of examples using different permittivity profiles. In addition, one should explore the possibility of relaxing the constraints on the current distribution (Equation 2-131). Perhaps the first extension should be an investigation of whether or not the method can be used if the current distribution consists of a circular ring of current. This would be one of the easiest current distributions to generate and one of the easiest about which to measure the resulting magnetic field. The questions of resolution in depth, accuracy of the results, and actual limit of the depth to which the moisture content can be measured, should also be investigated.

LIST OF REFERENCES

(1) Lukshin, A.A., T.I. Rumyantsova, and V.P. Kovrigo, "Magnetic Susceptibility of Main Soil Types of the Udmurt ASSR," Soviet Soil Science, N° 1, Jan., 1968.

(2) Edlefsen, N.E., "A Review of the Results of Dielectric Methods for Measuring Moisture Present in Materials," Agricultural Engineering, Vol. 14, 1933.

(3) Balls, W.L., "Rapid Estimation of the Water Content in Undisturbed Soil and Bales of Cotton," Nature, Vol. 129, 1932.

(4) Balls, W.L., "Capacitance Hygroscopy and Some of its Applications," Nature, Vol. 130, 1932.

(5) Cashen, G.H., "Measurements of the Electrical Capacity and Conductivity of Soil Blocks," Journal of Agricultural Science, Vol. 22, 1932.

(6) Edlefsen, N.E., "A New Capillary Potentiometer," Western Society of Soil Science, 1934.

(7) Fletcher, J., "A Dielectric Method of Determining Soil Moisture," Proceedings of the Soil Science Society of America, Vol. 4, 1939.

(8) Anderson, A.B.C., and N.E. Edlefsen, "The Electrical Capacity of the 2-Electrode Plaster of Paris Block As an Indicator of Soil Moisture Content," Soil Science, Vol. 54, July, 1942.

(9) Childs, E.C., "A Note on Electrical Methods of Determining Soil Moisture," Soil Science, Vol. 55, 1943.

(10) Wallihan, E.F., "Studies of the Dielectric Method of Measuring Soil Moisture," Proceedings of the Soil Science Society of America, Vol. 10, 1945.

(11) Thorne, M.D., and H.B. Russell, "The Dielectric Properties of Soil Moisture and Their Measurement," Proceedings of the Soil Science Society of America, Vol. 12, 1948.

(12) O'Konski, C.T., "Properties of Macromolecules V. Theory of Ionic Polarization in Polyelectrolytes," Journal of Physical Chemistry, Vol. 66, 1962.

(13) Schwan, H.P., G. Schwartz, J. Maczuk, and H. Pauly, "On the Low Frequency Dielectric Dispersion of Colloidal Particles in Electrolytic Solutions," Journal of Physical Chemistry, Vol. 66, 1962.

(14) Schwartz, G., "A Theory of the Low Frequency Dispersion of Colloidal Particles in Electrolyte Solution," Journal of Physical Chemistry, Vol. 66, 1962.

(15) Weibe, M.L., "Laboratory Measurements of the Complex Dielectric Constant of Soils," Technical Report RSC-23, Texas A&M Remote Sensing Center, College Station, Texas, Oct., 1971.

(16) Mandel, M. and A. Jenard, "Sur la Mesure de la Constante Dielectrique des Liquides Conducteurs - II," Bull. Soc. Chim. Belg., Vol. 59, 1963.

(17) Bockris, J. O'M. and A.K.N. Reddy, Modern Electrochemistry, Vols. I and II, Plenum Press, 1970.

(18) Dorsey, Noah Ernest, Properties of Ordinary Water Substance, Reinhold Publishing Corporation, 1953.

(19) Eisenberg, D. and W. Kauzmann, Structure and Properties of Water, Clarendon Press, 1969.

(20) Smiley, W.G. and A.K. Smith, "Electrode Polarization," Journal of the American Chemical Society, Vol. 64, 1942.

(21) Schwan, H.P., "Determination of Biological Impedances," Physical Technology in Biological Research, Vol. 6, Academic Press Inc., New York, 1963.

(22) Gardner, W.H., "Water Content," Methods of Soil Analysis, edited by C.A. Black, American Society of Agronomy, 1965.

(23) Ramo, S., J. Whinnery, and T. Van Duzer, Fields and Waves in Communication Electronics, John Wiley and Sons, 1967.

(24) Richards, L.A., "Physical Condition of Water in Soil," Methods of Soil Analysis, edited by C.A. Black, American Society of Agronomy, 1965.

(25) Dutt, G., and P. Low, "Relationship Between the Activation Energies for Deuterium Oxide Diffusion and Exchangable Ion Conductance in Clay Systems," Soil Science, Vol. 93, No. 3, March, 1962.

(26) Baver, L.D., Soil Physics, John Wiley and Sons, New York, 1956.

(27) Schofield, R.K., "Soil Temperature Variations," Quart. J. Roy. Met. Soc., Vol. 66, 1940.

(28) Marchenko, V.A. and Z.S. Agranovitch, The Inverse Problem of Scattering Theory, Gordon and Breach, New York, 1963.

(29) Sharpe, C.B., "The Synthesis of Infinite Lines," Quarterly of Applied Mathematics, Vol. 21, No. 2, July, 1963.

(30) Becher, W.D., Vertical Geoelectric Exploration Utilizing Nonuniform Transmission Line Theory, Ph.D. Thesis, University of Michigan, 1968.

(31) Slichter, L.B., "An Inverse Boundary Value Problem in Electrodynamics," Physics (now known as Journal of Applied Physics), Vol. 4, No. 12, Dec., 1933.

(32) Waite, W.P., K.R. Cook, and B.B. Bryan, "Broad Spectrum Microwave Systems for Remotely Measuring Soil Moisture Content,"Water Resources Research Center, University of Arkansas, Publication No. 18, September, 1973.

(33) Lytle, R. Jeffrey, "Measurement of Earth Medium Electrical Characteristics: Techniques, Results, and Applications," Lawrence Livermore Laboratory, Report No. UCRL-51479, Nov. 12, 1973.

APPENDICES

APPENDIX I

DATA TABLES

Preliminary Investigation

The tables in this section give the measured capacitance, resistance, permittivity, and conductivity for various samples of soil. A complete discussion of how the data were obtained can be found in Chapter 3 of Part I.

Crider Clay 26% Moisture Content

Frequency kHz	Capacitance pF	Resistance kΩ
20	1570	0.350
50	490	0.340
100	245	0.336
200	144	0.332
500	91	0.325
1000	74	0.317
2000	63.5	0.302

Crider Clay 28.9% Moisture Content

Frequency kHz	Capacitance pF	Resistance kΩ
20	1040	1.88
50	435	1.86
100	255	1.84
200	160	1.83
500	98.5	1.79
1000	74	1.765
2000	59	1.71

Crider Clay 29.1% Moisture Content

Frequency kHz	Capacitance pF	Resistance kΩ
20	1010	2.2
50	410	2.16
100	235	2.14
200	146	2.12
500	91	2.08
1000	69.5	2.04
2000	56	1.97

Crider Clay 30.2% Moisture Content

Frequency kHz	Capacitance pF	Resistance kΩ
20	1120	1.775
50	455	1.775
100	260	1.74
200	159	1.725
500	95	1.69
1000	70	1.67
2000	55	1.62

Crider Clay 30.4% Moisture Content

Frequency kHz	Capacitance pF	Resistance kΩ
20	1210	1.70
50	485	1.68
100	275	1.665
200	168	1.64
500	100	1.62
1000	72.5	1.58
2000	56	1.535

Crider Clay 31.7% Moisture Content

Frequency kHz	Capacitance pF	Resistance kΩ
20	1150	1.66
50	475	1.635
100	270	1.62
200	164	1.60
500	96.5	1.575
1000	70	1.55
2000	53	1.50

Crider Clay 32.6% Moisture Content

Frequency kHz	Capacitance pF	Resistance kΩ
20	1190	1.665
50	490	1.64
100	285	1.62
200	175	1.60
500	102.5	1.565
1000	77.5	1.535
2000	60	1.49

Crider Clay 34.8% Moisture Content

Frequency kHz	Capacitance pF	Resistance kΩ
20	1050	2.20
50	420	2.17
100	245	2.14
200	154	2.12
500	98	2.08
1000	77	2.04
2000	65	1.97

Crider Clay 35.3% Moisture Content

Frequency kHz	Capacitance pF	Resistance kΩ
20	1220	1.89
50	475	1.865
100	270	1.85
200	165	1.83
500	103	1.795
1000	79	1.76
2000	65	1.71

Crider Clay 36.7% Moisture Content

Frequency kHz	Capacitance pF	Resistance kΩ
20	895	2.47
50	370	2.43
100	222	2.41
200	144	2.38
500	95	2.34
1000	76.5	2.30
2000	66	2.22

Crider Clay 40.0% Moisture Content

Frequency kHz	Capacitance pF	Resistance kΩ
20	670	0.242
50	277	0.239
100	166	0.238
200	108	0.236
500	72	0.232
1000	58	0.230
2000	50	0.225

Crider Clay 41.3% Moisture Content

Frequency kHz	Capacitance pF	Resistance kΩ
20	940	0.209
50	390	0.206
100	232	0.204
200	148	0.2015
500	96	0.198
1000	76	0.1945
2000	64.5	0.189

Crider Clay 41.3% Moisture Content

Frequency kHz	Capacitance pF	Resistance kΩ
20	960	0.206
50	390	0.204
100	233	0.203
200	149	0.200
500	93	0.1975
1000	77	0.194
2000	65	0.190

Crider Clay 42.7% Moisture Content

Frequency kHz	Capacitance pF	Resistance kΩ
20	865	0.259
50	340	0.256
100	200	0.254
200	129	0.251
500	86	0.248
1000	70.4	0.244
2000	61.5	0.237

Crider Clay 42.8% Moisture Content

Frequency kHz	Capacitance pF	Resistance kΩ
20	720	0.272
50	285	0.270
100	167	0.267
200	108	0.264
500	72	0.260
1000	59	0.256
2000	51	0.250

Crider Clay 42.9% Moisture Content

Frequency kHz	Capacitance pF	Resistance kΩ
20	1070	0.260
50	437	0.256
100	250	0.252
200	161	0.249
500	104	0.244
1000	83.5	0.255
2000	72.2	0.245

(Held in container longer than usual)

Crider Clay 43.4% Moisture Content

Frequency kHz	Capacitance pF	Resistance kΩ
20	770	0.250
50	322	0.247
100	190	0.244
200	128	0.242
500	84	0.238
1000	68	0.233
2000	58.5	0.227

Crider Clay 45.4% Moisture Content

Frequency kHz	Capacitance pF	Resistance kΩ
20	745	0.220
50	310	0.218
100	187	0.216
200	123	0.215
500	83	0.212
1000	67.5	0.209
2000	58	0.204

Miami Silt Loam 8.4% Moisture Content

Frequency kHz	Capacitance pF	Resistance kΩ
20	150	1.43
50	84.5	1.40
100	65	1.39
200	53	1.37
500	41	1.30
1000	31.5	1.21
2000	24.6	1.14

Miami Silt Loam 8.7% Moisture Content

Frequency kHz	Capacitance pF	Resistance kΩ
20	100	1.34
50	86	1.325
100	65	1.31
200	53.5	1.285
500	42.5	1.23
1000	32.5	1.155
2000	24.5	1.07

Miami Silt Loam 9.93% Moisture Content

Frequency kHz	Capacitance pF	Resistance kΩ
20		
50	18.6	2.5
100	34.5	2.69
200	43.5	2.6
500	42	1.4
1000	33.5	0.74
2000	24	0.44

Miami Silt Loam 10.0% Moisture Content

Frequency kHz	Capacitance pF	Resistance kΩ
20	130	1.40
50	77.5	1.39
100	60	1.39
200	50	1.36
500	39.8	1.31
1000	31.5	1.23
2000	25	1.15

Miami Silt Loam 10.1% Moisture Content

Frequency kHz	Capacitance pF	Resistance kΩ
20	71	15
50	48	15
100	40	15
200	40.5	15
500	41	11
1000	35.5	6.9
2000	26.5	4.0

Miami Silt Loam 10.8% Moisture Content

Frequency kHz	Capacitance pF	Resistance kΩ
20	70.0	9.9
50	56.0	9.9
100	55.5	9.9
200	57.0	9.6
500	54.0	7.1
1000	44.5	4.5
2000	31.0	2.75

Miami Silt Loam 14.9% Moisture Content

Frequency kHz	Capacitance pF	Resistance kΩ
20	250	80
50	138	20
100	74	15
200	46	14.7
500	34	11.4
1000	31.5	8.7
2000	27.5	5.3

Miami Silt Loam 15.0% Moisture Content

Frequency kHz	Capacitance pF	Resistance kΩ
20	320	61
50	200	20
100	122	13
200	75.5	9.8
500	51.5	7.4
1000	43	5.4
2000	35	3.35

Miami Silt Loam 17.0% Moisture Content

Frequency kHz	Capacitance pF	Resistance kΩ
20	152	2.38
50	104	2.35
100	92	2.33
200	85.5	2.28
500	78.3	2.06
1000	68	1.675
2000	49.5	1.24

Miami Silt Loam 17.1% Moisture Content

Frequency kHz	Capacitance pF	Resistance kΩ
20	125	1.35
50	71	1.34
100	55	1.331
200	47	1.32
500	40	1.288
1000	35.5	1.223
2000	29.5	1.11

Miami Silt Loam 18.9% Moisture Content

Frequency kHz	Capacitance pF	Resistance kΩ
20	410	0.48
50	140	0.475
100	79	0.470
200	53.5	0.478
500	38.5	0.472
1000	31.5	0.461
2000	28.0	0.450

Miami Silt Loam 24.6% Moisture Content

Frequency kHz	Capacitance pF	Resistance kΩ
20	58.5	4.86
50	35.7	4.81
100	30.3	4.80
200	28.3	4.77
500	26.5	4.65
1000	25.5	4.40
2000	24.0	3.60

80% Kaolinite/20% Chelsea Sand-33.6% M.C.

Frequency kHz	Capacitance pF	Resistance kΩ
20	59	7.8
50	38.5	7.6
100	31	7.5
200	27	7.3
500	23	6.9
1000	21	6.2
2000	19.3	5.4

3/64 shrinkage from sides, firmly packed

80% Kaolinite/20% Chelsea Sand-35.9% M.C.

Frequency kHz	Capacitance pF	Resistance kΩ
20	23	83
50	20	83
100	18.7	76
200	16.7	64
500	14.5	51
1000	13.7	37
2000	12.6	21.6

80% Kaolinite/20% Chelsea Sand-36.0% M.C.

Frequency kHz	Capacitance pF	Resistance kΩ
20	27.5	∞
50	26.5	∞
100	26.5	1000
200	26.5	800
500	25.8	104
1000	24.0	32.9
2000	21.0	1.32

80% Kaolinite/20% Chelsea Sand-38.1% M.C.

Frequency kHz	Capacitance pF	Resistance kΩ
20	26	10,000
50	26	8,000
100	26	1,400
200	26	300
500	25.5	65
1000	25	20
2000	24	

80% Kaolinite/20% Chelsea Sand-43.6% M.C.

Frequency kHz	Capacitance pF	Resistance kΩ
20	27.0	∞
50	26.5	∞
100	26.5	∞
200	26.5	∞
500	26.5	400
1000	26.0	100
2000	25.5	40

Muck Soil 9% Moisture Content

Frequency kHz	Capacitance pF	Resistance kΩ
20	7.4	10,000
50	7.1	9,000
100	6.85	4,000
200		
500	6.4	800
1000	6.25	420
2000	6.1	220

Muck Soil 11.1% Moisture Content

Frequency kHz	Capacitance pF	Resistance kΩ
20	12.2	1000
50	11.1	1000
100	10.0	1000
200	9.2	700
500	8.4	350
1000	8.1	170
2000	7.6	70

Muck Soil 0% Moisture Content

Frequency kHz	Capacitance pF	Resistance kΩ
20		
50	9.45	1800
100	8.80	1020
200	8.25	580
500	7.45	284
1000	7.05	167
2000		

Muck Soil 0% Moisture Content

Frequency kHz	Capacitance pF	Resistance kΩ
20	4.8	10,000
50	4.65	10,000
100	4.6	10,000
200		
500	4.5	6,000
1000	4.5	3,000
2000	4.45	1,100

Muck Soil 11.7% Moisture Content

Frequency kHz	Capacitance pF	Resistance kΩ
20	16.0	1000
50	15.9	1000
100	15.0	1000
200	13.6	1000
500	13.5	
1000	13.5	500
2000	13.1	

Muck Soil 13.6% Moisture Content

Frequency kHz	Capacitance pF	Resistance kΩ
20	15.3	1000
50	13.2	1000
100	11.7	800
200	10.5	400
500	9.7	170
1000	8.8	110
2000	8.4	64

Muck Soil 16.2% Moisture Content

Frequency kHz	Capacitance pF	Resistance kΩ
20	32.0	500
50	27.0	280
100	23.5	150
200	20.6	100
500	16.7	54.5
1000	14.7	32.8
2000		

Muck Soil 15.8% Moisture Content

Frequency kHz	Capacitance pF	Resistance kΩ
20	82	17.6
50	67.5	17.25
100	54	15.9
200	41.5	13.6
500	31	10.4
1000	25	8.0
2000	20.5	6.0

Muck Soil 16% Moisture Content

Frequency kHz	Capacitance pF	Resistance kΩ
20		
50	30.9	194.5
100	25.9	186.8
200	21.3	168.3
500	17.3	147.0
1000	14.7	124.2
2000		

Muck Soil 25.2% Moisture Content

Frequency kHz	Capacitance pF	Resistance kΩ
20	62	40.0
50	54	26.1
100	39.2	19.8
200	33	17.9
500	25	13.5
1000	20.8	10.6
2000	17	7.7

Data of doubtful validity

Muck Soil 32.1% Moisture Content

Frequency kHz	Capacitance pF	Resistance kΩ
20	130	4.22
50	59	4.12
100	44.5	4.08
200	38.0	3.98
500	31.5	3.67
1000	25.8	3.36
2000	20.3	2.69

Muck Soil 32.5% Moisture Content

Frequency kHz	Capacitance pF	Resistance kΩ
20	136	2.52
50	68	2.55
100	50	2.66
200		
500	30.5	2.56
1000	26.6	2.40
2000	20.0	1.90

Silt Loam 15.8% Moisture Content

Frequency kHz	Capacitance pF	Resistance kΩ
20	4.75	∞
50	4.60	10,000
100	4.62	10,000
200	4.52	9,000
500	4.45	4,000
1000	4.40	1,400
2000	4.35	760

Sand, Oven Dry

Frequency kHz	Capacitance pF	Resistance kΩ
20	4.9	10,000
50	4.8	10,000
100	4.75	10,000
200	4.75	10,000
500	4.7	9,000
1000	4.65	4,000
2000	4.65	

Sand 5.79% Moisture Content

Frequency kHz	Capacitance pF	Resistance kΩ
20	25.5	68
50	19.5	62
100	15.9	55.5
200	12.7	48
500	10.4	38
1000	8.9	31.5
2000	7.8	24.8

Sand 4.56% Moisture Content

Frequency kHz	Capacitance pF	Resistance kΩ
20	24.5	71
50	21.0	68
100	17.6	57
200	13.6	46
500	11.4	37
1000	9.2	27
2000	8.2	20

Toggle switch used - nickel plate

Sand 3.87% Moisture Content

Frequency kHz	Capacitance pF	Resistance kΩ
20	25.0	68
50	19.1	64
100	16.3	57
200	14.2	47
500	10.7	38
1000	9.2	29
2000	7.9	22

Toggle switch used

Sand 6.46% Moisture Content

Frequency kHz	Capacitance pF	Resistance kΩ
20	25.5	52
50	19.0	49
100	16.6	44.5
200	13.0	35.9
500	11.1	27.5
1000	9.3	24
2000	8.7	

Properties of Miami Silt Loam
In the 5 - 40 MHz Range

These data were collected using the General Radio 1606 R-F Bridge. The procedures used to prepare the samples and collect the data are presented in Chapter 5 of Part I. A description of Miami Silt Loam is given in Appendix II.

The symbols used in the tables are as follows:

f = frequency in MHz

x*f = the product of reactance in ohms and frequency in MHz

R = resistance in ohms

ε = relative permittivity

Log ε = logarithm to base 10 of ε

σ = conductivity in mhos/meter

M.C. = moisture content

Miami Silt Loam, 9.1% M.C.

f	x*f	R	ε	σ	Log ε
5	391	148	9.91	0.0055	0.996
10	920	90.0	9.84	0.0057	0.993
20	1685	44.7	8.07	0.0051	0.907
40	1965	15.7	7.86	0.0058	0.895

Miami Silt Loam, 9.9% M.C.

f	x*f	R	ε	σ	Log ε
5	287	103	14.9	0.0077	1.17
10	571	74.0	11.6	0.0088	1.06
20	1020	45.0	9.69	0.0100	0.98
40	1620	20.0	8.47	0.0096	0.92

Miami Silt Loam, 10.3% M.C.

f	x*f	R	ε	σ	Log ε
5	556	140	12.4	0.0046	1.09
10	1000	88.0	9.99	0.0052	0.99
20	1560	42.0	8.69	0.0055	0.93
40	2030	15.3	7.68	0.0054	0.88

Miami Silt Loam, 10.5% M.C.

f	x*f	R	ε	σ	Log ε
5	360	121	13.0	0.0064	1.11
10	703	80.0	11.0	0.0073	1.04
20	1185	46.5	9.16	0.0084	0.96
40	1782	18.0	8.23	0.0077	0.91

Miami Silt Loam, 12.4% M.C.

f	x*f	R	ε	σ	Log ε
5	404	127	12.8	0.0059	1.10
10	826	82.5	10.7	0.0063	1.03
20	1360	42.0	9.3	0.0068	0.970
40	1836	13.9	8.5	0.0059	0.930

Miami Silt Loam, 15.8% M.C.

f	x*f	R	ε	σ	Log ε
5	176	78.0	17.4	0.0111	1.24
10	420	55.0	15.8	0.0119	1.20
20	797	29.0	14.6	0.0122	1.16
40	1130	10.0	13.4	0.0106	1.12

Miami Silt Loam, 18% M.C.

f	x*f	R	ε	σ	Log ε
5	442	120	14.3	0.0056	1.15
10	812	69.0	12.8	0.0063	1.10
20	1220	31.8	11.4	0.0069	1.05
40	1578	10.0	10.2	0.0059	1.00

Miami Silt Loam, 21.2% M.C.

f	x*f	R	ε	σ	Log ε
5	143	65.0	20.7	0.0134	1.31
10	302	48.0	17.0	0.0155	1.23
20	600	30.0	14.8	0.0170	1.17
40	995	12.3	13.8	0.0151	1.14

Miami Silt Loam, 24.1% M.C.

f	x*f	R	ε	σ	Log ε
5	334	95.0	18.0	0.0074	1.25
10	491	56.0	16.0	0.0105	1.20
20	475	28.5	13.6	0.0091	1.13
40	1460	8.20	11.1	0.0057	1.04

Miami Silt Loam, 9.5% M.C., 0.2% Salt

f	x*f	R	ε	σ	Log ε
5	130	73.0	15.6	0.0127	1.19
10	311	57.6	13.0	0.0140	1.11
20	665	39.5	11.0	0.0152	1.04
40	1200	19.6	10.0	0.0148	1.00

Miami Silt Loam, 10.3% M.C., 0.2% Salt

f	x*f	R	ε	σ	Log ε
5	261	108	13.0	0.0078	1.11
10	578	74.0	11.7	0.0087	1.06
20	1010	46.0	9.5	0.0101	0.978
40	1595	22.5	8.1	0.0106	0.909

Miami Silt Loam, 13.0% M.C., 0.2% Salt

f	x*f	R	ε	σ	Log ε
5	67	46.5	20.9	0.0207	1.32
10	169	40.0	16.2	0.0220	1.20
20	396	30.1	13.5	0.0237	1.13
40	830	17.0	12.3	0.0226	1.09

Miami Silt Loam, 15.7% M.C., 0.2% Salt

f	x*f	R	ε	σ	Log ε
5	75	48.0	21.6	0.0198	1.33
10	184	38.7	18.1	0.0219	1.25
20	409	27.9	15.2	0.0238	1.18
40	780	14.4	14.2	0.0232	1.15

Miami Silt Loam, 17.8% M.C., 0.2% Salt

f	x*f	R	ε	σ	Log ε
5	148	57.5	25.9	0.0143	1.41
10	307	48.6	16.8	0.0153	1.22
20	677	35.0	12.6	0.0151	1.10
40	1000	18.2	11.2	0.0184	1.04

Miami Silt Loam, 18.2% M.C., 0.2% Salt

f	x*f	R	ε	σ	Log ε
5	110	45.0	32.3	0.0187	1.50
10	210	33.0	25.0	0.0223	1.39
20	360	24.0	17.9	0.0270	1.25
40	680	13.1	15.7	0.0266	1.19

Miami Silt Loam, 19.1% M.C., 0.2% Salt

f	x*f	R	ε	σ	Log ε
5	425	99.0	18.1	0.0061	1.25
10	470	66.2	12.7	0.0104	1.10
20	1100	30.0	12.4	0.0078	1.09
40	1236	9.55	12.6	0.0087	1.10

Miami Silt Loam, 22.0% M.C., 0.2% Salt

f	x*f	R	ε	σ	Log ε
5	25	29.0	21.0	0.0349	1.32
10	84	26.5	19.7	0.0355	1.29
20	238	21.0	18.2	0.0364	1.26
40	570	12.4	17.0	0.0322	1.23

Miami Silt Loam, 10% M.C., 0.4% Salt

f	x*f	R	ε	σ	Log ε
5	86	54.0	19.5	0.0175	1.29
10	189	42.4	15.8	0.0204	1.20
20	416	31.1	13.2	0.0227	1.12
40	870	37.2	12.0	0.0242	1.08

Miami Silt Loam, 12.3% M.C., 0.4% Salt

f	x*f	R	ε	σ	Log ε
5	74	44.0	25.1	0.0213	1.40
10	162	35.8	19.0	0.0240	1.28
20	361	28.2	14.3	0.0256	1.15
40	770	16.0	13.1	0.0243	1.11

Miami Silt Loam, 15.9% M.C., 0.4% Salt

f	x*f	R	ε	σ	Log ε
5	189	45.2	40.2	0.0136	1.60
10	228	30.5	28.7	0.0217	1.45
20	372	21.0	21.2	0.0268	1.32
40	610	12.0	17.2	0.0295	1.23

Miami Silt Loam, 18.9% M.C., 0.4% Salt

f	x*f	R	ε	σ	Log ε
5	53	33.0	32.5	0.0286	1.51
10	135	25.7	29.3	0.0315	1.46
20	250	18.0	23.3	0.0376	1.36
40	420	10.9	19.4	0.0434	1.28

Properties of Some Soils in the 250 - 450 MHz Range

These data were collected using the General Radio 1602 Admittance Meter. The procedures used to prepare samples and collect data are presented in Chapter 5, Part I. Descriptions of the soils used in the investigation are summarized in Appendix II. The computer program used to convert the data into permittivities and conductivities is listed in Appendix IV.

The symbols used in the tables are as follows:

f = frequency in MHz

B = susceptance in mhos

G = conductance in mhos

ε = relative permittivity

Log ε = logarithm to base 10 of ε

σ = conductivity in mhos/meter

M.C. = moisture content

* = denotes samples prepared with salt

Miami (Lab Prepared), 9% M.C.

f	B	G	ε	Log ε	σ
250	0.0139	0.0008	4.97	0.697	0.008
300	0.0176	0.0012	4.90	0.690	0.010
350	0.0219	0.0017	4.77	0.679	0.012
450	0.0350	0.0035	4.73	0.675	0.014

Miami (Lab Prepared), 10.2% M.C.

f	B	G	ε	Log ε	σ
250	0.0148	0.0011	5.60	0.748	0.010
300	0.0189	0.0015	5.52	0.742	0.012
350	0.0238	0.0022	5.45	0.736	0.014
450	0.0392	0.0046	5.37	0.730	0.016

Miami (Lab Prepared), 12.8% M.C.

f	B	G	ε	Log ε	σ
250	0.0161	0.0017	6.45	0.810	0.015
300	0.0207	0.0023	6.37	0.804	0.018
350	0.0263	0.0032	6.25	0.796	0.019
450	0.0451	0.0072	6.16	0.790	0.021

Miami (Lab Prepared), 14.0% M.C.

f	B	G	ε	Log ε	σ
250	0.0182	0.0015	7.76	0.890	0.013
300	0.0237	0.0023	7.65	0.884	0.016
350	0.0313	0.0033	7.66	0.885	0.017
450	0.583	0.0095	7.50	0.875	0.020

Miami (Lab Prepared), 15.0% M.C.

f	B	G	ε	Log ε	σ
250	0.0209	0.0014	9.34	0.970	0.011
300	0.0277	0.0021	9.20	0.964	0.013
350	0.0369	0.0041	9.04	0.956	0.018
450	0.792	0.0117	8.92	0.950	0.016

Miami (Lab Prepared), 17.6% M.C.

f	B	G	ε	Log ε	σ
250	0.0239	0.0023	11.0	1.04	0.017
300	0.0322	0.0035	10.8	1.03	0.019
350	0.0446	0.0058	10.6	1.02	0.021
450	0.114	0.0304	10.4	1.02	0.023

Miami (Lab Prepared), 18.8% M.C.

f	B	G	ε	Log ε	σ
250	0.0270	0.0028	12.6	1.10	0.019
300	0.0372	0.0044	12.3	1.09	0.021
350	0.0532	0.0078	12.1	1.08	0.023
450	0.169	0.0686	11.9	1.07	0.025

Miami (Lab Prepared), 21.0% M.C.

f	B	G	ε	Log ε	σ
250	0.0341	0.0043	15.8	1.20	0.025
300	0.0499	0.0075	15.5	1.19	0.027
350	0.0802	0.0161	15.3	1.18	0.028
450	-0.178	0.485	15.2	1.18	0.030

Miami (Lab Prepared), 22.0% M.C.

f	B	G	ε	Log ε	σ
250	0.0481	0.0053	20.9	1.32	0.023
300	0.0798	0.0120	20.6	1.31	0.025
350	0.173	0.0492	20.1	1.30	0.026
450	-0.148	0.0265	19.8	1.29	0.028

Miami (Lab Prepared), 24.2% M.C.

f	B	G	ε	Log ε	σ
250	0.0579	0.0069	23.7	1.37	0.025
300	0.107	0.0192	23.4	1.37	0.027
350	0.315	0.184	23.2	1.36	0.029
450	-0.105	0.118	22.9	1.36	0.031

Miami (Field, 3" †) 8.6% M.C.

f	B	G	ε	Log ε	σ
250	0.0134	0.0010	4.59	0.662	0.010
300	0.0169	0.0021	4.55	0.658	0.018
350	0.0211	0.0031	4.51	0.654	0.022
450	0.0328	0.0076	4.48	0.651	0.032

† refers to depth below surface of earth at which sample was caken.

Miami (Field, 3"), 11.5% M.C.

f	B	G	ε	Log ε	σ
250	0.0153	0.0022	5.90	0.771	0.020
300	0.0195	0.0037	5.84	0.766	0.029
350	0.0246	0.0053	5.78	0.762	0.033
450	0.0407	0.0120	5.75	0.760	0.039

Miami (Field, 3"), 17.0% M.C.

f	B	G	ε	Log ε	σ
250	0.0258	0.0043	12.0	1.08	0.030
300	0.0356	0.0074	11.9	1.07	0.037
350	0.0504	0.0136	11.8	1.07	0.042
450	0.118	0.102	11.7	1.07	0.051

Miami (Field, 3"), 19.4% M.C.

f	B	G	ε	Log ε	σ
250	0.0283	0.0092	13.4	1.12	0.060
300	0.0394	0.0144	13.3	1.12	0.064
350	0.0564	0.0259	13.2	1.12	0.067
450	0.0641	0.180	13.2	1.12	0.070

Miami (Field, 3"), 22.6% M.C.

f	B	G	ε	Log ε	σ
250	0.0423	0.0172	19.5	1.29	0.081
300	0.0640	0.0337	19.3	1.28	0.085
350	0.0919	0.0911	19.0	1.28	0.090
450	-0.110	0.0704	19.0	1.27	0.096

Miami (Field, 3"), 23.2% M.C.

f	B	G	ε	Log ε	σ
250	0.0557	0.0215	23.7	1.37	0.078
300	0.0928	0.0566	23.6	1.37	0.084
350	0.0607	0.222	23.4	1.37	0.094
450	-0.0873	0.0268	23.4	1.37	0.102

Miami (Field, 3"), 24.0% M.C.

f	B	G	ε	Log ε	σ
250	0.0530	0.0338	24.0	1.38	0.122
300	0.0726	0.0795	23.8	1.37	0.130
350	0.0020	0.177	23.6	1.37	0.134
450	−0.0785	0.0301	23.4	1.37	0.140

Miami (Field, 3"), 24.0% M.C.

f	B	G	ε	Log ε	σ
250	0.0484	0.0348	22.9	1.36	0.135
300	0.0615	0.0755	22.7	1.35	0.146
350	0.0084	0.150	22.5	1.35	0.152
450	−0.0766	0.0357	22.5	1.35	0.158

Miami (Field, 18"), 8.8% M.C.

f	B	G	ε	Log ε	σ
250	0.0135	0.0009	4.68	0.670	0.009
300	0.0171	0.0016	4.63	0.666	0.013
350	0.0213	0.0034	4.59	0.662	0.024
450	0.0335	0.0073	4.58	0.661	0.030

Miami (Field, 18"), 10.0% M.C.

f	B	G	ε	Log ε	σ
250	0.0141	0.0022	5.13	0.710	0.021
300	0.0179	0.0029	5.08	0.706	0.024
350	0.0224	0.0049	5.05	0.703	0.033
450	0.0356	0.0102	5.01	0.699	0.039

Miami (Field, 18"), 15.0% M.C.

f	B	G	ε	Log ε	σ
250	0.0174	0.0067	7.43	0.871	0.057
300	0.0224	0.0090	7.38	0.868	0.063
350	0.0284	0.0134	7.34	0.866	0.072
450	0.0444	0.0339	7.33	0.865	0.084

Miami (Field, 18"), 16.0% M.C.

f	B	G	ε	Log ε	σ
250	0.0217	0.0074	9.98	0.999	0.079
300	0.0288	0.0108	9.93	0.997	0.088
350	0.0379	0.0175	9.84	0.993	0.100
450	0.0617	0.0627	9.77	0.990	0.109

Miami (Field, 18"), 17.8% M.C.

f	B	G	ε	Log ε	σ
250	0.0244	0.0088	11.4	1.06	0.063
300	0.0327	0.0142	11.4	1.05	0.074
350	0.0446	0.0239	11.3	1.05	0.081
450	0.0573	0.100	11.3	1.05	0.092

Miami (Field, 18"), 18.6% M.C.

f	B	G	ε	Log ε	σ
250	0.0301	0.0127	14.4	1.16	0.079
300	0.0413	0.0213	14.2	1.15	0.088
350	0.0554	0.0425	14.2	1.15	0.100
450	−0.0199	0.146	14.1	1.15	0.109

Miami (Field, 18"), 20.4% M.C.

f	B	G	ε	Log ε	σ
250	0.0358	0.0179	17.1	1.23	0.096
300	0.0499	0.0322	16.9	1.23	0.105
350	0.0606	0.0721	16.9	1.22	0.120
450	−0.0798	0.101	16.7	1.22	0.125

Miami (Field, 18"), 22.0% M.C.

f	B	G	ε	Log ε	σ
250	0.0385	0.0231	18.6	1.27	0.115
300	0.0530	0.0429	18.4	1.26	0.123
350	0.0590	0.0921	18.3	1.26	0.128
450	−0.0849	0.0759	18.2	1.25	0.135

Miami (Field, 18"), 23.0% M.C.

f	B	G	ε	Log ε	σ
250	0.0433	0.0250	20.4	1.31	0.112
300	0.0621	0.0510	20.4	1.31	0.119
350	0.0591	0.126	20.4	1.31	0.124
450	−0.0887	0.0507	20.4	1.31	0.130

Miami (Field, 18"), 23.18% M.C.

f	B	G	ε	Log ε	σ
250	0.0457	0.0299	21.6	1.33	0.125
300	0.0629	0.0623	21.5	1.33	0.132
350	0.0344	0.141	21.4	1.33	0.140
450	-0.0813	0.0426	21.3	1.33	0.147

Miami (Field, 36"), 9.0% M.C.

f	B	G	ε	Log ε	σ
250	0.0135	0.0012	4.67	0.670	0.012
300	0.0171	0.0023	4.63	0.666	0.019
350	0.0224	0.0036	4.59	0.662	0.025
450	0.0333	0.0077	4.56	0.659	0.032

Miami (Field, 36"), 11.1% M.C.

f	B	G	ε	Log ε	σ
250	0.0139	0.0020	5.01	0.710	0.019
300	0.0178	0.0033	5.01	0.710	0.027
350	0.0224	0.0048	5.01	0.710	0.032
450	0.0357	0.0100	5.01	0.710	0.038

Miami (Field, 36"), 14.0% M.C.

f	B	G	ε	Log ε	σ
250	0.0171	0.0034	7.08	0.850	0.030
300	0.0219	0.0053	6.99	0.845	0.038
350	0.0282	0.0079	6.97	0.843	0.044
450	0.0483	0.0201	6.90	0.839	0.051

Miami (Field, 36"), 18.6% M.C.

f	B	G	ε	Log ε	σ
250	0.0251	0.0098	11.8	1.07	0.069
300	0.0337	0.0146	11.7	1.07	0.074
350	0.0457	0.0235	11.6	1.06	0.077
450	0.0712	0.103	11.4	1.06	0.080

Miami (Field, 36"), 21.0% M.C.

f	B	G	ε	Log ε	σ
250	0.0392	0.0138	18.2	1.26	0.070
300	0.0580	0.0270	17.9	1.25	0.078
350	0.0881	0.0690	17.9	1.25	0.083
450	−0.118	0.0967	17.8	1.25	0.088

Miami (Field, 36"), 22.2% M.C.

f	B	G	ε	Log ε	σ
250	0.0479	0.0313	22.3	1.35	0.125
300	0.0661	0.0658	22.1	1.34	0.130
350	0.0339	0.150	21.8	1.34	0.135
450	−0.0829	0.0408	21.6	1.33	0.140

Chelsea (Lab Prepared), 2.3% M.C.

f	B	G	ε	Log ε	σ
250	0.0128	0.0010	4.19	0.622	0.010
300	0.0161	0.0014	4.13	0.616	0.012
350	0.0200	0.0018	4.10	0.613	0.013
450	0.0310	0.0031	4.05	0.607	0.014

Chelsea (Lab Prepared), 4.0% M.C.

f	B	G	ε	Log ε	σ
250	0.0136	0.0009	4.77	0.679	0.009
300	0.0173	0.0013	4.75	0.677	0.0105
350	0.0217	0.0019	4.72	0.674	0.013
450	0.0347	0.0035	4.68	0.671	0.014

Chelsea (Lab Prepared), 5.4% M.C.

f	B	G	ε	Log ε	σ
250	0.0142	0.0016	5.19	0.715	0.015
300	0.0182	0.0020	5.16	0.713	0.0165
350	0.0229	0.0029	5.15	0.712	0.019
450	0.0372	0.0054	5.11	0.708	0.020

Chelsea (Lab Prepared), 7.0% M.C.

f	B	G	ε	Log ε	σ
250	0.0159	0.0021	6.34	0.802	0.019
300	0.0204	0.0030	6.25	0.796	0.023
350	0.0261	0.0045	6.22	0.794	0.027
450	0.0447	0.0106	6.19	0.792	0.031

Chelsea (Lab Prepared), 8.6% M.C.

f	B	G	ε	Log ε	σ
250	0.0164	0.0025	6.61	0.820	0.022
300	0.0212	0.0033	6.61	0.820	0.024
350	0.0274	0.0045	6.61	0.820	0.026
450	0.0491	0.0107	6.66	0.824	0.028

Chelsea (Lab Prepared), 9.1% M.C.

f	B	G	ε	Log ε	σ
250	0.0177	0.0039	7.50	0.875	0.034
300	0.0231	0.0053	7.46	0.873	0.037
350	0.0300	0.0074	7.43	0.871	0.039
450	0.0542	0.0186	7.41	0.870	0.041

Chelsea (Lab Prepared), 10.1% M.C.

f	B	G	ε	Log ε	σ
250	0.0185	0.0045	7.99	0.903	0.038
300	0.0242	0.0059	7.94	0.900	0.040
350	0.0318	0.0084	7.94	0.900	0.042
450	0.0603	0.0226	7.96	0.901	0.043

Crider (Lab Prepared), 14.5% M.C.

f	B	G	ε	Log ε	σ
250	0.0130	0.0031	4.37	0.640	0.030
300	0.0163	0.0035	4.25	0.628	0.030
350	0.0197	0.0069	4.17	0.620	0.050
450	0.0290	0.0130	4.07	0.610	0.060

Crider (Lab Prepared), 16.0% M.C.

f	B	G	ε	Log ε	σ
250	0.0133	0.0062	4.69	0.671	0.060
300	0.0164	0.0083	4.56	0.659	0.070
350	0.0201	0.0099	4.48	0.651	0.070
450	0.0287	0.0179	4.36	0.640	0.080

*Crider (Lab Prepared), 17.0% M.C.

f	B	G	ε	Log ε	σ
250	0.0128	0.0125	4.76	0.678	0.120
300	0.0152	0.0155	4.68	0.670	0.130
350	0.0171	0.0194	4.52	0.655	0.140
450	0.0195	0.0299	4.41	0.644	0.150

Crider (Lab Prepared), 18.6% M.C.

f	B	G	ε	Log ε	σ
250	0.0141	0.0107	5.48	0.739	0.100
300	0.0169	0.0137	5.31	0.725	0.110
350	0.0203	0.0164	5.20	0.716	0.110
450	0.0262	0.0284	5.07	0.705	0.120

Crider (Lab Prepared), 21.6% M.C.

f	B	G	ε	Log ε	σ
250	0.0146	0.0120	5.95	0.775	0.110
300	0.0176	0.0154	5.83	0.766	0.120
350	0.0204	0.0202	5.73	0.758	0.130
450	0.0241	0.0346	5.62	0.750	0.140

*Crider (Lab Prepared), 22.5% M.C.

f	B	G	ε	Log ε	σ
250	0.0157	0.0174	7.24	0.860	0.150
300	0.0182	0.0221	7.05	0.848	0.160
350	0.0207	0.0272	6.93	0.841	0.160
450	0.0185	0.0455	6.76	0.831	0.170

Crider (Lab Prepared), 25.0% M.C.

f	B	G	ε	Log ε	σ
250	0.0185	0.0134	8.55	0.932	0.110
300	0.0227	0.0181	8.29	0.919	0.120
350	0.0267	0.0255	8.14	0.911	0.130
450	0.0284	0.0516	7.94	0.899	0.140

Crider (Lab Prepared), 26.5% M.C.

f	B	G	ε	Log ε	σ
250	0.0192	0.0143	8.99	0.954	0.115
300	0.0237	0.0187	8.75	0.942	0.120
350	0.0280	0.0267	8.61	0.935	0.130
450	0.0286	0.0561	8.41	0.925	0.140

*Crider (Lab Prepared), 27.4% M.C.

f	B	G	ε	Log ε	σ
250	0.0196	0.0180	9.59	0.982	0.140
300	0.0232	0.0242	9.31	0.969	0.150
350	0.0257	0.0336	9.14	0.961	0.160
450	0.0120	0.0627	9.02	0.955	0.180

Crider (Lab Prepared), 29.2% M.C.

f	B	G	ε	Log ε	σ
250	0.0219	0.0207	11.1	1.04	0.150
300	0.0258	0.0287	10.8	1.03	0.160
350	0.0276	0.0413	10.7	1.03	0.170
450	0.0085	0.0759	10.4	1.02	

*Crider (Lab Prepared), 30.6% M.C.

f	B	G	ε	Log ε	σ
250	0.0234	0.0216	12.1	1.08	0.150
300	0.0285	0.0313	12.0	1.08	0.160
350	0.0303	0.0476	12.0	1.08	0.170
450	-0.0092	0.0843	12.0	1.08	0.180

Crider (Lab Prepared) 32.0% M.C.

f	B	G	ε	Log ε	σ
250	0.0298	0.0216	15.0	1.17	0.130
300	0.0374	0.0341	14.6	1.16	0.140
350	0.0442	0.0555	14.4	1.15	0.140
450	-0.0305	0.106	14.1	1.15	0.150

Crider (Lab Prepared), 34.4% M.C.

f	B	G	ε	Log ε	σ
250	0.0318	0.0291	16.8	1.22	0.160
300	0.0373	0.0463	16.3	1.21	0.170
350	0.0307	0.0756	16.0	1.20	0.180
450	-0.0512	0.0822	15.6	1.19	0.180

*Crider (Lab Prepared), 36.4% M.C.

f	B	G	ε	Log ε	σ
250	0.0354	0.0345	18.9	1.27	0.170
300	0.0398	0.0576	18.4	1.26	0.180
350	0.0211	0.0938	18.1	1.25	0.190
450	-0.0619	0.0614	17.7	1.25	0.200

Crider (Lab Prepared), 36.4% M.C.

f	B	G	ε	Log ε	σ
250	0.0421	0.0376	21.4	1.33	0.160
300	0.0476	0.0688	20.8	1.31	0.170
350	0.0193	0.119	20.4	1.31	0.170
450	-0.0697	0.0491	19.9	1.30	0.190

Crider (Lab Prepared), 40.0% M.C.

f	B	G	ε	Log ε	σ
250	0.0513	0.0465	25.0	1.39	0.160
300	0.0549	0.0956	24.3	1.38	0.165
350	-0.0227	0.149	23.8	1.37	0.166
450	-0.0726	0.0313	23.4	1.37	0.170

Crosby (Field, 18"), 14.0% M.C.

f	B	G	ε	Log ε	σ
250	0.0139	0.0074	5.13	0.710	0.070
300	0.0171	0.0098	5.04	0.702	0.080
350	0.0209	0.0122	4.98	0.697	0.083
450	0.0299	0.0221	4.91	0.691	0.091

Crosby (Field, 18"), 16.0% M.C.

f	B	G	ε	Log ε	σ
250	0.0173	0.0063	7.33	0.865	0.055
300	0.0221	0.0092	7.23	0.859	0.065
350	0.0279	0.0132	7.18	0.856	0.072
450	0.0445	0.0299	7.08	0.850	0.077

Crosby (Field, 18"), 19.8% M.C.

f	B	G	ε	Log ε	σ
250	0.0198	0.0113	9.12	0.960	0.090
300	0.0249	0.0158	8.91	0.950	0.100
350	0.0312	0.0223	8.81	0.945	0.104
450	0.0406	0.0553	8.71	0.940	0.113

Crosby (Field, 18"), 21.2% M.C.

f	B	G	ε	Log ε	σ
250	0.0236	0.0146	11.4	1.06	0.105
300	0.0305	0.0214	11.3	1.05	0.113
350	0.0377	0.0339	11.2	1.05	0.122
450	0.0255	0.0922	11.1	1.04	0.129

Crosby (Field, 18"), 24% M.C.

f	B	G	ε	Log ε	σ
250	0.0323	0.0231	16.2	1.21	0.130
300	0.0412	0.0380	15.9	1.20	0.140
350	0.0464	0.0664	15.7	1.19	0.143
450	-0.0524	0.0998	15.4	1.18	0.151

Crosby (Field, 18"), 25.8% M.C.

f	B	G	ε	Log ε	σ
250	0.0370	0.0294	18.7	1.27	0.145
300	0.0474	0.0514	18.6	1.27	0.151
350	0.0404	0.0976	18.4	1.26	0.155
450	-0.0751	0.0671	18.3	1.26	0.160

Crosby (Field, 18"), 26.8% M.C.

f	B	G	ε	Log ε	σ
250	0.0377	0.0327	19.4	1.28	0.156
300	0.0463	0.0573	19.2	1.28	0.162
350	0.0312	0.104	19.0	1.28	0.166
450	-0.0717	0.0595	18.8	1.27	0.175

APPENDIX II

DESCRIPTION OF SOME SOILS USED IN THIS INVESTIGATION

Chelsea

Chelsea is a moderately dark colored soil which is deep and well-drained. The surface of the soil (where samples for this investigation were collected) is dark brown, while the subsoil is yellowish red to reddish brown. The soil is more than 80% sand and contains very little organic matter. The wilting point moisture for the samples used in this investigation was 2.2%.

Crider

Where it occurs, Crider is a deep well-drained, gently sloping soil. Its surface layer consists of dark brown silt loam while the subsurface (where samples for this investigation were obtained) is silty clay or clay which is red. Crider contains between 27% and 40% clay. The wilting point of the samples used in this investigation was 18.5%.

Crosby

Crosby developed under hardwood forests and occurs on nearly level ground. It is somewhat poorly drained and dark

in color. On the surface there is a layer of silt loam and below that is brown silt loam (where samples for this investigation were taken). The subsoil consists of thick yellowish brown silty clay loam. The wilting point for samples used in this investigation was 14%.

Miami

Miami occurs in upland tills and moraines on sloping ground. It is well-drained, deep, and moderately dark in color. The soil is predominately silt, more than 66%. In the subsoil, however, both sand and clay content increase somewhat. The moisture wilting point for the samples used in this investigation was 8.8%.

APPENDIX III

ANALYSIS OF SAMPLE HOLDER-SOIL EQUIVALENT CIRCUIT

The circuit is shown in Figure A-1. The impedance of this circuit is

$$A\text{-}1 \qquad Z_{12} = \frac{\frac{R_1}{j\omega C_1}}{\frac{1}{j\omega C_1} + R_1} + \frac{\frac{R_2}{j\omega C_2}}{\frac{1}{j\omega C_2} + R_2}$$

$$= \frac{R_1}{1 + j_\omega C_1 R_1} + \frac{R_2}{1 + j\omega C_2 R_2}$$

$$A\text{-}2 \qquad Z_{12} = \frac{R_1 - j\omega C_1 R_1^2}{1 + \omega^2 C_1^2 R_1^2} + \frac{R_2 - j\omega C_2 R_2^2}{1 + \omega^2 C_2^2 R_2^2}$$

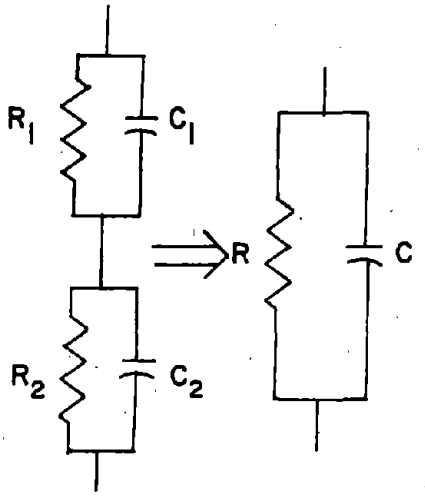

R_1 = Electrode resistance

C_1 = Electrode capacitance

R_2 = Sample resistance

C_2 = Sample capacitance

R = Measured resistance

C = Measured capacitance

Figure A-1. Sample Soil Holder Circuit.

$$\text{A-3} \quad Z_{12} = \frac{R_1(1 + \omega^2C_2^2R_2^2) + R_2(1 + \omega^2C_1^2R_1^2)}{(1 + \omega^2C_1^2R_1^2)(1 + \omega^2C_2^2R_2^2)} - \frac{j\omega[C_1R_1^2(1 + \omega^2C_2^2R_2^2) + C_2R_2^2(1 + \omega^2C_1^2R_1^2)]}{(1 + \omega^2C_1^2R_1^2)(1 + \omega^2C_2^2R_2^2)}$$

$$\text{A-4} \quad Z = \frac{R - j\omega CR^2}{1 + \omega^2R^2C^2}$$

$$\text{A-5} \quad \frac{R}{1 + \omega^2R^2C^2} = \frac{R_1(1 + \omega^2C_2^2R_2^2) + R_2(1 + \omega^2C_1^2R_1^2)}{(1 + \omega^2C_1^2R_1^2)(1 + \omega^2C_2^2R_2^2)}$$

Equating the imaginary part of Z to the imaginary part of Z_{12}

$$\text{A-6} \quad \frac{CR^2}{1 + \omega^2R^2C^2} = \frac{C_1R_1^2(1 + \omega^2C_2^2R_2^2) + C_2R_2^2(1 + \omega^2C_1^2R_1^2)}{(1 + \omega^2C_1^2R_1^2)(1 + \omega^2C_2^2R_2^2)}$$

From A-5

$$\text{A-7} \quad 1 + RC = \frac{R(1 + \omega^2C_1^2R_1^2)(1 + \omega^2C_2^2R_2^2)}{R_1(1 + \omega^2C_2^2R_2^2) + R_2(1 + \omega^2C_1^2R_1^2)}$$

Substituting into A-6

$$\text{A-8} \quad RC = \frac{C_1R_1^2(1 + \omega^2C_2^2R_2^2) + C_2R_2^2(1 + \omega^2C_1^2R_1^2)}{R_1(1 + \omega^2C_2^2R_2^2) + R_2(1 + \omega^2C_1^2R_1^2)}$$

Substituting into A-5

$$\text{A-9}\quad R = \left\{1 + \omega^2\left[\frac{C_1R_1^2(1 + \omega^2C_2^2R_2^2) + C_2R_2^2(1 + \omega^2C_1^2R_1^2)}{R_1(1 + \omega^2C_2^2R_2^2) + R_2(1 + \omega^2C_1^2R_1^2)}\right]^2\right\}$$

$$\times \left[\frac{R_1(1 + \omega^2C_2^2R_2^2) + R_2(1 + \omega^2C_1^2R_1^2)}{(1 + \omega^2C_2^2R_2^2)(1 + \omega^2C_1^2R_1^2)}\right]$$

Simplifying

$$\text{A-10}\quad R = \frac{R_1^2(1 + \omega^2R_2^2C_2^2) + 2R_1R_2(1 + \omega^2C_1R_1C_2R_2) + R_2^2(1 + \omega^2C_1^2R_1^2)}{R_1(1 + \omega^2R_2^2C_2^2) + R_2(1 + \omega^2C_1^2R_1^2)}$$

$$\text{A-11}\quad C = \frac{RC}{R} =$$

$$\frac{C_1R_1^2(1 + \omega^2C_2^2R_2^2) + C_2R_2^2(1 + \omega^2C_1^2R_1^2)}{R_1^2(1 + \omega^2R_2^2C_2^2) + 2R_1R_2(1 + \omega^2C_1R_1C_2R_2) + R_2^2(1 + \omega^2C_1^2R_1^2)}$$

$$\text{A-12}\quad C = \frac{C_1C_2}{C_1 + C_2}\ \frac{\omega^2 + (C_1^2R_1^2 + C_2^2R_2^2) + C_1C_2(R_1^2 + R_2^2/[C_1C_2(C_1 + C_2)^2R_1^2R_2}{\omega^2 + (R_1 + R_2)^2/[(C_1 + C_2)^2R_1^2R_2^2]}$$

$$\text{A-13}\quad R = \frac{R_1R_2(C_1 + C_2)^2}{R_1C_1^2 + R_2C_2^2}\ \frac{\omega^2 + (R_1 + R_2)^2/[(C_1 + C_2)^2R_1^2R_2^2]}{\omega^2 + (R_1 + R_2)/[R_1R_2(R_2C_2^2 + R_1C_1^2)]}$$

The final results are

$$\text{A-14}\quad C = \frac{C_1C_2}{C_1 + C_2}\ \frac{\omega^2 + \dfrac{C_1R_1^2 + C_2R_2^2}{C_1C_2(C_1 + C_2)R_1^2R_2^2}}{\omega^2 + \dfrac{(R_1 + R_2)^2}{(C_1 + C_2)^2R_1^2R_2^2}}$$

$$\text{A-15}\quad R = \frac{R_1R_2(C_1 + C_2)^2}{R_1C_1^2 + R_2C_2^2}\ \frac{\omega^2 + \dfrac{(R_1 + R_2)^2}{(C_1 + C_2)^2R_1^2R_2^2}}{\omega^2 + \dfrac{R_1 + R_2}{R_1R_2(R_2C_2^2 + R_1C_1^2)}}$$